2019

Increasing service life at bridge ends of moveable abutment bridges

Douglas Krapf
Iowa State University

Increasing service life at bridge ends of moveable abutment bridges

by

Douglas Krapf

A thesis submitted to the graduate faculty

in partial fulfillment of the requirements for the degree of

MASTER OF SCIENCE

Major: Civil Engineering (Structural Engineering)

Program of Study Committee:
Behrouz Shafei, Major Professor
Brent Phares
Vernon Schaefer

The student author, whose presentation of the scholarship herein was approved by the program of study committee, is solely responsible for the content of this thesis. The Graduate College will ensure this thesis is globally accessible and will not permit alterations after a degree is conferred.

Iowa State University

Ames, Iowa

2019

DEDICATION

This thesis is dedicated to my friends and family. To my fiancée, Megan, for her love and friendship throughout our time together. To my parents, Tom and Julie, for encouraging me to enter the field of civil engineering and giving me so much support.

TABLE OF CONTENTS

Page

LIST OF FIGURES

LIST OF TABLES

ACKNOWLEDGMENTS

I would like to thank my major professor, Behrouz Shafei, for his guidance throughout this project. His advice and supervision have been invaluable. I would also like to thank my committee members, Brent Phares and Vern Schaefer.

I would also like to thank Shahin Hajilar. His assistance was critical to my success, especially regarding the finite element modeling aspects of the project.

Thank you to Doug Wood and Owen Steffens for their help in field monitoring activities. Our time spent in the field included some difficult conditions from summer heat to below freezing temperatures.

Thank you to the Iowa Department of Transportation for sponsoring this research project and the input and information provided to me throughout the project.

Furthermore, I would also like to thank my friends Austin DeJong, Andrew Mock, and Lizzie Miller. Thank you to faculty, staff, and colleagues in the Iowa State Civil Engineering Department.

Finally, I would like to extend a special thanks to my entire family.

ABSTRACT

Integral and semi-integral abutment bridges have become increasingly popular in Iowa and across the country because they eliminate joints at the bridge ends. Expansion joints in bridge decks allow water to seep in and corrode bearings along with other structural elements in conventional bridge construction. An integral abutment connects the bridge deck and girders with the substructure in one piece to reduce maintenance and increase service life. The abutment moves with the rest of the bridge, and this movement introduces new issues with water drainage, soil settlement, soil erosion, and concrete cracking. The objective of this research was to evaluate improved bridge end details to increase service life and investigate limitations placed on the use of semi-integral abutment bridges. Research methods include a literature review, visual inspections, field monitoring, and finite element simulations.

An extensive literature review presents relevant research to improving performance of bridge ends. Abutments, approach slab, geotechnical aspects, drainage, and expansion joints are evaluated in detail. Innovative bridge abutments allow for elimination of conventional bearings and attempt to reduce issues associated with integral construction.

Semi-integral bridges and those with approach slabs attached to the abutment were inspected across the state of Iowa to assess performance of current design methods. Tied joint condition performance was unsatisfactory with measured openings much larger than initial construction. Joints between wingwalls and approach slabs were also in poor condition.

Two bridges were outfitted with a multitude of sensors including strain gauges and displacement transducers to measure concrete expansion and bridge displacement. A 184.5-foot 45-degree skew semi-integral abutment provided abutment displacements and earth pressures behind the abutments. A 375-foot integral abutment bridge with 15-degree skew was also monitored for joint movements and strain in the approach slabs.

Finite element models were created to investigate the sliding of approach slabs on the soil below. Simulated bridge expansion provides insight into approach slab behavior and tie bar stresses due to friction. Parametric studies were completed on various approach slab properties including friction with soil, soil stiffness, tie bar style, and bridge skew. The outcome of this study includes recommendations for improving bridge end drainage and provides insight into skewed approach slab behavior.

CHAPTER 1. INTRODUCTION

1.1 Overview

An increased focus on life-cycle cost of transportation infrastructure results in attempts to lower costs in areas other than just initial construction. There are additional aspects including maintenance, repair, operation, and disposal. The other component of life-cycle cost is the service life. How long can the structure safely perform its intended function? By increasing service life, the costs are spread over a longer period of time. One of the major contributors to bridge deterioration and increased repair work is bearings. Girders in conventional bridges are placed on bearings which are located directly below joints at the end of the bridge, and when joints degrade over time they leak surfacewater and de-icing chemicals onto the bridge bearings (Hassiotis et al. 2006). Bearings are eliminated entirely through the use of integral or semi-integral abutment bridges. These "jointless" bridges expand and contract as one piece during temperature changes, pushing on the soil at either end. The movement must be accommodated somehow, and frequently presents design challenges that shorten the service life. The issue of unsatisfactory drainage remains and designs often do not adequately remove water away from bridge components. Water that infiltrates the bridge ends may increase settlement or contribute to erosion of the embankment. The worst case involves water flowing under the abutment and exposing the steel piles, leading to corrosion and possibly compromising the structural capacity of the foundation. Many factors seen in Figure 1.1 contribute to an equally large number of metrics of poor performance, including the "bump" at the end of the bridge which is a symptom of approach slab settlement (Briaud et al. 1997).

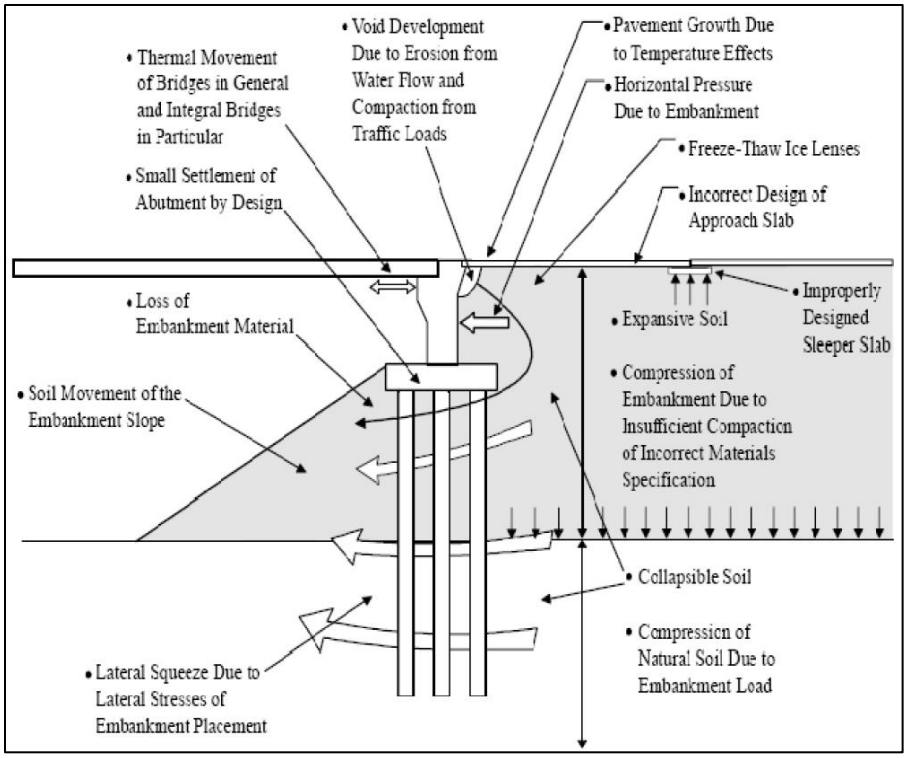

Figure 1.1. Factors Contributing to the "Bump" at the end of the Bridge (Briaud et al. 1997)

1.2 Research Needs and Motivations

Integral and semi-integral abutment bridges are currently limited in use for low and moderate span lengths to restrict bridge movement. They are also limited to certain skews to limit secondary forces (Bakeer et al. 2005). The limits placed on their use is different in every state and depends on many factors. As research continues to push the boundaries of jointless bridge design, there are many aspects of bridge design and detailing that need to catch up. For example, although research may show foundation piling is sufficient to allow for integral bridges over a given length, other bridge details like a tied approach slab connection, wingwalls, and drainage details may not be able to accommodate the expected bridge movements (Olson et al. 2013). There is no consensus on how best to detail most any of the parts listed, thus the variety seen when reviewing other state's standards. This is the

main motivation of the research presented in this thesis that will help Iowa DOT and other Midwestern transportation agencies to improve long term performance of many key bridge aspects.

1.3 Research Objectives

Objectives were used to focus research effort including collection of information relevant to increasing bridge end service life and development of recommendations and guidelines. Information was accumulated through multiple sources by completing different tasks such as a comprehensive literature review, survey of state DOTs, bridge inspections, field instrumentations and monitoring, and finite element modeling. The process began with a thorough review of current literature on relevant topics including integral abutments, semi-integral abutments, tied approach slabs, bridge end erosion, and bridge drainage. A survey of state DOTs provided insight into practices of other neighboring states around Iowa that experience similar climate. Seven different bridges in the state of Iowa with semi-integral abutments or tied approach slabs were inspected for signs of soil settlement, concrete cracking, poor joint performance, and poor drainage. These inspections provided real examples of problems contributing to poor bridge service life. In order to support recommendations made for increasing service life, two bridges were instrumented with an array of sensors to record various measurements of long periods of time. Finite element (FE) modeling also allowed for investigation of bridge properties to make additional design recommendations.

1.4 Thesis Outline

This thesis is organized into chapters by the different tasks that were completed in order to accomplish the research objectives. Beginning after the introductory chapter, chapter 2 presents the literary review information pertaining to the many complicated aspects of

bridge ends. The chapter is split into sub-categories to further separate information on abutments, approach slabs, drainage, soil and geotechnical engineering, and bridge drainage. Chapter 3 discusses the preparation and overview of a survey sent to state DOTs on the topic of bridge end service life. The eleven-question survey covers semi-integral abutments, sleeper slabs, expansion devices, and drainage in an attempt to gain information not publicly available in state DOT bridge design manuals. Chapter 4 shows results of the visual inspections done for 7 different bridges of varying ages, span lengths, skews, and traffic levels. The inspections illustrate how poor design and detailing leads to degradation and shortens service life, which leads to costly repair or replacement. Chapter 5 begins with the techniques used for installing strain gauges, crackmeters, earth pressure sensors, and displacement transducers on two Iowa bridges for long-term monitoring. The data is processed and reveals how temperature changes affect bridge behavior. Chapter 6 details the creation and calibration of FE models and the parametric studies used to determine the effects of changing bridge properties on concrete and steel stresses and other performance metrics. Chapter 7 provides a conclusion of the research efforts that includes recommendations being made to Iowa DOT for the improvement of bridge end service life through abutment, approach slab, and drainage details.

CHAPTER 2. LITERATURE REVIEW

2.1 Overview

The goal of this literature review is to compile relevant research studies and systematically present the important findings of each after outlining important objectives, test methods, and limitations. The information is grouped into multiple categories involving the overall performance of integral and semi-integral abutment bridges. Research focused on abutment and backfill details, approach slab details, geotechnical performance and specifications, proper drainage, and expansion joint devices. Since the focus of the review is broad and many important conclusions are included, the proper context by which the conclusions and recommendations are formulated is included where necessary.

2.2 Abutment Details

2.2.1 Length and Skew Limits

Mistry (2005) provided an overview of jointless bridges including the reason for transition away from conventional bridges, an explanation of what integral abutments are, the many advantages of jointless bridges, and an extensive list of best practices and details. Deck joints are sometimes not given the proper attention during installation and can lead to larger problems with rather expensive bearings. Eliminating joints and bearings can prevent future structural issues and additional costs. Jointless bridges simplify design, widening and replacement, offer lower future maintenance costs, and can expedite construction among other advantages. The most significant practice the author notes is the standardized use of sleeper slabs to control the crack between approach slab and pavement. Important design detail recommendations are made to tie approach slabs to abutments with hinge-type reinforcing, use generous shrinkage reinforcement in the deck slab above the abutment,

design wingwalls as small as possible to make them easier to move with the bridge, and to use cantilevered turn-back wingwalls instead of transverse wingwalls for shallow superstructures.

Surveys are a useful tool to gain insight on the current practice of engineers across the country. Since the design of integral abutment bridges and approach slabs lacks a standard process, continuous surveys are required to stay up to date. Maruri and Petro (2005) summarized results from a survey sent to all fifty states about their use of integral abutments and jointless bridges in which thirty-nine responded. The survey included "questions about the number of integral abutments designed, built and in service, the criteria used for design and construction, including maximum span lengths, total length, skews and curvature and problems experienced with integral abutment bridges". A majority of states limit the total length and skew of integral abutment bridges; the variation and range of limits show the lack of uniformity and standardization between states. Ninety percent of states responded that their policy was to eliminate as many joints as possible and use jointless construction in new bridge design. White (2008) conducted a survey of bridge designers in seven European countries about the use of integral and semi-integral abutment bridges in their respective countries. The results were able to highlight some interesting differences in design practices between Europe and the United States. The design earth pressure for abutment backwalls varied between full passive pressure and a value between at-rest and passive pressure. Approach slabs were not required to be used with integral abutment bridges but were recommended by most countries. U-wingwalls parallel to the bridge centerline are in use which is similar to practice in the United States (US), but wingwalls were cast both with the superstructure of a semi-integral abutment and with the stationary substructure of a semi-

integral abutment. Overall, there are some significant differences between practice in Europe and the US that appear to be driven by empirical results and the successful performance of past projects. Surveys are especially helpful for recording the limits placed upon different types of design limitations placed on jointless bridges. Length limitations of integral abutment bridges built on H-piles in sand were investigated by Dicleli et al. (2003). The authors used SAP2000 to create an FE model and complete a parametric study to examine effects on maximum displacement capacity of the bridge, which assumed 0° skew. Displacement capacity was found to decrease with stiffer foundation soil and larger/stiffer bridges in terms of span lengths and cross-sectional stiffness. It was recommended that piles are placed in the strong axis direction for bending for low-cycle fatigue performance, but if flexural capacity of the abutment controls displacement, then they should be oriented with weak axis in bending. Concrete bridges were determined to be less sensitive to temperature variations and the maximum length limit in cold climates is 190 meters (623 feet) while steel bridges in cold climates should be limited to 100 meters (328 feet) in cold climates. Dunker and Abu-Hawash (2005) provided a history of the use and expansion of integral abutment bridges in Iowa. The simple cantilever pile model developed at Iowa State allowed for changes to the length and skew limits for integral abutment bridges (IAB). Thermal expansion and contraction of the bridge introduce second-order bending effects to the piles and increase stresses. Limiting the piles to elastic stresses was conservative, so piles were allowed to deform plastically. Allowing a hinge does not affect the pile strength since the strains are considered residual. The 2002 limits encompassed 90% of a particular group of bridges compared to 70% with the 1988 policy limits showing how effective the changes were in allowing for the construction of more jointless bridges. As part of their bridge design

manual, Idaho DOT (2008) produced a set of guidelines for the design of integral abutment bridges. Length limitations are set as 650 feet for concrete structures and 350 feet for steel structures. Wingwalls are to be parallel with the girders for all bridges, and piles are to be oriented for bending in the strong axis regardless of the bridge skew. Hassiotis et al. (2006) combined the results of bridge monitoring with a finite model created using ABAQUS producing a design guide which limited integral designs to a length of 460 feet and skew of 30°.

Olson et al. (2009) aimed to expand the limitations for integral abutment bridges in the state of Illinois. The study included FE modeling, and the development of instrumentation plans for future Illinois bridges. LPILE and FTOOL were used for 2-D FE modeling and SAP2000 was used for 3-D. It was found that a continuous connection between approach slab and abutment/deck results in stress well above tensile rupture strength of typical concrete materials and a hinged connection provides much lower stresses. The FE models produced many recommendations for IDOT, including the use of compacted select granular backfill behind the abutment. In order to increase IAB limitations, it was recommended to predrill pile locations to 8 feet, and either reduce pile embedment in pile caps from 2 feet to 6 inches or include hinge details similar to that used by the Virginia DOT. Length and skew limitations were provided for concrete piles, and two sizes of steel piles for both strong and weak axis bending in Table 2.1 and Table 2.2.

Table 2.1. Allowable Length and Skew Combinations for Integral Abutment Bridges using HP12x53 Piles Oriented for Strong Axis Bending (Olson et al. 2009)

	Grade 36 steel		Grade 50 steel		Grade 60 steel	
	Maximum length (feet)	Skew (degrees)	Maximum length (feet)	Skew (degrees)	Maximum length (feet)	Skew (degrees)
No moment reduction (i.e., current IDOT design)	140	0 - 30	240 120	0 - 30 30 - 60	320 190	0 - 30 30 - 60
Predrill to 8 ft	160	0 - 30	300 160	0 - 30 30 - 60	360 240	0 - 30 30 - 60
Hinge at pile cap/pile interface	400 250	0 - 30 30 - 60	600 440	0 - 30 30 - 60	700 550	0 - 30 30 - 60
Hinge at pile cap/abutment interface	600 440	0 - 30 30 - 60	900 680	0 - 30 30 - 60	1000 850	0 - 30 30 - 60

Table 2.2. Allowable Length and Skew Combinations for Integral Abutment Bridges Using HP12x53 Piles Oriented for Weak Axis Bending (Olson et al. 2009)

	Grade 36 steel		Grade 50 steel		Grade 60 steel	
	Maximum length (feet)	Skew (degrees)	Maximum length (feet)	Skew (degrees)	Maximum length (feet)	Skew (degrees)
No moment reduction (i.e., current IDOT design)	Not recommended		160 120	0 - 30 30 - 60	240 180	0 - 30 30 - 60
Predrill to 8 ft	160	0 - 30	280 240	0 - 30 30 - 60	380 320	0 - 30 30 - 60
Hinge at pile cap/pile interface	300 240	0 - 30 30 - 60	440 400	0 - 30 30 - 60	600 540	0 - 30 30 - 60
Hinge at pile cap/abutment interface	450	0 - 60	700	0 - 60	900	0 - 60

LaFave et al. (2016) and (2017) completed a systematic study on the behavior of integral abutment bridges under thermal loading. The authors completed a parametric analysis of chosen primary and secondary parameters in the first study (2016a) and compared with field monitoring results on two Illinois bridges in the second one (2016b). Primary parameters were abutment skew, pile size, span length, and number of spans which used a matrix of 38 model batches to see trends in the overall behavior. Full bridge models were created using SAP2000 software, and approach slabs were not included since bridge behavior

was not affected by their presence. Stress levels in the real bridge approach slabs were low-magnitude and did not have significant effects. Overall bridge expansion in the models was around 90% of free expansion predicted by the effective expansion length (EEL). Increasing skew created increasing thermal displacements at the acute bridge corners, a finding that was also confirmed by field data. Larger pile sizes, like HP16s and HP18s, were found to be feasible and allow for longer EELs so long as increased forces and moments in the abutment and superstructure could be accommodated.

Olson et al. (2013) continued the investigation into the Illinois DOT length and skew limits for integral abutment bridges building off previous work by Olson et al. (2009). The main objective of the research was to use 3-D SAP2000 models to complete a parametric study of the effects on IAB behavior. Various parameters such as bridge length, skew, interior span length, pile type and size, live loading, and pile orientation were studied using 200 different full bridge FE models. All models considered only a 2-lane bridge and in order to determine length and skew limits piles were taken to first yield as opposed to allowing plastic deformation as some states do in design. Some general trends were found across the different models including the fact that greater abutment rotation, due to less restraint, results in lower pile stresses. Longer intermediate spans between supports also increased pile stresses. Skew has large effects on IAB behavior regardless of many other parameters. The authors noted that the largest amount of bridge expansion occurs parallel to the bridge's longitudinal axis, so it was proposed to place piles with webs parallel to that axis regardless of the bridge skew. This "strong-axis alternate" orientation in Figure 2.1 provided pile stresses 20%-30% lower than either weak-axis or strong-axis piles, and it was recommended that IDOT consider the use of strong-axis alternate orientation. The limitations seen in

Figure 2.2 below are based strictly on the performance of the pile foundation and do not account for other structural or non-structural bridge components. The study resulted in additional recommendations for IDOT including the use of compacted granular backfill behind abutments. For skews less than 45° the passive pressure that develops resists thermal expansion, and the backwall friction helps to resist transverse abutment movements for all bridges regardless of skew.

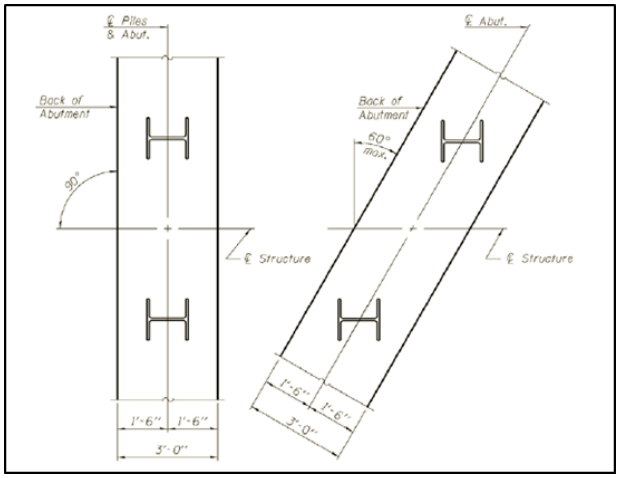

Figure 2.1. Proposed Strong-Axis Alternative Pile Orientation for Illinois IABs Founded on H-Piles (Olson et al. 2013)

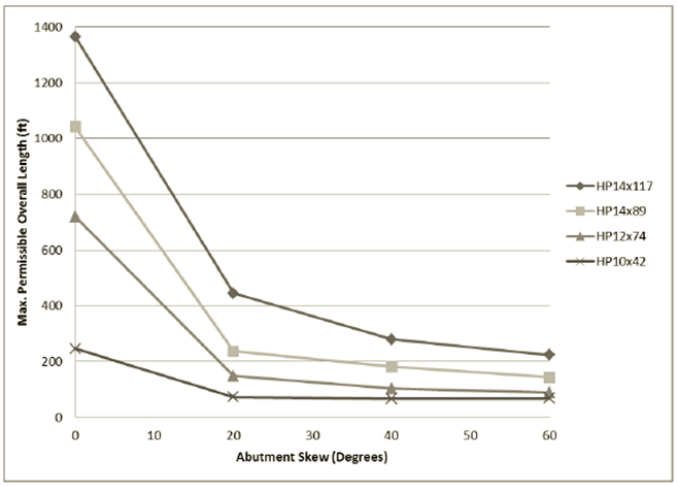

Figure 2.2. H-Pile Summary: Permissible IDOT IAB Lengths vs. Skew (100-ft Intermediate Spans) (Olson et al. 2013)

In 2013, the Illinois DOT issued a memorandum to all bridge designers. The memorandum adopted a new pile orientation for abutments which is the exact opposite of the "strong-axis alternate" proposed by Olson et al. (2013), saying the "pile web is always perpendicular to the centerline of the structure". Integral abutment limits were increased to a length of 550 feet and skews up to 45°. The corbel was eliminated and absorbed into the abutment cap. The integral abutment pile selection chart seen in Figure 2.3. is a function of effective expansion length (EEL) and skew. The EEL must be calculated accounting for the centroid of stiffness of the abutments. EEL is calculated the same for concrete and steel bridges and is equal to or greater than half the total expansion length depending on whether the centroid of stiffness lies at the center of the bridge or is shifted towards one abutment.

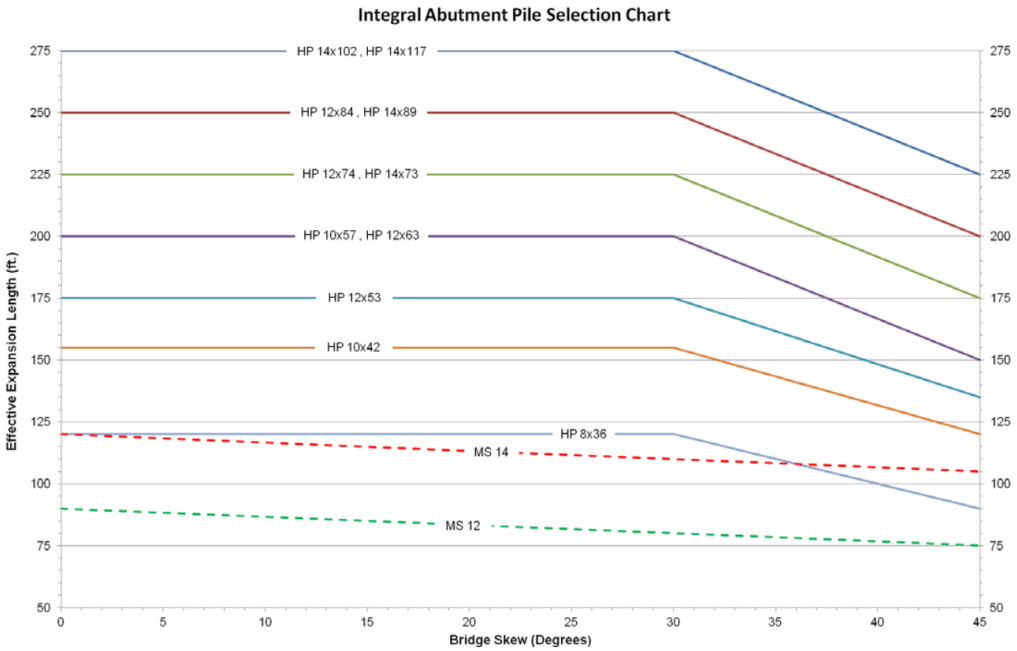

Figure 2.3. Integral Abutment Pile Selection Chart Based on EEL (Illinois DOT 2013)

2.2.2 Earth Pressure and Forces on Abutments

The pressure experienced by an abutment backwall in an integral or semi-integral bridge is an important yet complex issue. Hassiotis et al. (2006) worked together with the

New Jersey DOT to fully evaluate integral abutments for use in place of bridges with bearings. The extremely extensive evaluation included monitoring of an integral abutment bridge, and a finite element model all culminating in recommendations and a design guide for integral bridges. The review of the current practice at the time concluded that additional research was needed in the development of passive earth pressures behind the abutment due to cyclic loading. A 298-foot long integral abutment bridge with 15° skew and piles oriented for weak-axis bending was fitted with a multitude of sensors. The results of the monitoring period combined with a finite model created using ABAQUS lead to a large number of recommendations for integral bridges. The approach slab should be connected to the abutment with a moment connection allowing for rotation and designed as a simply supported span in case of a loss of soil support underneath a majority of the length. Since passive pressures behind the abutment can increase over time and were found to be larger than typical design values, passive pressure should be calculated with a maximum density of the soil and a maximum internal angle of friction. The obtuse corner of a skewed bridge will see a larger pressure than the acute corner due to unequal movement, and geosynthetics may be able to reduce passive pressure build-up. Bonczar et al. (2005) examined the effects of soil properties on the behavior of piles and abutments using both 2-D and 3-D finite element models created using GT-STRUDL Structural Design & Analysis Software. Abutment backfill was modeled as non-linear springs in the finite FEM models. Earth pressures were found to be higher when loose material was used to surround the top of piles, due to lower constraint and higher movement. The equivalent cantilever method provided a great correlation for pile moments for bridge expansion and was conservative for contraction. According to Idaho DOT (2008), the earth pressure on the abutment is calculated using full

passive pressure for the top third varying linearly to at-rest earth pressure at the bottom of the abutment. A design check for lateral forces is also provided that compares lateral capacity of piles and soil pressure on wing walls to the moment created by eccentricity of soil forces at either end of the bridge. Field monitoring of integral abutment bridges is rather common due to the insight the data can provide about the real-world performance of experimental details. However; monitoring is typically done for 1 to 2 years at the most, just enough to capture a full seasonal cycle. Kim and Laman (2012) instrumented four bridges for which monitoring periods lasted between 2.5 and 7 years. Many responses were measured using the 240 total sensors including abutment displacement and rotation, backfill pressure, girder rotation and moments, pile forces, and approach slab strain. Based on temperature readings, AASHTO LRFD (2010) design temperature ranges for concrete were found to be conservative and the difference between ambient temperature and superstructure temperature was negligible. The thermal loading produced nonlinear and irreversibly increasing abutment displacements over time. Earth pressure in all four bridges reached passive pressure values, making it an appropriate design choice to use full passive pressure. A difference was observed in the girder rotation and abutment rotation values indicating the assumption of a fully fixed connection may not be entirely accurate and further investigation may be required. Thermal loading of the superstructure must be taken into account, as positive thermal loading creates negative bending in the girders and negative thermal loading creates positive bending.

Arenas et al. (2013) investigated the behavior of IABs with MSE walls when subject to thermal movements. Only full integral abutments with MSE walls on three sides forming a U-back configuration were considered. The study included a survey of state DOTs across the United States, a 3-D numerical model, an analysis of corrugated steel pipes that surround

piles, and a parametric study to develop a spreadsheet to aid in design for thermal responses. The survey received responses from 21 agencies where it was discovered that almost all agencies used a skew limit of 30°, and 71% of agencies oriented piles for weak-axis bending only. Abutment design earth pressures varied across the board between active, at-rest, passive, or a combination of earth pressures. The 3-D numerical model created using FLAC3D software determined that surrounding piles with corrugated steel pipes and filling them with loose sand does not reduce pile loading due to stiffening after cyclic loading, so it was recommended that the Virginia DOT end the practice to reduce costs. Final conclusions note that earth pressure increases during a one-year cycle to reach a peak value increase of up to 60% over the first year, with an increase of only 6% the following year seen in Figure 2.4. The use of elasticized EPS, which was found to be rare in the completed survey, reduced lateral earth pressures according to the numerical analyses supporting its use by VDOT. The numerical analysis also showed transverse displacements of skewed bridges reached magnitudes similar to longitudinal displacements.

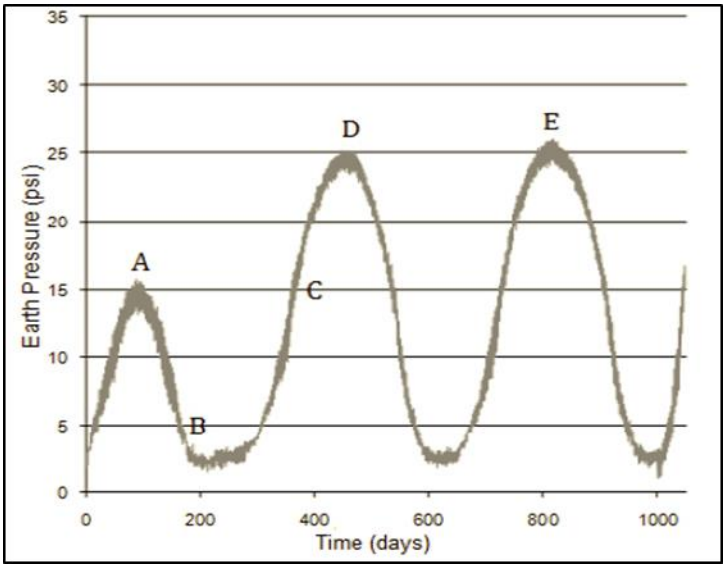

Figure 2.4. Earth Pressure behind the Abutment (Arenas et al. 2013)

Kong et al. (2015) instrumented the first fully integral abutment bridge constructed in the state of Louisiana in 2011. Louisiana has unique soil conditions, which is why there was a lack of information on IAB behavior for engineers to use. The Caminada Bay Bridge has long continuous spans, deep precast prestress concrete piles, and very soft soil conditions creating additional challenges. Monitoring was concentrated on the first 11 spans with an integral abutment at one end, 10 bents rigidly connected to the 300-foot continuous slab, and simply supported at the other end. Extensive temperature data showed a temperature variation at a central bent deck surface large enough to possibly cause cracking of the concrete deck with seasonal temperatures variations within the design values of AASHTO LRFD. Soil behavior at the abutment proved to be non-linear and extremely complicated with restraints accumulating over time, but it was found that effects of abutment movement were negligible at a distance of 6.9 feet away from the abutment. Kong et al. (2016) continued studying the Caminada Bay Bridge in Louisiana. The monitoring data that was obtained was used to validate a 3-D finite element model in the program ANSYS. A parametric study examined the effects of support conditions, soil types, and joint connections between the piles and bents on the overall bridge behavior. Free supports at the bridge ends allowed for larger displacements inducing the largest positive and negative bending moment on the pile; however, high compressive strains develop in the bridge deck under fixed support conditions. This illustrates a trade-off between superstructure and substructure performance when examining where thermal expansion is accommodated. Loose sand backfill was found to result in lower backfill pressures when compared to dense sand. The soil surrounding the piles was found to have the largest effect on the bridge. When changing soft soil to stiff soil the maximum displacements were decreased by 1.5 times, but pile strains

increased 70% and slab negative strains increased by 48%.

Varmazyar et al. (2017) analyzed the performance of a new backfill method to improve soil interaction with the bridge structure during cyclic movements. The problem of high earth pressures and "ratcheting" of backfill was outlined as a reason for the study. Ratcheting causes increasing earth pressures on an integral bridge abutment over time as the bridge contracts and backfill collapses into the void, before being compressed in the next expansion cycle. Traditional backfill is constructed in layers or lifts, and when combined with a large area occupied by the approach slab results in a significant amount of time required for construction. The proposed solution used a compressible inclusion (CI) made of resilient Expanded Polystyrene (EPS) attached to the abutment backwall with a backfill consisting of cement stabilized sand or no-fines mass concrete behind it. The intent of this detail is to reduce lateral earth pressures, accommodate expansion and contraction movements, and prevent settlement or voids below the approach slab all while reducing construction cost through reduced cost and time of installation. The authors created a 2-D finite element model using PLAXIS 2D software which included the bridge abutment, foundation pile, bridge deck, and backfill. Models were created for both a traditional backfill and the proposed solution so that results could be compared. Four cycles of expansion and contraction of 10mm, 30mm, and 100mm were applied to simulate thermal movements of a bridge. The CI with CSS model showed decreased lateral earth pressures on the abutment, with a spike at the soil just below the abutment (Figure 2.5), and much lower residual total displacements meaning a reduction of ratcheting effects (Figure 2.6). The proposed design performed better at a lower cost and would shorten construction times.

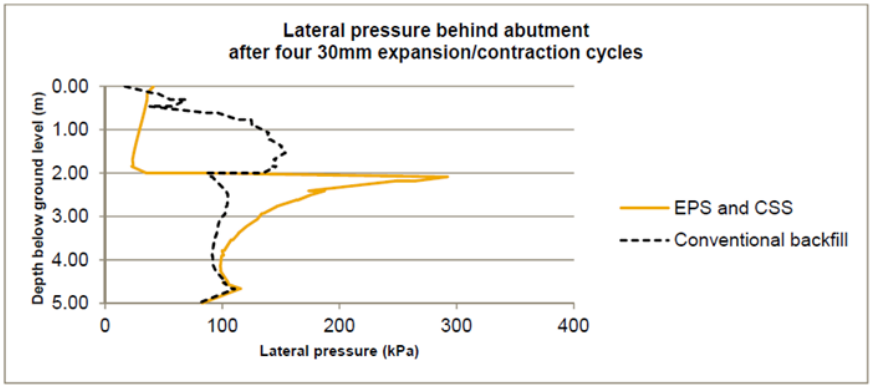

Figure 2.5. Comparison of Horizontal Stress behind Abutment after Fourth Cycle of 30mm Bridge Expansion (Varmazyar et al. 2017)

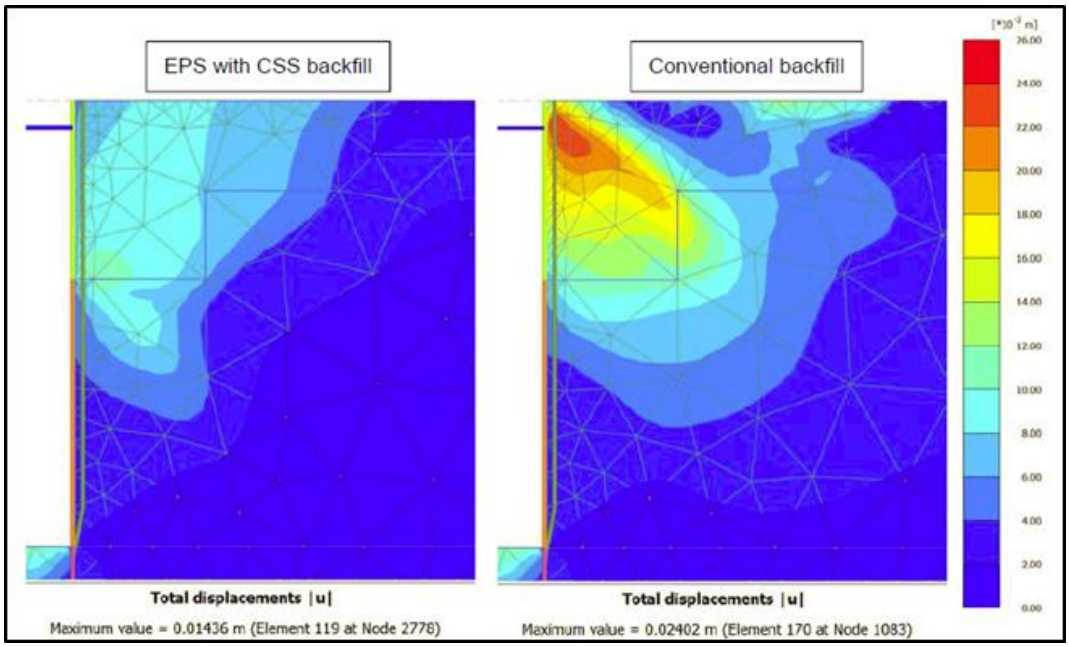

Figure 2.6. Comparison of Total Displacement in Backfill After Bridge Deck Contracting to Original Length Following Fourth Cycle of 30mm Bridge Expansion (Varmazyar et al. 2017)

The first six prototype semi-integral bridges constructed in the state of Louisiana were evaluated by Bakeer et al. (2005) to determine if they had performed satisfactorily since construction. All six bridges were inspected, and two were selected for a structural/geotechnical analysis and finite element analysis respectively. All the bridges used the same abutment design detail shown in Figure 2.7 which utilized geosynthetics to

reinforce the embankment behind the abutment and allow for a gap between abutment backwall and embankment. The gap's purpose is to accommodate longitudinal expansion of the abutment. During bridge inspections, it was found the gaps were performing as intended and had not closed or filled with any significant amount of material. Additional results of the inspections showed the semi-integral bridges outperforming similar conventional bridges based on a rating system of each bridge component. The ANSYS model was used to complete a parametric study examining the effects of thermal loading, settlement of the approach, and bridge skew. No overstressing was detected in any components for temperature gradient loading or for skew of 30°; however, cracking was seen in the approach settlement model and was the reason for a weak joint (saw-cut joint) being included in the design of Bridge I-2 at 10 feet away from the abutment backwall. Final recommendations include the use of a sleeper slab and compressible joint at the end of the approach, a vertical gap of at least 6 inches behind the backwall, and the use of a weak joint as an internal hinge in the approach slab at one-quarter the length away from the backwall.

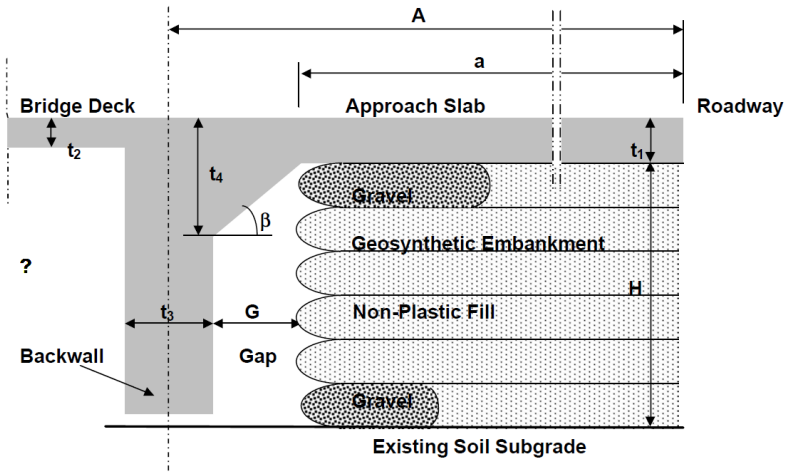

Figure 2.7. Details of Louisiana DOTD Prototype Semi-Integral Bridge Design (Bakeer et al. 2005)

2.2.3 Unique Abutment Details

In cases where limitations disqualify the use of integral or semi-integral abutments, other options are available. Aktan et al. (2008) completed an extensive investigation of link slabs used in jointless bridges along with performance and details at the end of the bridge including abutments and approach slabs. Two different bridge types were considered including deck-sliding-over-backwall and semi-integral abutment. The literature review revealed only continuous bottom reinforcement should be used to prevent moment transfer in deck-sliding-over-backwall bridges (Figure 2.8) and FE modeling confirmed that stresses over the abutment are reduced with the improved detail. For semi-integral abutments an inclined bar should be used with a construction joint for to serve the same purpose of moment and stress reduction by acting as a hinge allowing the approach slab end to rotate when backfill inevitably settles. Friction between the approach slab and subgrade did not create any appreciable stresses in the approach slab in the FE models. It was recommended that the construction joint be placed at the span side abutment face for deck-sliding-over-backwall and at the approach side abutment face for semi-integral abutments. Aktan and Attanayake (2011) also investigated link slabs, deck-sliding-over-backwall abutments, and semi-integral abutments for bridges with high skew (over 20 degrees). This study complements a previous work, Aktan et al. (2008), which considered bridges with less than 20-degree skew. The authors instrumented a bridge with 42-degree skew and measured displacements. Skewed bridges expand and contract along an axis between the two acute bridge corners, instead of just longitudinally along the axis of the girders. Deck-sliding-over-backwall bridges can be restrained longitudinally by restraining the center girder using concrete keys. A 1” layer of expanded polystyrene is placed between the backwall and bottom surface of the approach slab shown in Figure 2.9.

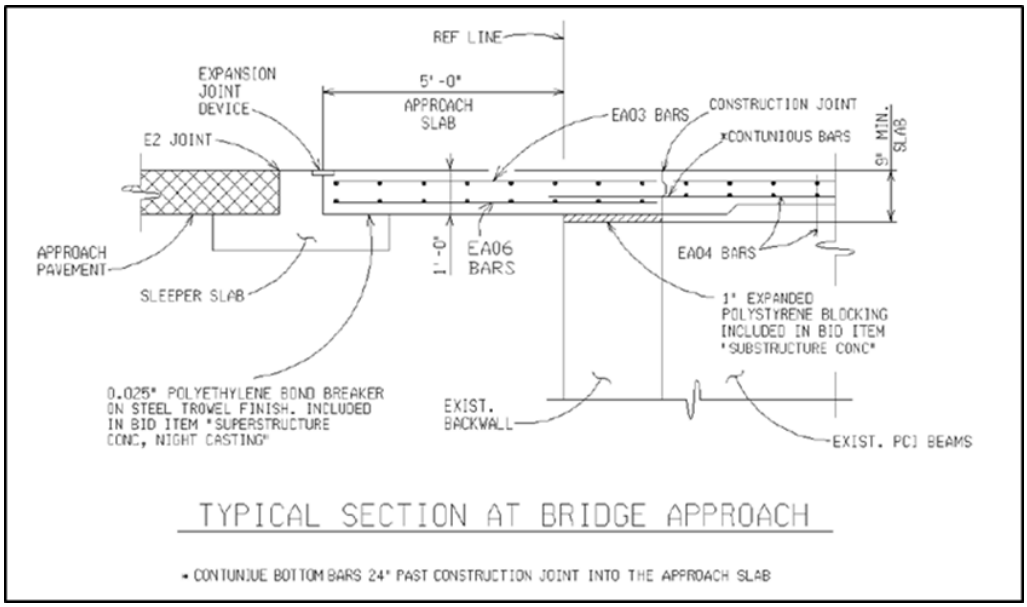

Figure 2.8. Proposed Dependent Backwall Configuration, i.e. Construction Joint over the Backwall Face at the Span Side with Continuous Bottom Reinforcement (Aktan et al. 2008)

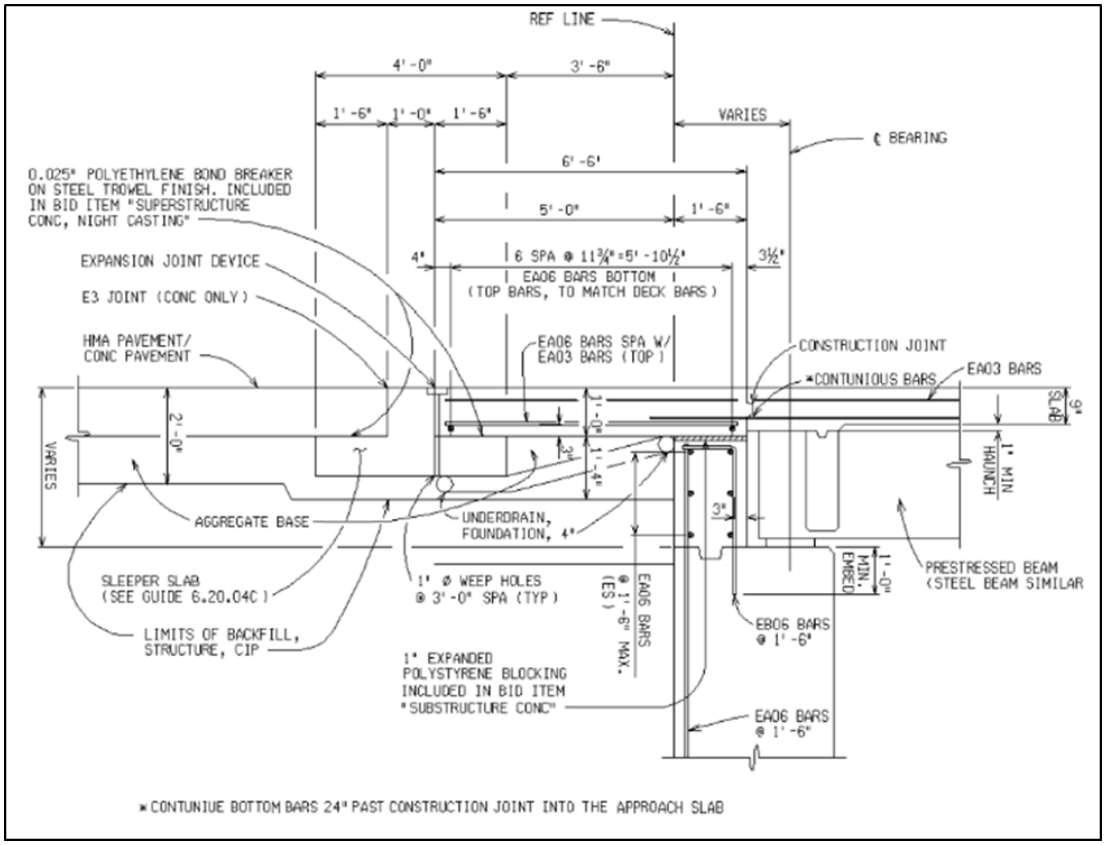

Figure 2.9. Deck Sliding over Backwall (Aktan and Attanayake 2011)

A similar longitudinal restraint concept applies for semi-integral abutments (Figure 2.10), except transverse movement is restrained by rub plates on a wingwall at the acute corner. The use of an EPS layer behind the backwall was recommended to reduce passive pressures. The use of a 0.025" thick polyethylene beneath the approach slab can reduce friction, something that should be done for all surfaces of the approach slab to facilitate free movement.

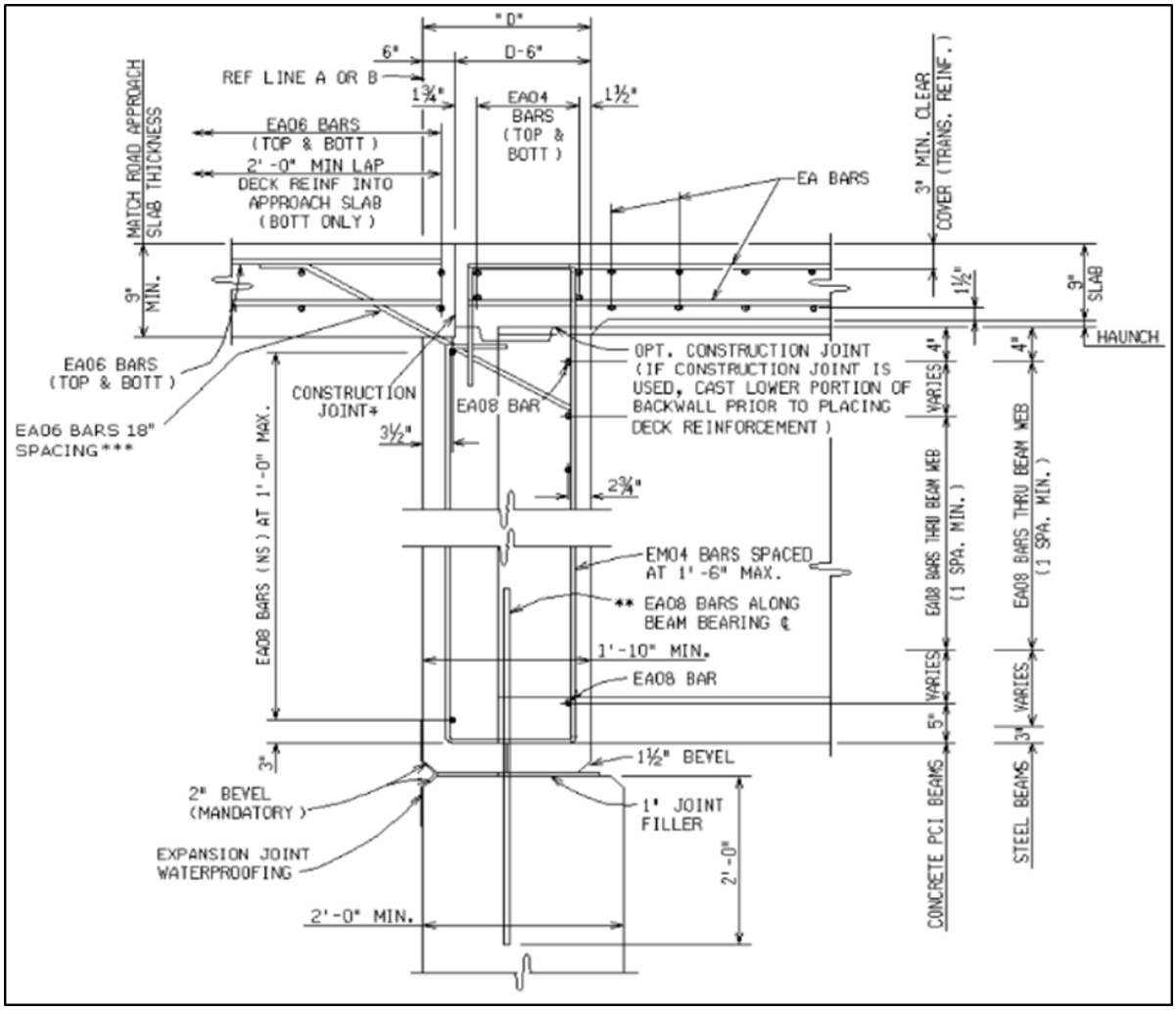

Figure 2.10. Semi-Integral Abutment Details (Aktan and Attanayake 2011)

Like Michigan DOT, Virginia DOT also has jointless bridge design options that are not traditional integral or semi-integral. Weakley (2005) covered a set of guidelines for

designing jointless bridges for the Virginia Department of Transportation. Three different types, integral, semi-integral, and deck sliding over backwall, are used depending on length, skew, and anticipated abutment movement limits. The backwall for fully integral bridges is designed to handle passive earth pressures. If the bridge is skewed, piles must accommodate lateral loading as well. Semi-integral designs are used when the minimum pile length of 25 feet cannot be used for construction of a fully integral bridge. Skewed bridges result in lateral movements that must be resisted so that movement is limited to the longitudinal direction. Rub plates are placed at the acute corners of bridges made of stainless steel to bear on wingwalls and the wing haunch is a vertical cantilever and must be reinforced more heavily to account for this loading. A deck extension configuration (Figure 2.11) eliminates the deck joint at the abutment by extending the bridge deck over the backwall. The joint is relocated and a ½" layer of polystyrene is placed horizontally between the abutment and deck above. Lateral movement and rotation due to skew may still occur so rub plates are used as they are for semi-integral bridges. VDOT uses elasticized expanded polystyrene (EPS) to replace backfill in contact with the abutment backwall to reduce passive pressures and settlement. The use of the elasticized EPS mitigates the effect of ratcheting which occurs during bridge shrinkage. The previous connection between approach slab and abutment used two layers of bars continuing into the bridge deck. Cracking problems occurred with cracks appearing at the end of the bars due moments caused by settlement, so the change was made to a single layer of bars angled into the abutment to allow rotation. A new jointless bridge detail known as the "Virginia Abutment" was created to work in any scenario that includes a double backwall with large drainage area and expansion joint between the semi-integral-like abutment and second backwall. The Virginia Abutment (Figure 2.12) uses an isolated

backwall located behind an integral backwall. A tooth joint is located at the bridge deck surface between the two abutment walls. There is a large void space between the two and concrete is covered with an epoxy coating to facilitate drainage. The void space is large enough that it can be easily maintained and cleared of any possible debris. Thermal expansion and contraction of the bridge is accommodated without any interaction with the soil. There do not appear to be any research studies done specifically on the Virginia Abutment; however, they are in use by VDOT. The following is an excerpt from the VDOT Manual of the Structure and Bridge Division: "When beyond the limits of the selection criteria indicated above for full integral abutments, semi-integral abutments or conventional cantilever abutments with deck slab extensions and the decision is made not to pursue a design waiver, Virginia Abutments shall be used."

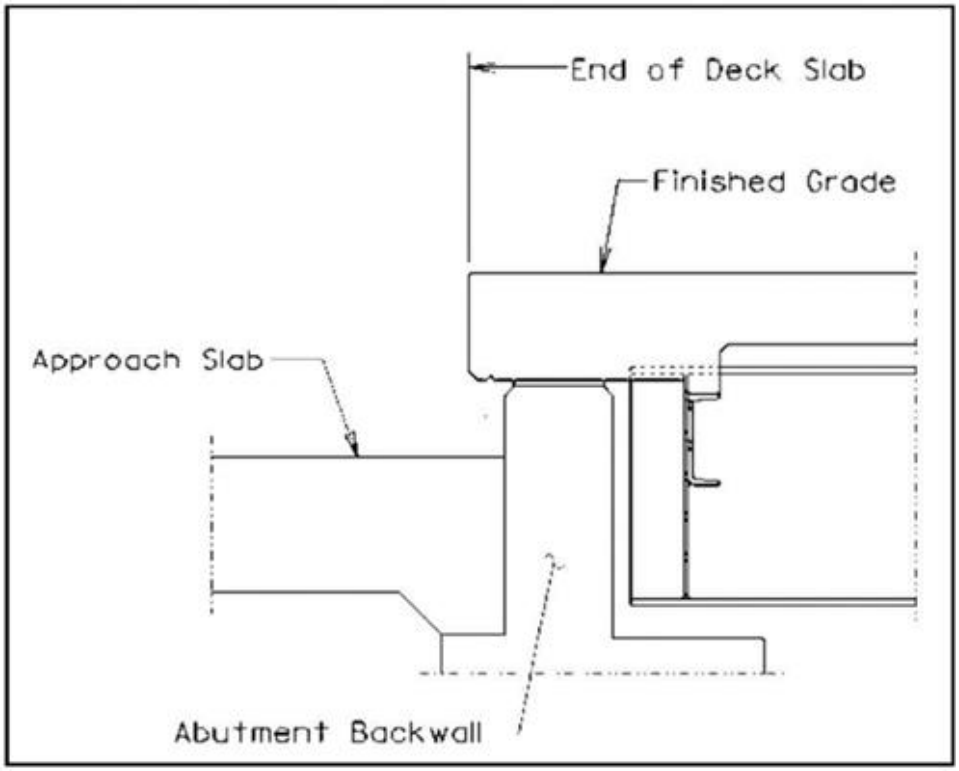

Figure 2.11. Deck Extension (Weakley 2005)

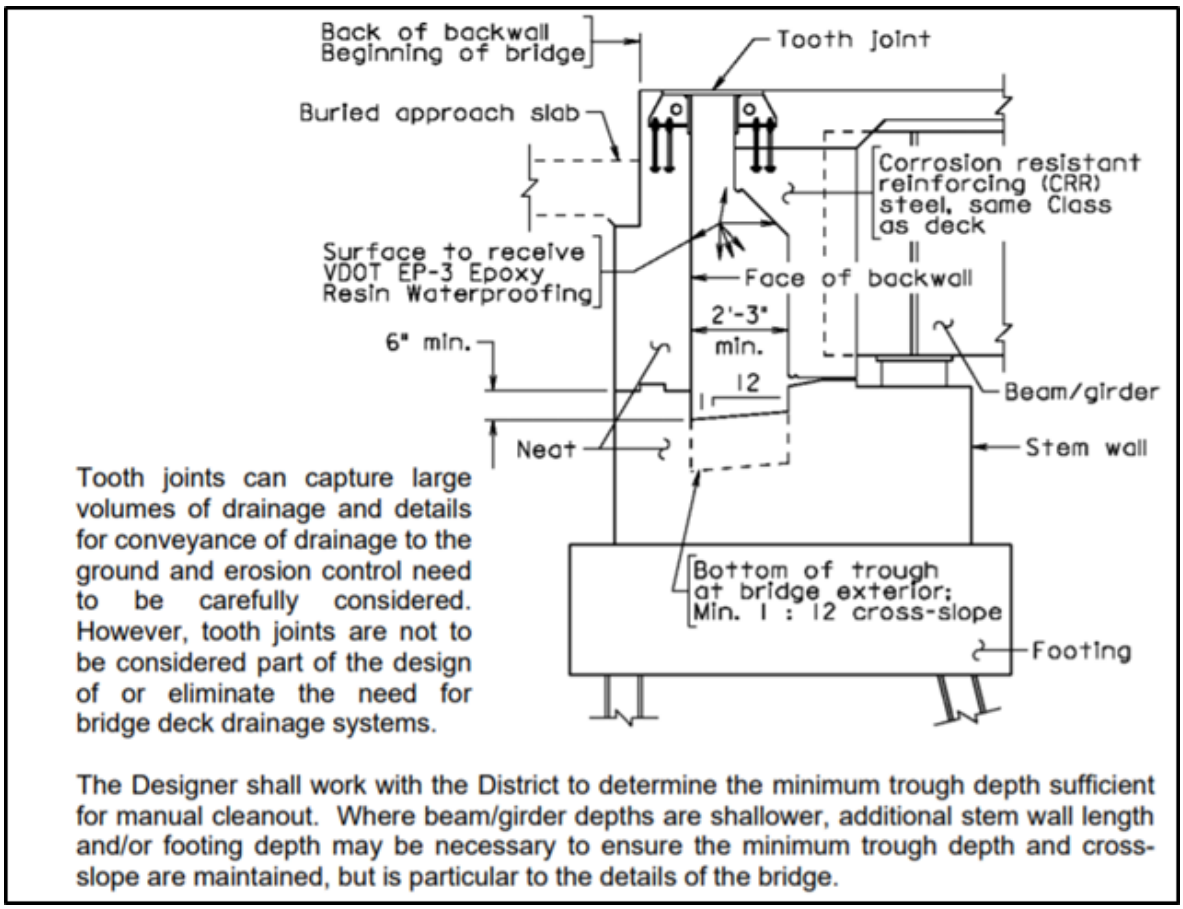

Figure 2.12. Example Detail of Virginia Abutment (VDOT Manual of the Structure and Bridge Division p.17.01-4)

Hoppe and Eichenthal (2012) conducted field monitoring of a highly skewed semi-integral bridge for the Virginia DOT. The 100’ foot one span bridge with 45-degree skew was monitored for 5 years. One abutment utilized a 15” layer of expanded polystyrene (EPS) as an elastic inclusion per VDOT policy (Figure 2.13). The inclusion was combined with a well-graded backfill separated by geotextile drainage fabric since VDOT had determined uniformly-graded backfill was causing approach slab settlement in previous studies. Piles were oriented for bending in the strong direction since it was noted that semi-integral abutments do not transfer lateral thermal loading to piles. Instead, this lateral load was resisted by a concrete buttress at the acute corner of the bridge since highly skewed bridges

tend to rotate with expansion. Approach slabs were not used in construction and after the monitoring period the approach areas had performed well. A finite element model created in SAP2000 determined that a new buttress location in the abutment near the acute corner of the bridge shown in Figure 2.14 may be more effective. The study also recommended that semi-integral bridge limitations be increased from 30 to 45 degrees, K_h values with and without elastic inclusions should be modified, and wingwalls should be designed for larger earth pressures than K_a to prevent the cracking that was observed. Hoppe et al. (2016) summarized the advancements in jointless bridge design implemented by the Virginia DOT. In addition to much of the work done in Hoppe and Eichenthal (2012), the authors explain the design priority of VDOT when choosing an abutment type. Full integral is the primary choice for new bridges, but if length and skew restrictions require it a semi-integral design is used. If limitations are still not satisfied then the bridge design becomes deck-extension, and finally the Virginia abutment. The Virginia abutment detail allows for jointless design in any scenario using a semi-integral abutment with an isolated backwall that does not apply any bridge movements to the backfill. A large recess exists between the two and is open on both sides to allow for drainage without the possibility of blockage due to its size. The four different jointless bridge types provide options for VDOT to utilize jointless design to lower lifecycle costs and adapt to unique and challenging conditions.

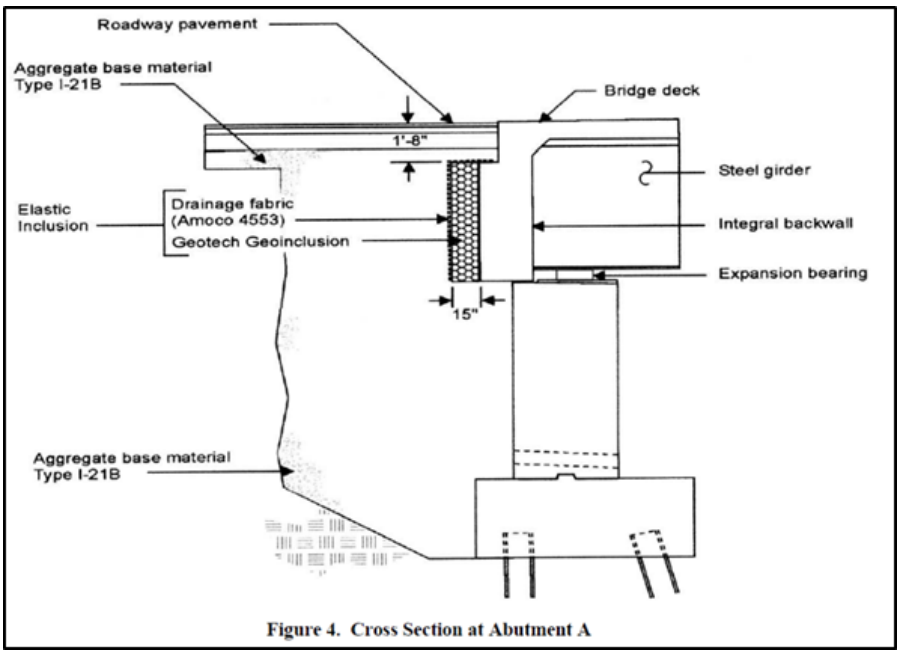

Figure 2.13. Cross Section at Abutment Showing Elastic Inclusion (Hoppe and Eichenthal 2012)

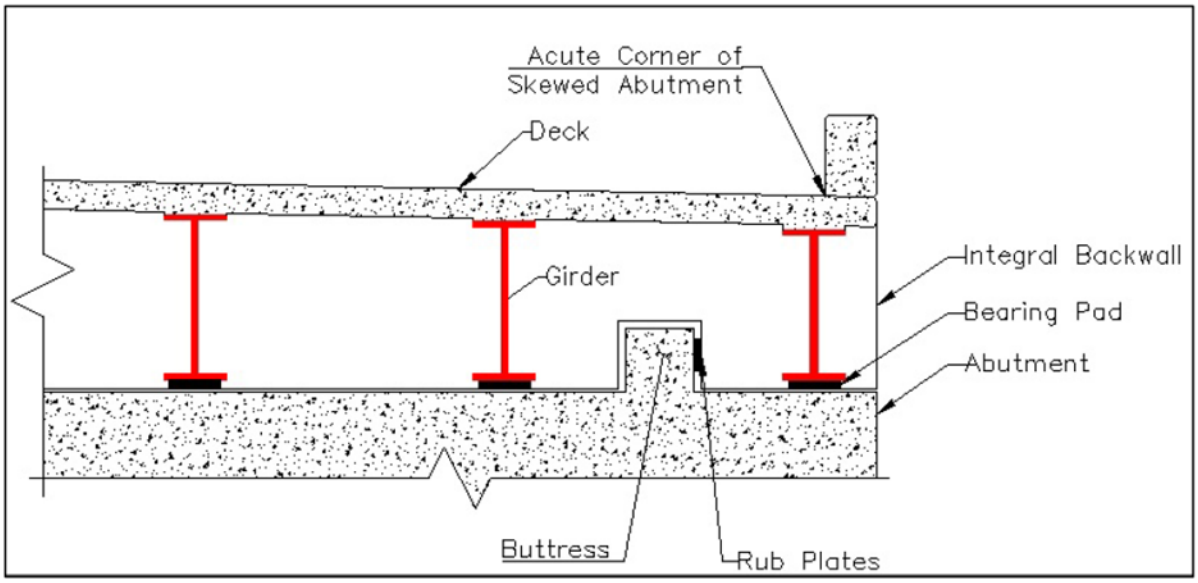

Figure 2.14. Proposed Buttress at Semi-Integral Bridges (Hoppe et al 2016)

Rub Plates (Figure 2.15) can be used with concrete end restraints to facilitate smooth movement and reduced friction. VDOT design uses two stainless steel rub plates cast into the concrete using shear studs. The plates are designed to resist horizontal forces due to thermal

induced passive earth pressures and must accommodate longitudinal movement. Aktan and Attanayake (2011) included the use of rub plates with their recommended abutment details for MDOT. Rub plates can be placed on the deck, abutment, or used in a concrete key system. The concrete key system was described as the most promising for deck-sliding-over-backwall abutments. Michigan DOT has not yet adopted the girder end restraint details. Concrete shear key and rub plate details from the study are still under discussion by MDOT per correspondence with Vladimir Zokvic, P.E. at MDOT on 9/11/2018.

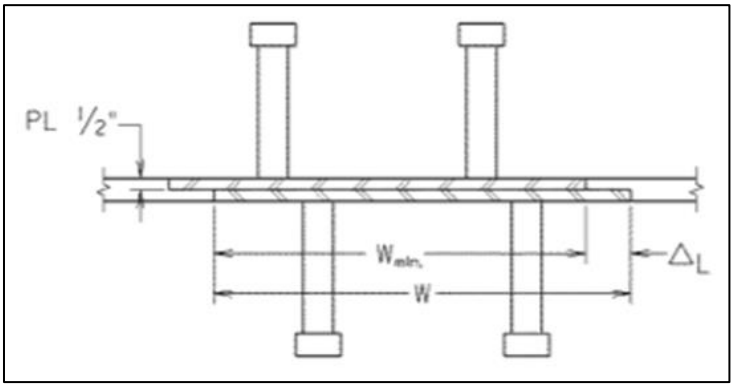

Figure 2.15. VDOT Rub Plate Example Design Calculations (VDOT Manual of the Structure and Bridge Division p.17.08-22)

High skew angles can complicate bridge behavior and have a negative effect on performance if a bridge is not properly detailed. Biana (2010) presented a unique design completed in the United Kingdom to overcome some difficult design restraints (Figure 2.16). The result was a composite semi-integral bridge with a high skew of 36 degrees. Longitudinally guided bearings control lateral movement of the bridge to keep it aligned. Behind the abutment a loose limestone layer was intended to accommodate longitudinal movement, sandwiched between the abutment and a solid concrete block layer which holds back compacted limestone backfill. After 21 months there were no signs of distress in the approach slab joint to the bridge deck.

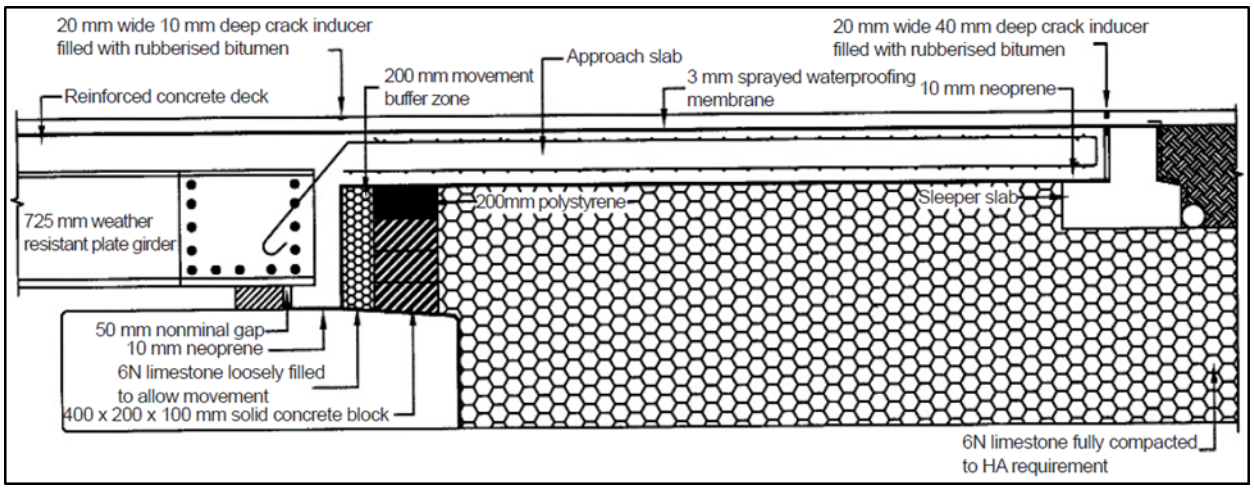

Figure 2.16. Abutment and Approach Slab Cross Section (Biana 2010)

2.3 Approach Slab Details

Approach slabs are intended to provide a smooth transition from the pavement road surface onto the bridge deck. If they are of sufficient length, a change in elevation at either end leads only to a small change in slope of the slab. Approach slabs that are designed thick enough and with enough reinforcement are able to span gaps or voids caused by erosion. Overall performance of an approach slab used on an integral or semi-integral bridge is affected by many factors and much research has been done to remedy the problems associated with them. Seo et al. (2002) completed a thorough investigation of the bump at the end of the bridge in Texas. The study included a survey of Texas DOT districts, finite element (FE) model of embankment soil under different conditions, monitoring of two bridges in Houston, and testing of a 1/20th scale bridge transition model all resulting in a proposed approach slab design to improve performance. The questionnaire highlights settlement of embankment fill followed by erosion as the top causes of the bump, though use of an approach slab minimizes the problem. The ABAQUS model used plane strain to simplify conditions and included many loading conditions using distributed and point loads.

The numerical analyses found that 80% of the maximum settlement occurs in the first 20 feet of soil near the abutment for a uniform load case. Final recommendations included using quality backfill and compacting to 95% of Modified Proctor, and an approach slab that is at least 20 feet long. Puppala et al. (2009) created a synthesis of practically all previous research and information on the performance of approach slabs. Causes of the "bump" include consolidation settlement, poor compaction of backfill, poor drainage and erosion, design detail specifics, skew, and seasonal temperature variations. In order to improve soil conditions, different methods can be used such as replacement of embankment soil, using surcharge loads, and dynamic compaction. Embankments can be reinforced using stone columns, compaction piles, driven piles, or more commonly used geosynthetic reinforcement. MSE walls, lightweight fill, flowable fill, are all viable options for improving the performance of backfill behind an abutment. Approach slab design is extremely important as longer approach slabs are less sensitive to settlement at the ends, but they should be designed to span between the abutment and the other end. Using a thicker slab is the most effective way to reduce tensile stresses that can cause cracking and proper compaction is necessary under sleeper slabs just as it is under the approach slab. After reviewing all previous research, the authors ranked all possible methods for preventing approach slab settlement in Table 2.3.

Table 2.3. Ranking Analysis of Mitigation Techniques for Bridge Approach Settlement (Puppala et al. 2009)

New or Maintenance Measure	Mitigation Method	Technique Feasibility (a)			Construction Requirements (b)			Cost Considerations (c)			Overall Performance (d)			Is this method recommended for present research?
		Ineffective	Effective but under research	Proven, well design method	Low	Medium	High	Low	Medium	High	Not proven	Ineffective	Effective	
Novel Methods for Foundation and Fill Improvement	MSE Walls/GRS		✓				✓			✓	✓			✗
	Geofoam		✓			✓			✓		✓			✓
	Lightweight Fill		✓			✓			✓		✓			✓
	Flowable Fill		✓		✓				✓		✓			✓
	DSM		✓		✓				✓				✓	✓
	CFA		✓			✓			✓		✓			✓
	Concrete Injection Columns		✓			✓				✓	✓			✗
	Geopiers		✓			✓			✓				✓	✓
Maintenance Measures	HMA Overlay			✓		✓		✓				✓		✗
	Mud/ Slab Jacking		✓		✓			✓					✓	✓
	Slab Replacement			✓		✓			✓			✓		✗
	Grouting			✓	✓				✓		✓			✗
	Urethane Injection		✓		✓					✓	✓			✓

a – Whether the method is in the research stage or the implementation stage; b – Difficulties in construction; i.e., the need of using heavy equipment; c – Costs vary from low to high based on material, equipment and mobilization costs

Luna et al. (2008) sought to improve practices in Missouri related to approach slabs since Missouri DOT was not satisfied with their performance based on a survey of DOT districts. Approach slabs were rated one of three designations with only 68% performing with no apparent issues, and 15% requiring corrective action. Two different bridges in two different areas of the state with differing soil conditions were examined and finite element models were created using PLAXIS. The models provide an upper and lower bound for approach settlement and allow for prediction of settlement based on conditions and construction staging. It was determined that the construction sequencing and staging had a large effect on overall performance and that construction of the approach slab should be delayed as long as possible to allow for settlement of the embankment before placement of the final grade. The sleeper slab drain should be placed below the bottom of the sleeper slab and 2 feet of crushed rock should be used below the sleeper and approach slab. The abutment should not include any notches or overhangs and the backwall should be straight in order to

facilitate good compaction. Finally, backfill should be compacted to 95% for the entire height of the approach embankment under the approach slab, sleeper, and pavement.

The connection between approach slab and abutment is extremely important due its location and the forces it experiences. A tied approach slab should move with the bridge during expansion and contraction, but the connection joint should not open to allow penetration by surfacewater. Greimann et al. (2008) tested multiple approach slab details by completing monitoring of two bridges in Iowa. The bridges were identical three-span prestressed concrete girder bridges with different approach slabs. One bridge utilized a precast concrete approach slab which was anchored to the abutment using vertical reinforcing bars. The other bridge used a cast-in-place approach slab attached to the abutment in the same manner. The bridges were outfitted with many sensors to measure temperature, strain, and displacement in different locations like girders, on piles, in slabs, and set up to measure displacement of the abutments. Abutments may displace horizontally and rotate but results showed that the abutment's rotation was negligible, and displacement depended entirely upon a horizontal movement of the entire abutment. After calculating the coefficient of thermal expansion, it's possible to find the theoretical expansion and contraction of the bridge. The theoretical and experimental data followed the same trends until winter where "strain ratcheting" may explain some deviations. Results showed there are forces present in the approach slabs at the expansion joints which must be accounted for in design. Approach slabs performed well initially, and overall bridge behavior seemed to follow short and long-term cycles as temperature changed over time. Unfortunately, later inspections revealed an opening of the joint as time progressed. The bridge construction differed only in the type and size of approach slab used and showed different behavior leading to the belief that the type

and/or size plays a role in the behavior of not only the approach slab itself, but the bridge superstructure. Nadermann et al. (2010) complemented the work of Greimann et al. (2008) by using a similar approach to study an approach slab to abutment connection in the state of Iowa. The approach detail used precast panels with a cast-in-place shoulder and inclined tie bars between abutment and approach (Figure 2.17). The shoulders were instrumented with strain gauges and crackmeters were placed at the joints. Similar trends in temperature were found as the slab acted as an insulator from daily extreme temperatures. Temperatures also followed shot-term and long-term cycles over the course of the monitoring period. Based on strains seen in the approach slab there is a force in the expansion joint. The coefficient of friction between approach slab and soil below reached much higher levels than in Greimann et al. (2008) and it is believed this is because low temperatures caused soil to freeze to the slab. The approach slabs functioned well over the monitoring period from October 2008 to January 2010.

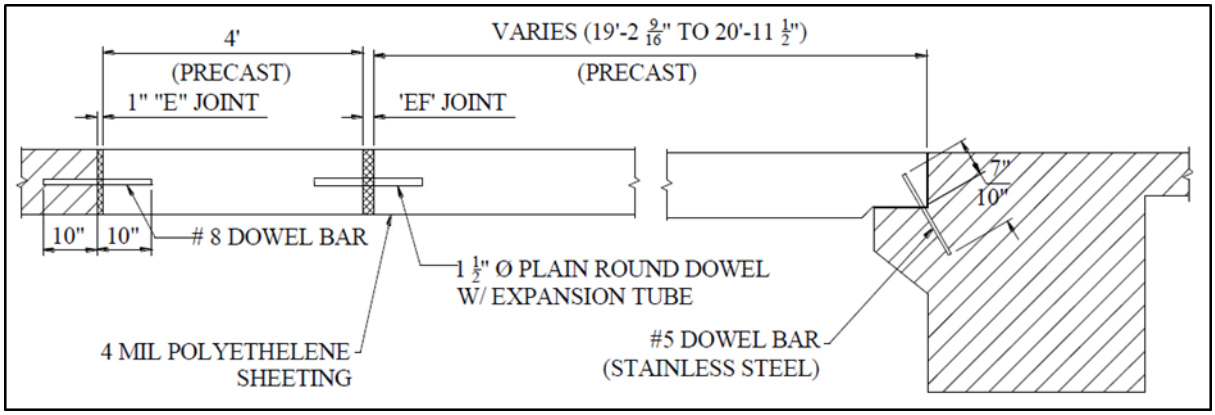

Figure 2.17. Elevation View of Precast Approach Slab (Nadermann et al. 2010)

Research is focused mainly on settlement of the approach slab and embankment, with little focus on the forces in tie bars or friction force under the approach slab. Often in finite element models the approach slab has been neglected due to negligible effects on the

movement of abutments and the bridge, which are the focus of the study. LaFave et al. (2016) found no impact on bridge behavior since forces were negligible in the superstructure due to approach slab friction under positive thermal loading. Their assumption from the parametric study was validated by monitoring results. According to Olson et al. (2009) the presence of an approach slab in their finite element model did not significantly affect stresses in the bridge deck. It is apparent that measures should still be taken to reduce friction since sliding can affect the backfill and slab itself. According to Aktan and Attanayake (2011) it is vital to reduce friction on approach slab surfaces, which can be accomplished by placing a 0.025" thick polyethylene sheet between backfill and the approach slab. Mistry (2005) and Thiagarajan et al. (2012) both recommended two layers of polyethylene sheets and Phares and Dahlberg (2015) recommended one. There were no other friction reduction methods found in the literature search. Hassiotis et al. (2006) recommended ensuring that the surface of sub-base course follows and is parallel to the roadway grade and cross slope. A filter fabric "or some type of bond-breaker" such as polyethylene sheets is also recommended for placement between the sub-base course and approach slab.

Oliva and Rajek (2011) used a parametric study to determine the effects of different design parameters on the rotation and strain of approach slabs. The goal was to determine the typical rotation that occurs so that it could be accounted for by engineers in designing approach slab connections at both ends. A finite element model was created using ABAQUS software (Figure 2.18) that represented a typical integral abutment bridge. The model included a "settlement trench" which was represented by a lack of backfill under a triangular portion of the approach slab and at the abutment face. This trench accounted for the fact that due to settlement or erosion there is often a lack of support under the approach slab as the

bridge ages. Results of the parametric study were categorized and judged on the flexural strain seen in the approach slab and the amount of rotation of the approach slab at the abutment. The settlement trench only had a significant impact when the length reached 6' of more while approach slab length had little effect on strain or rotation. Varying soil parameters were also investigated and it was found that the loose soil condition introduced cracking of the approach slab under truck loading, the only condition to do so. The cracking was eliminated with the use of an 8 ksi strength concrete suggesting that a precast approach slab could remedy the effects of poor soil conditions. Overall, rotations for all cases and parameters, except the loss soil condition, generally remained under 0.002 radians which means this is a magnitude that should be accounted for in design. As part of their parametric study, the authors also included approach slab length as a variable. After using three different lengths, they determined using approach slab strains (Table 2.4 and Table 2.5) that length only had a small effect on the behavior of the slab. All three cases used the same geometry as the base model and assumed moderately stiff soil. None of the lengths experienced cracking.

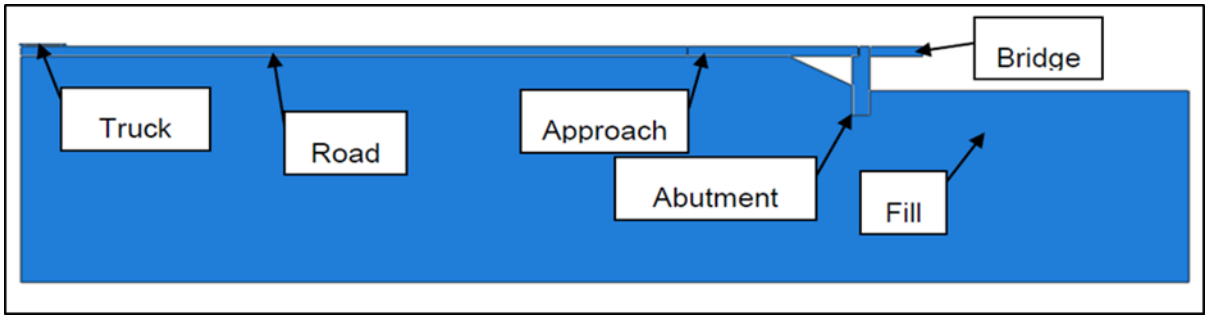

Figure 2.18. Components Considered in Numerical Model Showing Settlement Trench (Oliva and Rajek 2011)

Table 2.4. Maximum Principle (Tensile) Strains with Location (Oliva and Rajek 2011)

Case	Strain	Location
20'	8.21E-05	15'-6"
15'-8"	8.23E-05	11'-2 1/4"
10'	7.67E-05	6'-0"

Table 2.5. Minimum Principle (Compressive) Strains with Location (Oliva and Rajek 2011)

Case	Strain	Location
20'	-9.15E-05	16'-0 3/4"
15'-8"	-9.04E-05	11'-9"
10'	-8.47E-05	6'-6 1/2"

Nassif et al. (2009) compared the performance of the existing New Jersey standard approach details with two different prototype standards by field monitoring and finite element modeling. The two designs considered were embedded-beam (EB) shown in Figure 2.19 and continuous thickness (CT). The CT design offers an increased thickness over the traditional, and the EB design places effective beams inside the slab every 1.8 meters in both directions to create plates that support only one wheel load of a HS-20 truck at a time. ABAQUS was used to create a 2-D FE model using shell and spring elements along with a full 3-D model of solid elements to model soil behavior. Both designs provided a minimum 2.8 times the cracking capacity of the existing New Jersey design, and the EB design entraps cracks within “plates” surrounded by effective beams. The EB design was recommended for adoption by NJDOT for future approach slabs.

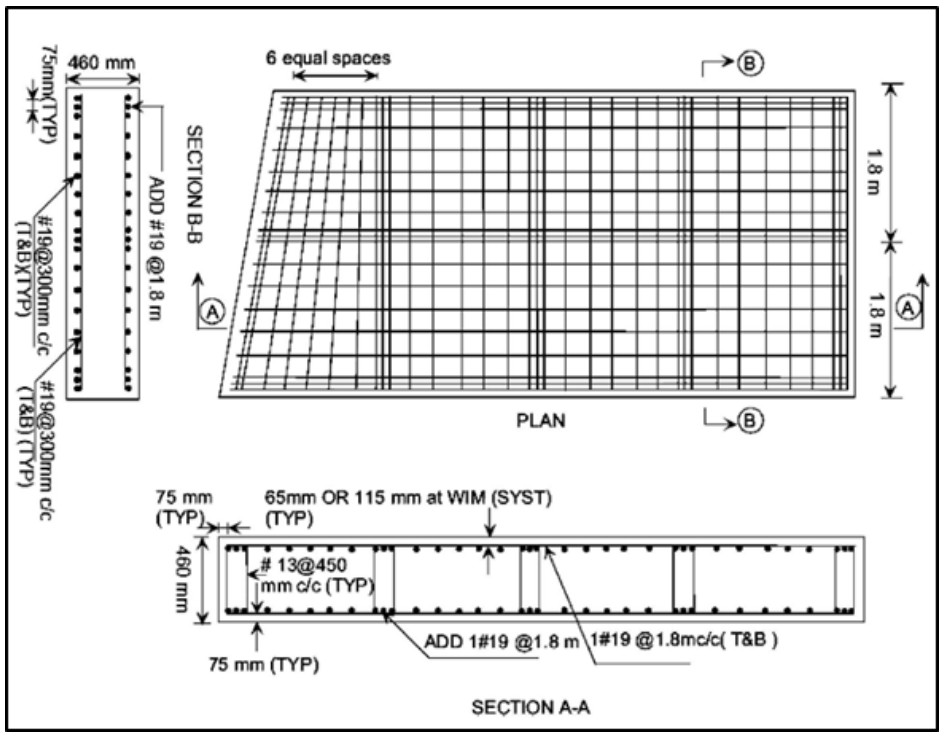

Figure 2.19. Reinforcement Details of an Embedded Beam (EB) Approach Slab (Nassif et al. 2009)

Yasrobi et al. (2016) surveyed 28 states about the issue of approach slab settlement. Settlement was found to be a common problem across the country (Figure 2.20) and states were organized into categories based on what percentage of bridges experienced settlement. The responses to many other questions could then be compared with the performance groups to determine if certain practices were required in better performing states. If responses did not correlate with the performance groups, then it could be seen that the parameter most likely has little or no effect on approach slab settlement. The survey asked the states what the cause of settlement is, to which the most popular answer was poor construction, followed by high embankment fill. Based on an examination of each question, the authors were able to create a list of recommendations for design and construction that should have a tangible effect on approach slab settlement. Approach slabs should be 12-16 inches thick and less

than 30 feet long to maintain proper structural stiffness and rigidity to avoid large deflection under load due to a loss of support, and a reinforced foundation should be used under a sleeper slab if one is included. Well-graded pervious backfill should be used in lieu of poorly-graded and should be compacted to 95% of the standard Proctor density. It was recommended to use geotextile reinforcement under the approach slab, and construction requirements should be revised or developed for the construction sequence, construction method, compaction method, and compaction control.

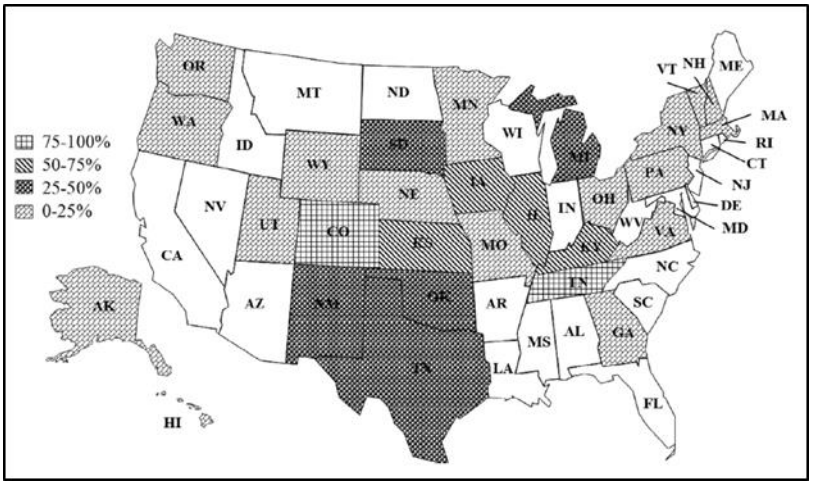

Figure 2.20. Percentages of Bridges with Approach Slab Settlement in Reporting States (Yasrobi et al. 2016)

Chen and Abu-Farsakh (2016) experimented with a new approach slab design to replace Louisiana's current standard at the time due to problems with the bump at the end of the bridge. The plan was to create a stiffer slab by thickening and use of a higher reinforcement ratio, and to reinforce the soil under the sleeper slab using two geogrid layers. The approach slab was intended to span the gap between the bridge abutment and sleeper slab when backfill support was inevitably lost. Both the new (Figure 2.21) and old designs were implemented on the same bridge, one at each end, so that they could be directly compared. The new design located on the West side used a slab thickness of 16" and length

of 40’ supported by a 3’ 11” sleeper slab. The new design outperformed the old after 1.5 years both visually and according to monitoring data. The roughness profile showed a smoother surface with less bump and there was less cracking at the approach to pavement joint. Sensors showed earth pressures decreased over time as load was spread out to the slab ends as intended on the new design, while earth pressures increased under the old design possibly due to lower slab rigidity. The geogrid reinforcement under the sleeper slab performed well and strains were measured to be under the typical manufacturer design value.

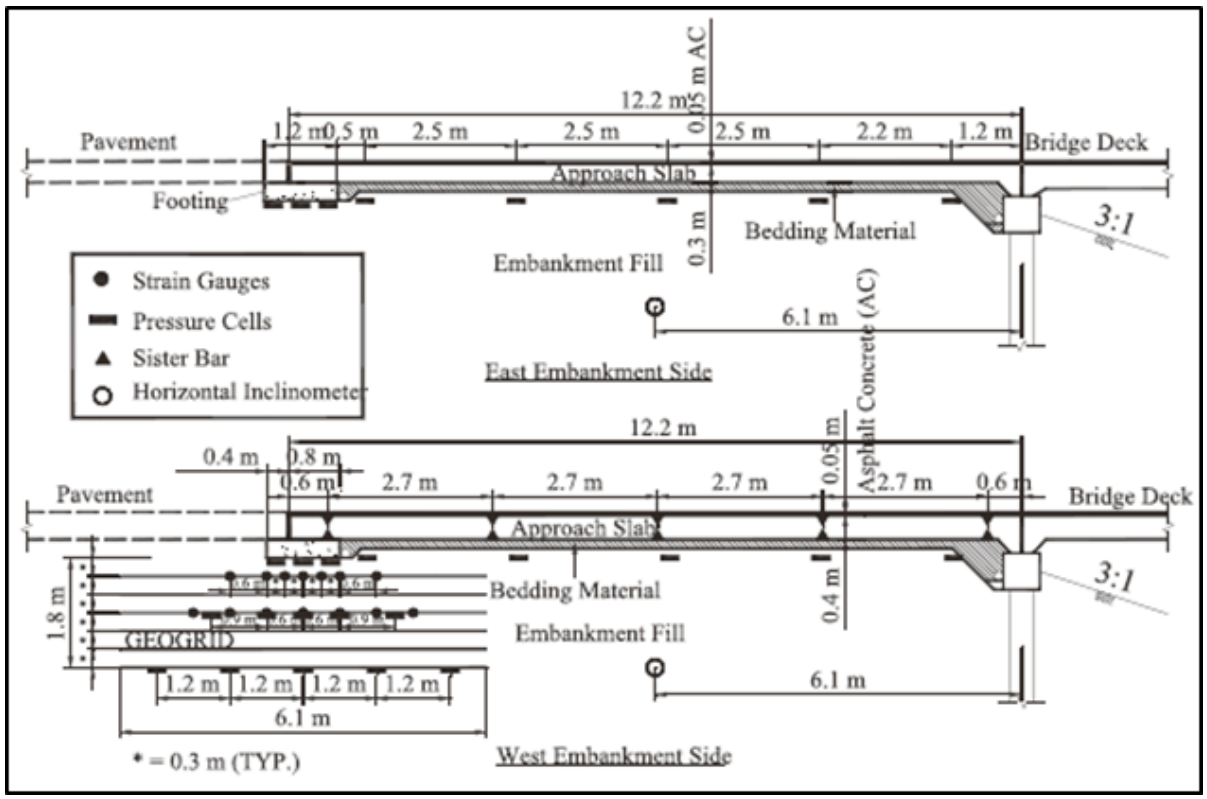

Figure 2.21. Standard and New Approach Slab Design Systems (Chen and Abu-Farsakh 2016)

2.4 Geotechnical Design

Dupont and Allen (2002) outlined the causes of differential settlement of bridge approaches as the following: compression of embankment fill, settlement of foundation soil beneath the embankment, poor design or construction practices, and poor drainage practices. A look at current practice began with a survey of all 50 states in which it was found only 21 states used special procedures when backfilling around integral abutments and end bents. The authors noted that some states appeared to view the approach slab as the overall solution to bridge approach problems, instead of design feature in need of additional improvement. Many conclusions were reached in order to alleviate future approach problems including approach settlement periods/using surcharge loading, lowered approach slabs with asphalt overlays, and designing maintenance plans simultaneously with construction plans. Other more viable or effective methods include improving drainage on/ around approaches, reducing embankment side slopes, and longer/stronger approach slabs. Robison and Luna (2004) accurately modeled the deformation and settlement of bridge approach embankments in Missouri using PLAXIS software. By accurately modeling the staged construction process the structurally important deflection, which occurs after the completion of the approach slab, can be determined and minimized on future projects. Other recommendations for MoDOT include enhanced soil exploration for high embankments (10 to 20 feet), the use of geosynthetics, and the use of select drainage material underneath the entire slab and sleeper beam. Some additional recommendations for better geotechnical performance of the embankment are provided by Luna et al. (2008). A recommendation was made to include exploratory boreholes 30-50 feet away from the abutment in the location of the approach embankment. Embankment slopes should be limited to 2.5H:1V to increase stability, and geosynthetic reinforcing should be considered for embankments higher than 10 feet.

Horvath (2005) examined the geotechnical issues that accompany integral-abutment bridges (IAB). The author states that the problems with IABs are geotechnical in nature, so it would follow that solutions should be geotechnical as well. Many solutions do not address the discontinuity between the moving structure and stationary soil. As the structure contracts in winter, a soil wedge moves inward and downward into the opening gap behind the abutment. This creates a long-term problem in addition to the passive pressure on the abutment during the summer. The "ratcheting" increases the passive pressure seen by the backwall over time. The movement of soil means that a loss of support will occur under the approach slab no matter what kind of soil is used or how well it is compacted. Compressible inclusions were found to be unable to hold back the active pressure of the slumping soil since they were elastic enough to accommodate the expansion of the bridge in the first place. Two different details were proposed in Figure 2.22, with the first more promising and cost-effective than the second. The first uses a compressible inclusion in combination with a mechanically stabilized earth (MSE) embankment which gives the soil enough strength to avoid falling into the void. The inclusion acts as a joint, while also insulating the soil against temperature changes, and possibly aiding in drainage. Passive pressures are reduced to increase cost savings in design. The second detail is intended for soft soil under the approach embankment and utilizes a wedge of expanded polystyrene (EPS) with a compressible layer. In conclusion, any successful solution must support the soil on a year-round basis and be able to function as an expansion joint between the abutment and soil.

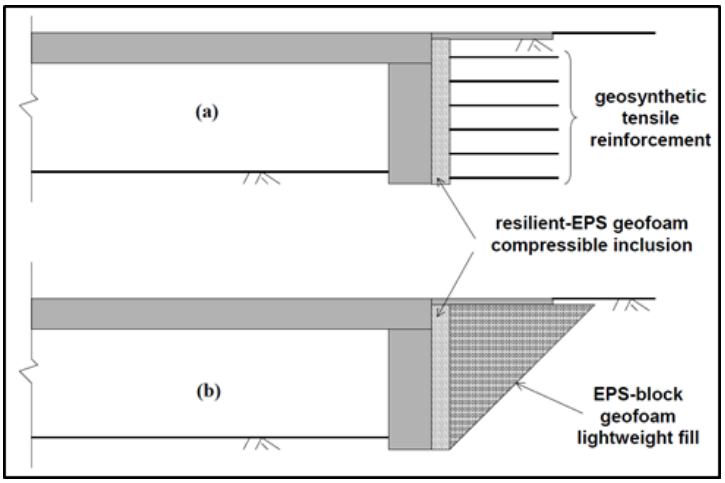

Figure 2.22. Proposed New IAB Design Alternatives (Horvath 2005)

Backfill is extremely important since it interacts with both the abutment and the approach slab placed on top of it. Abu-Hejleh et al. (2008) evaluated the Colorado DOT bridge approach design methods to determine their effectiveness and to provide additional recommendations moving forward. The practice at the time included three different methods for backfill: flowfill concrete, MSE Class 1 backfill, and MSE Class B free-draining backfill. Five different bridges were inspected and forensic investigation was done to determine the source of bridge bump problems. Performance of approaches using these methods improved over the previous methods but some settlement issues persisted. Flowfill was still recommended for unique scenarios where compaction is extremely difficult, but MSE Class B fill had the lowest unit cost over design life since there was no necessary repair reported. Final recommendations include the compaction of fill done wet of optimum and the use of surcharge preloading if possible. In order to better support the sleeper slab, two different methods were proposed in Figure 2.23. One included more MSE fill under the sleeper than the standard 4’ at the time of the study. The other detail used piles for supporting the sleeper slab. The sleeper slab and expansion joint above it may be installed up to 1 inch higher in

elevation than the design in order to account for post construction settlement if approved by the hydraulic, structural, and roadway engineers.

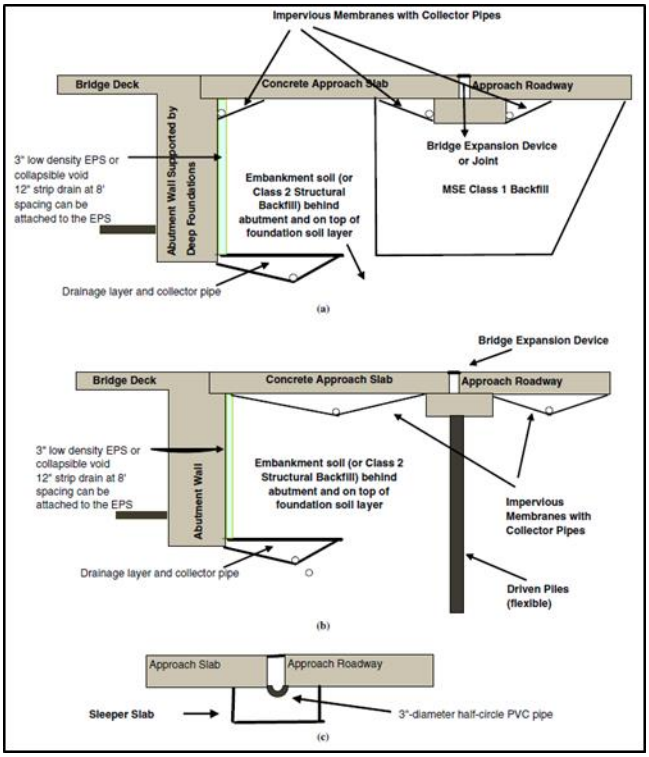

Figure 2.23. Recommended Supporting Systems and Drainage Details for Sleeper Slab: (a) Placement of MSE Wall under Sleeper Slab, (b) Use of Class 2 Backfill and Driven Piles to Support Sleeper Slab, and (c) Placement of Gutter and Half-Circle PVC Pipe to Drain Water (Abu-Hejleh et al. 2008)

Nebraska DOT has a rather unique practice that includes the use of helical piles at the end of an approach slab per correspondence with Mark Traynowicz of Nebraska DOT on 9/13/2018. Grade beams are used similarly to an approach slab and are almost always supported on piling. Nebraska allows HP, pipe, or concrete piles, but in the case of an approach slab replacement helical piles may be used as an alternate if they are the only piling required for the project.

2.5 Bridge End Drainage

Drainage is vital to bridge end design because of the effects poor drainage can have on the service life of a structure over time. An inspection of 74 Iowa bridges led to an investigation of approach slab performance by White et al. (2007). Void development due to backfill collapse, severe backfill erosion, poor surface and subsurface water management, and poor construction practices were identified as critical problems seen at some poorly performing bridge approaches. Elevation profiles of 38 bridge approaches were measured and the majority were found to require maintenance or repair based on a 1/200 slope criterion. Four different backfill samples were tested in a laboratory and bulking moisture contents ranged between 2-10%. Since field moisture contents were measured between 4-5%, the soils had a significant collapse potential which would result in voids beneath the approach slab. Compacting poorly graded granular backfill at a moisture content outside the bulking moisture content would reduce the potential for collapse. In order to minimize erosion, a gradation with less than 60% passing the No. 8 sieve should be used. A full height square abutment with paving notch is easier to construct and would facilitate better compaction around the abutment. Mekkawy et al. (2005) utilized the same bridge approach inspection results as White et al. (2007) to develop the Bridge Approach Drainage Model (BADM). The BADM is a ¼ scale model of an abutment backwall, backfill, and approach slab used to test different drainage techniques. The BADM was created to evaluate designs on the basis of surface/subsurface drainage and erosion on embankment and backfill materials, which are the two major causes of approach settlement in Iowa. Steady state flow from the expansion joint to drain pipe was achieved for each of the 13 models and allowed to run for 4 hours. Flow and settlement were measured, and the models were inspected for void formation and erosion. The poorest performing model of the group was the one which

simulated practices occurring in the field. Three details performed much better than the rest: a geocomposite drain with backfill reinforcement and moisture content above bulking, tire chips behind the bridge abutment, and porous backfill material for the entire depth behind the abutment.

All performance issues of jointless bridges like approach slab performance, embankment settlement, erosion, and abutment backwall earth pressures are all related due to the thermal movement of the bridge itself. Drainage design can have a huge impact on geotechnical aspects of the project. Miller et al. (2013) investigated the settlement of approach slabs in Oklahoma in order to provide recommendations to minimize settlement of future construction. After completing a literature review to determine the causes of settlement, a survey was sent to Oklahoma DOT Field Divisions to identify sites for inspection of bridge approach slabs. Thirty different bridges were inspected visually with fifteen showing representative examples of erosion and drainage concerns. Common issues include large voids appearing under approach slabs and abutments, and surface drainage was categorized as universally poor with separated joints or cracks allowing water infiltration. Staining on abutment walls indicated that soil loss was occurring through cracks in the abutment in some locations. Two bridges performed very well due to design changes in the drainage detailing. Shields Boulevard over I-35 included a neoprene sheet at the base of the abutment to block the hydraulic short circuit and prevent drainage from escaping under the abutment. Another example of poor detailing is that even when performing well drain outlets were allowing expelled water to flow back into embankments because of the outlet location. One recommendation was made to outlet drains near the bottom of slope walls into erosion resistant drainage ways and all drainage systems must be checked and maintained regularly.

Geomembranes can eliminate unwanted drainage paths and prevent short circuits under the abutment as shown in Figure 2.24. Construction of embankments should involve a complete settlement analysis which will illustrate the importance of the soil properties and identify issues with wetting-induced compression. Compaction should be made more accurate through the use of a relative density-based specification instead of a standard Proctor based specification.

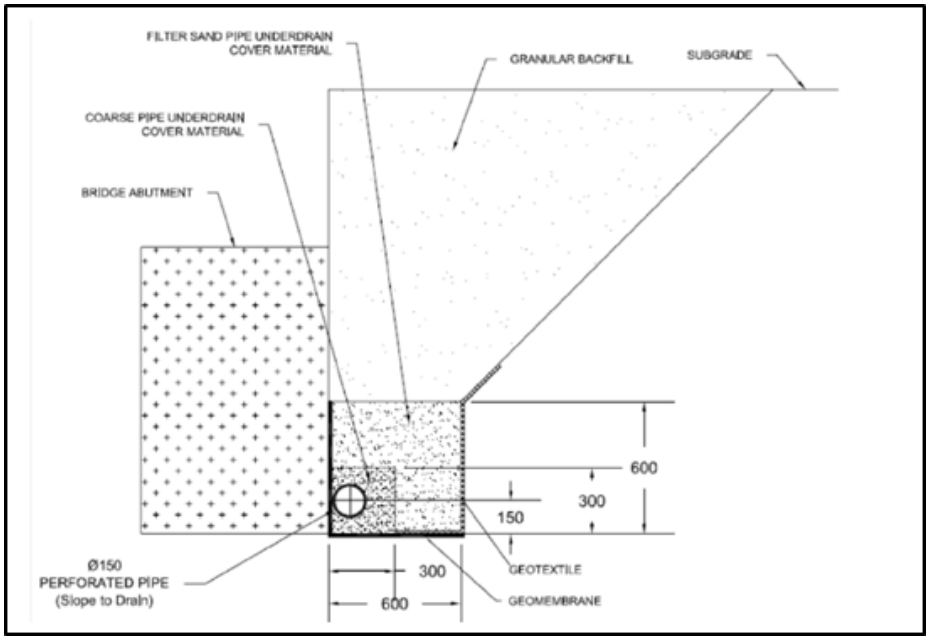

Figure 2.24. Proposed Abutment Backfill Drainage System with Geomembrane and Graded Granular Filter (units in mm) (Miller et al. 2013)

The practice of placing the concrete barrier rail on top of the approach slab is recommended for drainage purposes (Briaud et al. 1997). The detail shown in in Figure 2.25 has been referenced many times in various studies and shows the problem with placing the barrier on the wingwall. The joint between the approach slab and wingwall allows for water infiltration potentially leading to settlement or erosion of the embankment. There is no mention of possible consequences in terms of other aspects of approach slab performance.

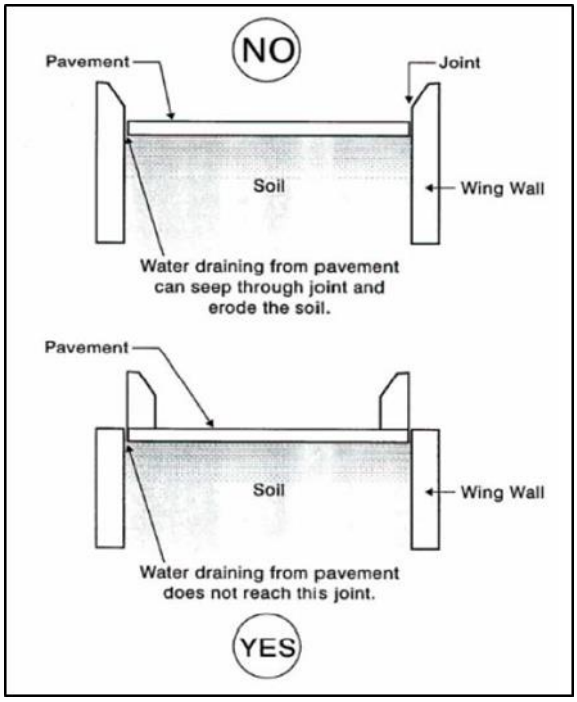

Figure 2.25. Cross Section of a Wingwall and Drainage System (Briaud et al. 1997)

Phares and Dahlberg (2015) evaluated the approach slab design used by the Wisconsin DOT after WISDOT made a change from using three expansion joints to using a single expansion joint due to difficulty in constructing the multiple joints. Twelve bridges were inspected, and a single soil sample was taken for laboratory analysis. Testing showed that increasing moisture content reduces the likelihood of collapse, an issue covered by White et al. (2007). The authors many general recommendations including the continued use of polyethylene sheeting under the approach slab and sleeper slabs. In order to maintain proper drainage several details are also recommended including full-width approach slabs, tiled drainage near the approach slab to pavement joint, surface drainage channels on embankments, drainage tiles in the embankments, drainage which can intercept water on the bridge deck before reaching the abutment to approach slab joint, and providing a drainage path for water that does infiltrate joints. Proper drain maintenance is key and should be

completed on a regular schedule. According to Puppala et al. (2009), proper drainage is extremely important to prevent water infiltration into the approach slab embankment resulting in erosion and a loss of support, so it is recommended to intercept deck surface water from the bridge before it crosses the joint to the approach slab, as previously noted by Phares and Dahlberg (2015) and Abu-Hejleh et al. (2008). Impervious membranes with collector pipes can be used to collect water that penetrates cracks and joints. Membranes can be limited to locations under joints to lower cost. A half circle PVC pipe under a joint can carry water to the sides of the approach and prevent infiltration.

Lenke (2006) conducted a thorough field evaluation of 19 bridges in New Mexico in conjunction with the New Mexico Department of Transportation. All 19 bridges were noted as having problems with approach. MSE walls showed fewer problems than other abutment systems due to better compaction and high-quality fill for improved drainage. NMDOT increased the use of wingwalls to reduce erosion and provide extra stability for backfill. The approach should be tied to barrier walls and wingwalls in order to prevent water intrusion into fill below the approach. It was recommended that corbels should not be used to support the approach slab because they make proper compaction difficult near the abutment.

2.6 Expansion Joints

Due to the unsatisfactory performance of the Minnesota DOT standard "E8" expansion joint, Reza (2013) investigated the standard practices of other states in terms of approach slab joint materials and details. The E8 joint was used between the approach slab and pavement and consists of a 4-inch-wide gap filled with a high density foam product (Evazote) attached to the inside walls of the joint by adhesive. The joint has often failed in winter as the bridge contracts and the joint opens due to breakage of the thin asphalt seal or failure of the adhesive. Joints at three different bridges were monitored using crackmeters to

determine the correct multiplier coefficient of 1.5 for calculating joint size. The multiplier is multiplied by the change in temperature, length, and coefficient of thermal expansion to compare with manufacturer ratings for joint types and sizes. The review of other states practice showed that strip seals should be considered for the expansion joint for new integral and semi-integral abutment bridges since it is the most popular choice and based on information on previous performance. However; using strip seals would require a new detail for where the joint meets the curb and increase costs slightly due to the need to extend the concrete barrier longer than was currently done. As a result of the studies by LaFave et al. (2016) and LaFave et al. (2017), it was recommended that IDOT consider alternative expansion joint details to their current strip seal, since longer bridges over 700 feet could result in a movement larger than the strip seal limit of 2 inches. According to Idaho DOT (2008) the joint between approach slab and sleeper slab should be designed only large enough that the joint does not completely close in maximum summer heat.

It appears that expansion joint issues are inevitable and unavoidable, thus the push for jointless bridge design. Miller et al. (2013) noted that "pavement surface joint seals were largely compromised and so the subsurface drainage must be designed with the expectation that water will enter the joints, potentially with enough erosive power to undermine approach slabs." There is little information available recommending any certain expansion device at the approach slab to sleeper slab joint, most studies simply state what joints are used and what problems are associated with them. In a set of design guidelines as part of the bridge design manual IdahoDOT (2008) says "The joint width at the end of the approach slab where it rests on the sleeper beam should only be large enough to prevent the joint from completely closing during hot weather, with an allowance for the minimum compressed width of the

joint seal material. It is not necessary to design the joint for the full movement range that would be required in a typical joint design."

The review of state DOTs surrounding Minnesota by Reza (2013) included what kind of expansion device was used at the approach slab to sleeper slab joint. South Dakota and Michigan used strip seals. Ohio was using an asphalt pressure relief joint. Problems led to a study with Iowa State by Phares et al (2011) in an attempt to remedy many problems with ride quality. Kansas utilized an approach slab overlapping 2 feet on an 8-foot sleeper slab with 6 feet of asphalt over the top. On the other side is another concrete slab overlapping 2 feet on the same sleeper slab that spans to another sleeper slab. Polytite waterproofing membrane was applied on all concrete surfaces in contact with asphalt. Ontario chose their expansion device based on the expected movement at the joint. Less than one inch resulted in use of an asphalt impregnated fiber board sealed by rubber asphalt. A sleeper slab with a closed cell neoprene seal was used for movement between 1 and 2 inches. Movements greater than 2 inches called for a strip seal.

CHAPTER 3. BRIDGE END SERVICE LIFE SURVEY

3.1 Survey Overview

A survey can prove especially helpful when collecting information on DOT practices. No two DOTs are identical, and all have different details, standards, and design processes. Although a large amount of information is available online in bridge design manuals and standard details, there is some information that is not posted for public access. A survey sent to individuals at each state DOT can provide inside information on design methodology and preference. Feedback on performance of certain bridge aspects is another high value result of a survey.

3.2 Survey Objective

Formulation of the survey began with the results of the literature review in Chapter 2. Any relevant questions to the topic were placed in a list to form categories matching those found in the chapter, including abutments, approach slabs, geotechnical issues, drainage, and expansion devices. The target amount of time to complete the survey was set at fifteen (15) minutes with questions requiring one to two minutes at most. Any longer and the likelihood that the survey is completed decreases, since the DOT employees participating are not being compensated in any way and likely have limited time. A first draft of the survey was presented at a Technical Advisory Committee meeting and recommendations were made to shorten the length from 20 questions and to review previous American Association of State Highway and Transportation Officials (AASHTO) surveys for overlap. AASHTO survey results were found online and North Central States (NCS) survey results were obtained from Iowa DOT. Multiple questions were eliminated to obtain a final length of 11 questions. The next step was to create the online format allowing for ease of use by the committee to allow

for a review before distribution to state DOTs. The survey was created using Qualtrics, which allows for a multitude of question formats including text entry, multiple choice, and file upload. The full list of questions included in the survey is available in Appendix A.

Since the survey was not distributed for responses there are no conclusions to be drawn from the data. However, it is expected that valuable insight will be gained in the practice of other state DOTs once results are available, especially regarding drainage and joint preferences. Of particular interest are the preferred joint type between approach slab and sleeper slab, drain maintenance, and the popularity of placing the concrete barrier rail on top of approach slabs. These aspects are not structural and cannot be evaluated using field monitoring with sensors or finite element modeling.

CHAPTER 4. BRIDGE VISUAL INSPECTIONS

Inspection of both semi-integral abutment bridges and bridges with tied approach slabs was used to examine details in practice to see possible deficiencies in real-world use. Seven bridges were chosen for inspection, with two locations having identical structures for a split roadway resulting in a total of nine structures inspected on September 21st and 24th of 2019. Bridges were chosen based on many factors including length, width, skew, abutment type, use of a tied approach, and availability for inspection. Since inspections were done without the use of extensive traffic control and did not close traffic lanes, certain bridges like those on highway I35 at the I80 interchange were eliminated from consideration. Otherwise, bridges with the most extreme lengths were chosen. The following bridges were inspected:

- 1215 Polk
- 310 Jasper (North and Southbound)
- 208 Bremer (North and Southbound)
- 108 Blackhawk
- 213 Cass
- 111 Pottawattamie
- 113 Cass

The plan for each bridge was to examine the entire bridge end including sleeper slabs (if present), approach slabs, deck joints, embankments, abutment faces, and bearings if possible. The focus included observing any signs of poor performance including cracking in any visible concrete surfaces, settlement of any structural members, erosion or voids in soil, expansion joint damage, and impediments to drainage. Approach slab section views are shown in Appendix B for each bridge except 113 Cass.

4.1 1215 Polk

1215 Polk is a 330-foot-long semi-integral bridge located in Urbandale, Iowa on 100th street at I-35/80. It has two identical spans and unique approach slabs at both ends due

to its proximity to stoplight intersections. The bridge is 101 feet wide and accommodates sidewalks along its length. The inspection began at the north end at the approach slab to sleeper slab CF-3 joint. Joint filler appeared to be missing along part of the length with debris filling the space. The north approach slab appeared in good condition with no visible settlement; however, a large amount of joint sealant was missing in the approach to abutment E joint. The embankment appeared intact with no serious erosion aside from areas with no plant cover a distance away from the bridge due to construction for an added interchange. The south approach slab to sleeper slab joint also had joint sealant missing and some expanding onto the roadway surface. The approach slab was in good condition along with the south abutment to approach joint except for excess sealant expanding out of the joint (Figure 4.1a). This sealant has the possibility of being caught by a snowplow or other vehicle and tearing out of the joint. The south embankment appeared OK minus a large void at the Southwest corner of the bridge at the end of the wingwall. The void measured 22” deep and was estimated to be about 2’ square in size. The embankment was not landscaped due to the interchange project and earthwork under construction, so it was unclear if that was a reason for area not filled with soil, or if it was created by erosion. Both the North and South abutments had a large amount of rust-colored staining present below the bearings (Figure 4.2). At the corners some water was still visible on the concrete surface (Figure 4.1b). The source of the water was not readily apparent, but it was assumed it came through the abutment. Another possible source for the abutment staining could be that it happened during bridge construction if beams were placed and rain occurred before the bridge deck was placed to cover the beams. In that case, the water present at the corners could have been left from a rain even before the time of inspection.

Figure 4.1. (a) South Bridge Deck to Approach Slab Joint with Excess Sealant (left), (b) Water and Abutment Staining at the Outermost Girder (right)

Figure 4.2. North Abutment Face

4.2 111 Pottawattamie

111 Pottawattamie is located in Pottawattamie County, Iowa on US-6 over Keg Creek. The 204.5’ long and 44’ wide bridge with 0° skew has semi-integral abutments. A CF2 joint lies between the 20’ precast approach slab and abutment, with a precast sleeper

slab supporting the other end of the approach. Beginning at the sleeper slab, joints were in OK condition. The approach slabs and entire bridge deck were covered in a polymer overlay consistent with available plans. The West approach slab was badly cracked across its entire width (Figure 4.3a). Joints at the abutment on both ends of the bridge were in poor condition with large amounts of sealant missing and debris filling the voids (Figure 4.3b). A 6” deep void was discovered at the abutment to approach joint where it met the barrier in the Southwest corner (Figure 4.4). Bridge surfacewater likely drains through the gap in the barrier instead of following the curb. Abutment faces did not have any staining, indicating there does not appear to be any water leaking through the abutment. Embankment condition was good with no obvious erosion except near the bridge piers.

Figure 4.3. (a) Transverse Approach Slab Crack (left), (b) Bridge Deck to Approach Slab Joint (right)

Figure 4.4. Void at the Intersection of Deck to Approach Joint and Barrier

4.3 113 Cass

113 Cass is located West of Massena, IA on IA-92 over a small creek. The semi-integral bridge was constructed in 2013 and is 120’ long and 44’ wide with a skew of 0°. Pavement approaching the bridge from either direction and along the shoulder of concrete panels was in poor condition and showed obvious settlement compared to the concrete. Joints at the end of the first approach slab section were in good condition since there is no movement accommodated at that location. The East approach slab had a transverse crack near its eastern end. Abutment to approach slab joints were in OK or poor condition with sealant missing and debris filling some of the joints. The curb joints between approach slab and wingwall were in extremely poor condition with sealant missing and large voids visible and each of the four corners of the bridge (Figure 4.5a). The North wingwall at the East end of the bridge appeared to be moving away from the approach slab based on the gap present at the joint and misalignment of the barriers (Figure 4.5b). The curb detail showing the “E”

joint can be seen in Figure 4.6. Embankments were in good condition and there was no staining on the abutment face. Bearings appeared to be working as intended.

Figure 4.5. (a) Approach Slab to Wingwall Joint Showing Separation (left), (b) Misaligned Wingwall and Barrier (right)

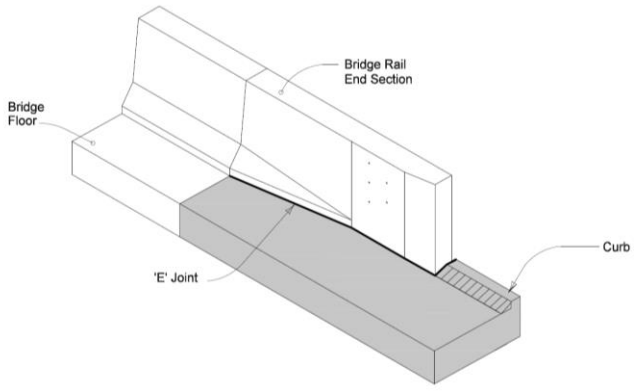

Figure 4.6. Iowa DOT Curb E Joint Detail (Iowa DOT).

4.4 213 Cass

213 Cass is in Cass County, Iowa on M56 over I-80. The bridge is 223.75’ long and 30’ wide with a skew of 7.75°. Past rehabilitation work included conversion to a semi-integral abutment and 20’ tied approach slab with a ¼” preformed joint at the abutment and CF2 joint at the sleeper slab. Sleeper to approach joints at both ends were in OK condition with some sealant missing and minor spalling. Approach slabs did not have any obvious cracking or settlement. Approach slab to abutment joints were in good condition with minor spalling at the North joint. Embankments and curbs were working as intended. Staining was visible on both North and South abutment faces at each bearing location but appeared to be left from before the rehabilitation and conversion to semi-integral abutments (Figure 4.7).

Figure 4.7. Abutment Face Showing the New Backwall on top of the Old Footing

4.5 310 Jasper

310 Jasper is located in Newton, Iowa on US-6 over I-80. There are two identical north and southbound bridges, and both were included as part of the inspection. The bridges are 232’ long and 32’ wide with a skew of 6.25°. A 2010 project saw the conversion to semi-integral abutments with tied approach slabs with a ¼” joint in-between. The approach uses a 20’ doubly-reinforced slab connected to a 4’ transition slab by an EF joint.

4.5.1 Northbound

The northbound bridge is in generally good condition. Beginning at the ends there is some joint sealant missing and the joint is open in the transition slab to pavement joint on the north end. The approach slab to transition slab joints were all in good condition. Approach slabs had no major cracking or settlement and appeared to be performing well. At the south end there is settlement of approximately 1" for pavement meeting concrete slabs in the shoulder. Drains exiting in the north embankment appear shorter than they should for proper drainage as they are partially obscured by the embankment. Abutment condition is good with visible no staining. Minor cracking and spalling of concrete were present at wingwalls and wingwall to approach slab joints at the beginning of the curbs (Figure 4.8a, b).

4.5.2 Southbound

The southbound bridge's condition is unsurprisingly very similar to the first. Joints between the transition slab and pavement are very poor and open with sealant missing. Abutment to approach joints appear in good condition apart from debris accumulating at the sides where the curb begins. Once again wingwalls show some minor seemingly random vertical cracking and minor spalling. Drains on the north end are very close to becoming blocked with debris piling up at the outlet and the NW drain completely closed (Figure 4.9a, b). In areas with pavement shoulders there is visible settlement compared to concrete panels.

Figure 4.8. (a) Concrete Cracking at the end of the Wingwall (left), (b) Additional Cracking at the end of the Wingwall (right)

Figure 4.9. (a) Blocked Embankment Drainage (left), (b) Additional Blocked Embankment Drainage (right)

4.6 208 Bremer (North and Southbound)

208 Bremer is located in Denver, Iowa on US-63 over 260th St. There are two identical northbound and southbound bridges constructed in 1994. They are three spans and 161’ long and 40’ wide with a skew of 2.25°. The bridge approach was redone with plans dated 2008 to use 20’ precast concrete panels. Slightly inclined rebar ties were embedded 1’ into the abutments and 4’ transition slabs were used between the approach slab and pavement. A ¼” joint exists at the abutment and an EF joint at the abutment to transition slab.

4.6.1 Northbound

EF joints between the approach slab and transition slab appeared to be in OK condition except for vegetation growing in the joints outside the traffic lanes. Approach slabs were also performing well except for some spalling on the north end (Figure 4.10a, b). Embankments used concrete slope protection under the bridge. On the north end there was a large gap between the inclined portion and flat section at the top of the embankment as if the entire concrete slope was sliding (Figure 4.11a). The slope portion was otherwise intact. The south end was performing even worse with a larger gap between the concrete slabs, broken sections around the pier columns, and a vertical settlement based off markings on the abutment. Repair work had attempted to fill the joints, but the material was cracked into pieces and joints have continued to open. At the west corner of the south abutment there was a large void at the corner of the abutment which measured 23” deep (Figure 4.12, Figure 4.13). The end of the tape measure was able to hook onto the underside of the concrete abutment.

4.6.2 Southbound

The southbound bridge condition was very similar to the northbound, including reasonable joint condition with some spalling of the approach slab at the abutment joint. Embankments and slope protection were just as poor with another large void located at the west side of the south abutment. The concrete slope protection was broken and there were large voids around the pier column bases (Figure 4.11b). The curb and joint between approach slab and barrier must not be effective in draining surfacewater for large voids to appear. There were also large amounts of settlement in the embankment that could have been caused by water infiltration.

Figure 4.10. (a) Deck to Approach Slab Joint Showing Severe Spalling (left), (b) Additional Deck to Approach Slab Joint Showing Severe Spalling (right)

Figure 4.11. (a) Typical Embankment Condition (left), (b) Embankment Condition at the Abutment (right)

Figure 4.12. Horizontal Void Created by the Embankment Pulling away from the Abutment

Figure 4.13. Measuring Tape Showing the Vertical Depth of the Void

4.7 108 Blackhawk

108 Blackhawk is a single span 130’ long, 40’ wide bridge. It is located west of Cedar Falls, Iowa on IA-57 over a small stream. The bridge uses a ¼” preformed joint at the abutment, a 20’ approach slab, and a CF-3 joint at the sleeper slab. Joints were in good condition with no large amounts of sealant missing or other common issues. Embankments we in good condition. The stream water levels were very high at the time of inspection, but the embankment did not appear to be experiencing erosion at the abutment face.

4.8 Joint Condition

Joints were measured at each bridge for both ends and Table 4.1 shows the recorded values taken with air temperatures ranging from 60-80° F. Joint widths at the time of construction were taken from bridge plans for comparison. Joint 1 is at the deck-to-approach slab joint, and Joint 2 is the next joint moving away from the bridge either between the approach slab and sleeper slab or between the approach slab and transition slab. Tied approach joint values show that the tied connections are not performing well. Over time a design value of ¼” has become in some cases up to a 1 5/8” opening. The decrease in joint width at the opposite end of the slabs clearly shows the movement of the approach slab away from the deck. Ideally there would be no movement at the tied approach, and the approach slab would move with the abutment and deck allowing all movement at the sleeper or transition slab joint. The tied connection details show for the most part vertical bars which, after initially good outlook as the subject of other studies (Greimann 2008), have performed poorly long-term. Semi-integral joints appeared to function as expected. Without any rebar to tie the approach slab to the bridge, the approach slabs would be pushed away from the bridge during expansion due to increasing temperatures. Then as temperatures decrease, the bridge contracts and without a tied connection to pull the slab with it, the joint would widen.

Table 4.1. Joint Measurements and Design Plan Values

Bridge				Joint 1		Joint 2	
				Design (in.)	Measured (in.)	Design (in.)	Measured (in.)
208 Bremer	Tied Approach	NB	North	0.25	1.5	3.5	2.5
			South	0.25	1.625	3.5	2.5
		SB	North	0.25	1	3.5	2.5
			South	0.25	1	3.5	1.75
108 Blackhawk	Tied Approach		East	0.25	1	3	2.875
			West	0.25	0.875	3	2.875
310 Jasper	Tied Approach	NB	North	0.25	0.875	3.5	2.75
			South	0.25	0.625	3.5	2.5
		SB	North	0.25	0.75	3.5	1.875
			South	0.25	0.625	3.5	2.125
213 Cass	Tied Approach		North	0.25	0.375	2.5	1.625
			South	0.25	0.5	2.5	2
111 Pottawattamie	Semi-Integral		East	2	1.5	N/A	N/A
			West	2	1.5	N/A	N/A
113 Cass	Semi-Integral		East	No Plans	1.875	No Plans	0.25
			West	No Plans	1.75	No Plans	0.375
1215 Polk	Semi-Integral		North	1	1.625	3	2
			South	1	2	3	1.5

CHAPTER 5. JASPER COUNTY 118 AND STORY COUNTY 118 INSTRUMENTATION

The instrumentation of two Iowa bridges was completed to further understand the behavior of integral and semi-integral abutment bridges in the real world. Multiple different types of sensors are used to obtain different measurements for each bridge. Strain gauges, earth pressure cells, crackmeters, and displacement meters are all used to gain important information over time.

5.1 Sensor Descriptions

All measurements were taken by Geokon vibrating wire (VW) gauges intended for long term use. Since the monitoring period of each of the bridges is at least one year, VW gauges are ideal for periodic data recording since continuous data is not necessary. The VW gauges are very resilient and must withstand the installation and construction process along with the exposure to the elements they may experience. The VW technology uses a steel wire located in each gauge tensioned at its two ends. When a measurement is taken the wire is plucked and vibrates at a certain frequency depending on the tension. The vibration is measured by an electromagnetic coil and can be converted into the applicable measurement of strain, pressure, or displacement. All the sensors contain an internal thermistor in order to measure temperature inside concrete if they are embedded, or external temperatures if they are attached to the exterior of the bridge. The wires for each sensor were ran to a central location at each end of the bridge to either a multiplexer or a datalogger. An additional wire was run the length of the bridge between the multiplexer location and the datalogger and attached to the exterior of the barrier wall.

5.5.1 Earth Pressure Cells

The Geokon Model 4810 “Fat Back” Pressure Cell was chosen for use since it is designed to measure earth pressures on the surface of concrete structures. The cells consist of two circular metal plates with a fluid trapped between them. As earth pressure on the exterior increases, so does the interior fluid pressure. The thicker back plate is designed to minimize any point loading effects. The 700 KPa range cells were chosen for use on Jasper County 118 by examining previous research for earth pressures recorded on similar bridges. The cells will provide a resolution of 0.175 KPa with an accuracy of 7 KPa.

5.1.2 Strain Gauges

The Geokon Model 4200 Strain Gauge was used for its intended purpose of being embedded inside concrete. The standard version was deemed satisfactory since extremely large strains or extremely high temperatures are not expected. The gauges are designed for embedment and long-term stability, a key factor when monitoring periods are expected exceed one year. The Model 4200 provides a resolution of 1.0 με and an accuracy of 15 με.

5.1.3 Crackmeters

The Geokon Model 4420 Crackmeter was designed for measuring movement across cracks or joints making it ideal for bridge applications. The crackmeter has ball joints at either end and accommodates threaded concrete anchors. By attaching the crackmeter across a joint the relative displacement between two objects can be measured. The range of the crackmeter for Jasper County 118 and Story County 118 were determined by calculating the theoretical free expansion of the bridges using Iowa DOT LRFD Bridge Design Manual Table 5.8.3.1.2.

$$\Delta_T = \alpha * L * (T_{MaxDesign} - T_{MinDesign})$$

Δ_T = design thermal movement range

α = coefficient of thermal expansion

L = expansion length

$T_{MaxDesign}$ = maximum design temperature

$T_{MinDesign}$ = minimum design temperature

For example, the Story County 118 movement range is computed as 30.5mm for the total length, making the 50mm range capable of accommodating errors in placing of the crackmeter at the correct extension length based on expected movement after installation. The 50mm range provides resolution of 0.0125mm with an accuracy of 0.05mm.

$$(6E-6)(375'+40')/2(100°\,F) = 1.49" \;=\; 37.9\,mm$$

5.1.4 Displacement Transducers

The Geokon 4427 Long Range Displacement Transducer is intended for measuring large displacements like those seen at an integral bridge abutment. The sensors consist of a spring drive motor connected to a lead screw. The rotation of the lead screw is converted into a linear displacement. The spring drive motor maintains a constant tension on the cable exiting the protective case. In the case of Jasper County 118 four Geokon 4427's were reused from past ISU projects and the calibration sheets were available from documentation kept by the ISU Structures Lab. The Geokon 4427 has a range of 1 meter with a resolution of 0.25mm and accuracy of 10mm.

5.2 Jasper County 118

Jasper County 118 (Jasper) is a bridge located near Kellogg, Iowa chosen for monitoring due to its 45° skew which matches the current maximum allowed by Iowa DOT for semi-integral abutments. The bridge is 184’ x 28’ and carries two lanes of traffic on HWY 6 over a railroad using three spans. The construction work included a deck overlay, and conversion to semi-integral abutments with complete reconstruction of the bridge approaches. The bearings remained unchanged, so the West end of the bridge remains stationary while the East end moves to accommodate and thermal expansion (Figure 5.1). The approach slab on the East end is tied to the abutment while the West end is not tied (Figure 5.2). It would follow that neither approach slab should experience any movement due to thermal expansion of the deck. Both ends of the bridge were monitored to determine whether it behaves as intended, as a precaution for the possibility of corroded bearings or other performance issues. The instrumentation plan seen in Figure 5.3 shows the location of sensors, which are identical for each end of the bridge. Displacement meters were placed at the acute bridge corners in orthogonal directions to measure not only longitudinal movement, but transverse movement as well. The large skew angle is likely to cause transverse movement in opposite directions at either end resulting in a slight rotation of the entire bridge. Crackmeters measured relative longitudinal movement between the bridge deck and approach slab at each corner. Earth pressure sensors located on the abutment backwall were placed at each corner to measure active and passive earth pressures. It was anticipated that pressure will differ between the gauges at the acute and obtuse corners of the bridge. Strain gauges were placed in the approach slab to measure any strains and forces that may occur. Should the bridge and bearings act as intended, strains in the approach slabs should be insignificant.

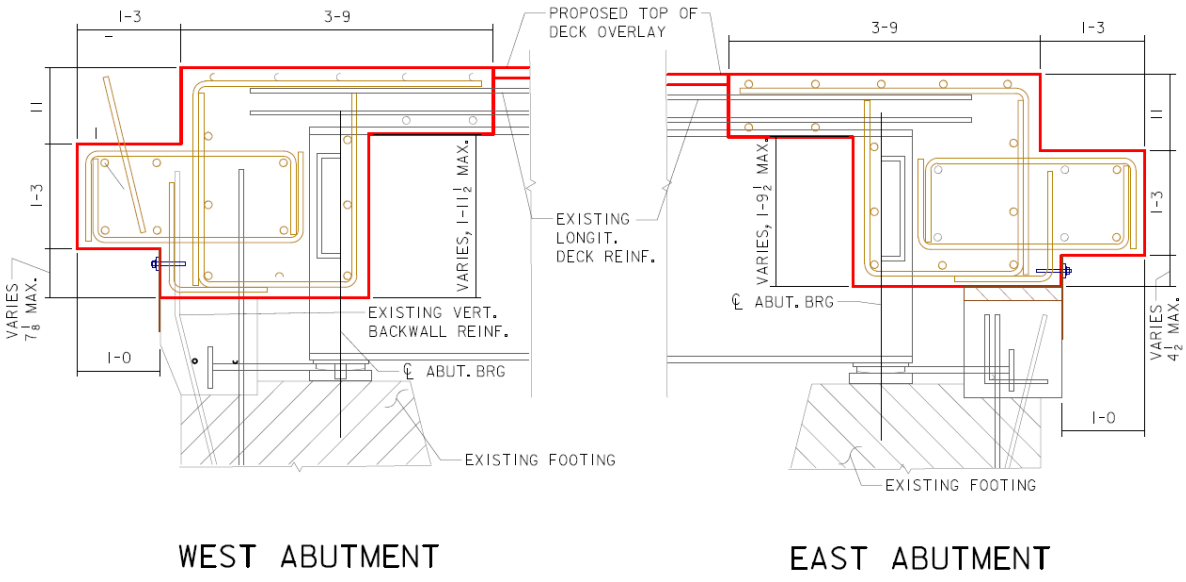

Figure 5.1. Jasper - East and West Abutments (Iowa DOT)

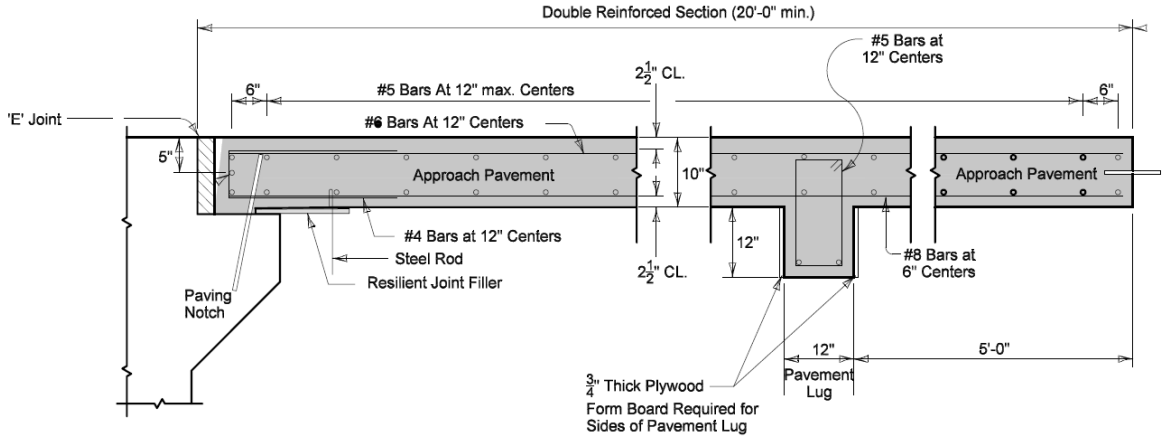

Figure 5.2. Jasper - Approach Slab Dimensions and Section View (Iowa DOT)

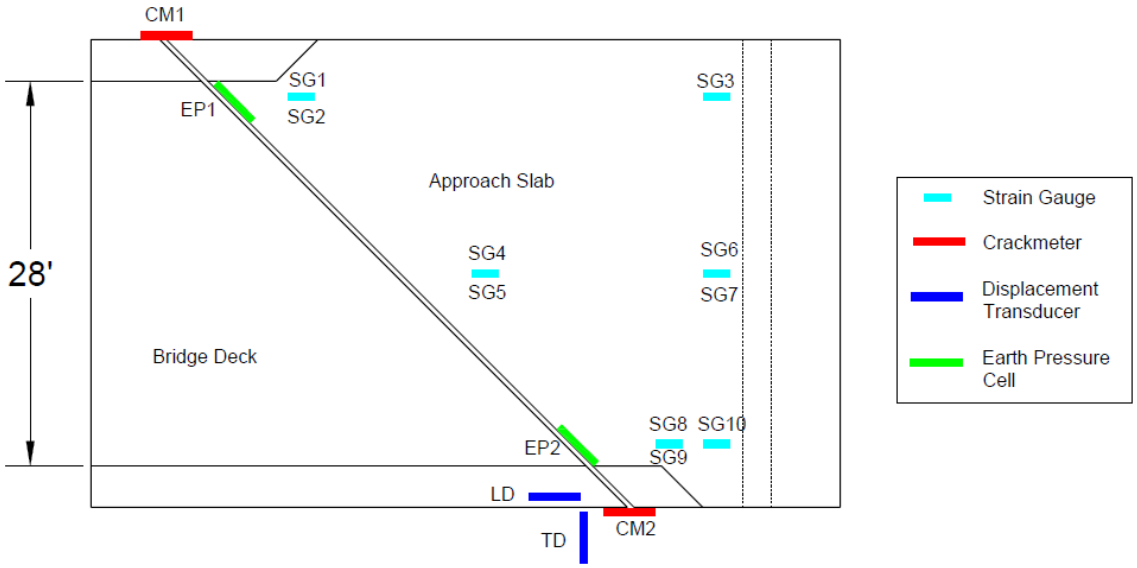

Figure 5.3. Jasper – Instrumentation Plan (Typical of East and West Ends)

5.2.1 Jasper Earth Pressure Sensor Installation Process

Sensor installation at Jasper County 118 began with earth pressure sensors at the West abutment out of necessity due to construction sequencing. The contractor completed the bridge deck replacement first, before constructing and pouring the semi-integral abutments. The abutment backwall was left exposed for earth pressure sensor installation before backfilling (Figure 5.4). Initially the sensors were intended to be placed on the same longitudinal axis as the outer bridge girders; however, due to the extreme 45° skew of the bridge and working space limitations they were placed closer to the center with the outside edge of the sensor on the girder axis. The decision was made to shift all other sensors to the same axis for the sake of consistency. The earth pressure sensors should illustrate how earth pressure along the backwall can vary due to skew. The sensors had been prepared by attaching an adhesive neoprene layer to the face to help distribute load for granular particles. A thick layer of mastic adhesive was applied to the back of the sensor and it was pressed

against the concrete surface causing mastic to flow out from behind. While the sensor was held in place, holes were drilled using a hammer drill for each of the four tabs for attachment. Concrete screws attached the sensor to the concrete and the excess mastic was removed from the edges. The wires were run around the abutment and kept tight to the concrete surface using small tabs and additional concrete screws. The final step included taking initial digit and temperature readings using a Geokon GK-404 readout unit on position “B”. The contractor was advised to use smaller 3/8” aggregate from a pile located on site to fill against the sensors.

Figure 5.4. Jasper - EP1-W Earth Pressure Sensor after Installation

5.2.2 Jasper Strain Gauge Installation Process

Shortly after backfilling the area, the contractor prepared the first half of the West approach slab by completing formwork and tying the rebar. Seven strain gauges were placed including three along the same axis as the obtuse corner earth pressure sensor, and four as close to the centerline of the roadway as possible. Strain gauges were placed according the

plan in Figure X with gauges 1, 3, 4, and 6 on the top layer of bars and gauges 2, 5, and 7 on the lower layer of bars. Small ½" rubber spacers were used to position the gauges with sufficient clearance to the bars with zip ties to hold them in place (Figure 5.5). The strain gauges were checked previously for proper function and set to the middle of their range of measurement per recommendation from the Geokon manual. Wires were zip tied periodically along their lengths to keep them tight to the bars. After the contractor poured the first half of the approach slab and tied the rebar for the second, the last three strain gauges were installed in the same manner as the first along the axis of the acute bridge corner earth pressure sensor. All wiring exited the slab on the North side and was bundled together for connection to a multiplexer. The earth pressure sensors and strain gauges on the East end of the bridge were installed in the same manner as the West one week later.

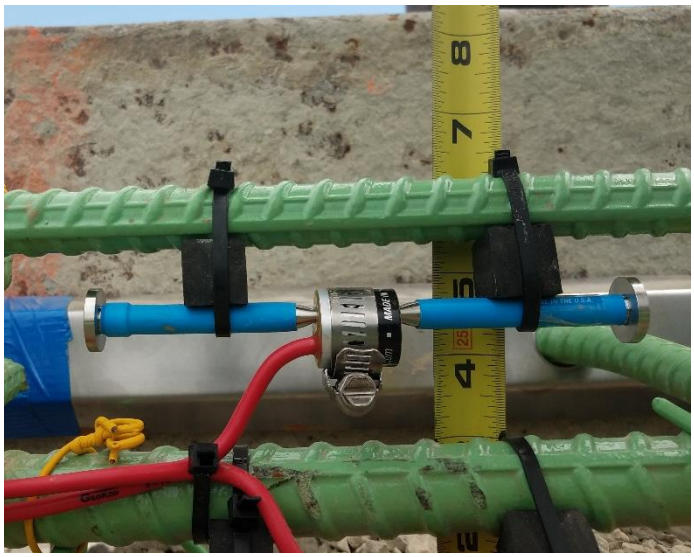

Figure 5.5. Jasper - Typical Strain Gauge Installation

5.2.3 Jasper Crackmeter Installation Process

Crackmeters were initially intended to attach to the vertical face on the side of the approach slab and the perpendicular end of the abutment. Unfortunately, the wooden posts

used to support the bridge guardrail were not accounted for in the initial planning, so a change was made to installation. The crackmeters were moved to the approach slab surface with the approval of Iowa DOT and protective covers were fabricated using a steel angle to prevent damage by snow plows (Figure 5.6a, b). The crackmeters are located under the barrier and will not be hit by traffic or the plow, but the snow itself is a concern. Crackmeters were installed per the Geokon manual and set at 25% of maximum extension. Since installation is occurring in the summer it is anticipated that the bridge will experience almost entirely contraction thus opening the joints between the abutment and approach slabs. The crackmeter located in the Northeast corner of the bridge was placed in a different location than the rest due to a different construction at that corner of the bridge. A large crash barrier prevented the crackmeter from attaching to the approach slab, so it was located across the joint between the bridge and stationary wingwall. Since the approach slab is not designed to move with the bridge, the crackmeter should theoretically measure the same joint movement. Unfortunately, since the railings were being installed by the contractor the same day as the crackmeters, the Northwest crackmeter cover was impacted by a large wooden post, causing a shear failure of the concrete screws allowing the metal cover to impact the sensor and shear the anchor. The crackmeter was removed and sent to Geokon for calibration check before being reinstalled at a later date.

Figure 5.6. Jasper - (a) Crackmeter without Protective Cover (left), (b) Crackmeter with Protective Cover Installed (right)

5.2.4 Jasper Displacement Transducer Installation Process

Measuring abutment displacement of integral or semi-integral bridges proves to be difficult due to the requirement of a stationary reference post somewhat near the abutment itself. Both settlement of the embankment and movement of the abutment itself can affect the reference post and skew results. A discussion between principle investigators of the project and the structures lab manager yielded no definitive preferred method. Using a reference post can be unreliable but using surveying equipment only provides periodic results unlike displacement sensors that can monitor hourly or daily. Data taken by total station may also miss seasonal extremes of movement since it is impossible to predict the coldest or warmest days of the year. Since Jasper County 118 is only a partial reconstruction project with no effect on the substructure, it was determined that a reference post should yield satisfactory

results. During construction a layer of embankment was removed and replaced to improve erosion protection, but the depth was limited. The method used a 1½" steel pipe driven 5 feet into the ground to reach frost depth and act as a reference post (Figure 5.7a). The Geokon 4427 was attached to the bridge abutment using concrete screws and a coupler attached to a cable which spans the distance to the reference post. At each acute bridge corner two displacement meters measure in orthogonal directions to measure longitudinal and transverse displacement (Figure 5.7b).

Figure 5.7. Jasper - (a) Displacement Transducer with Reference Post (left), (b) Longitudinal and Transverse Displacement Transducers Attached at the Acute Bridge Corner (right)

5.2.5 Jasper Datalogger Installation

The datalogger used to record measurements was installed with the last of the bridge sensors one day before the bridge opened for traffic. The sixteen wires on the West end of the bridge converge on a central location on the West abutment face to a multiplexer which can condense the data to be run through a single wire the length of the bridge. The single wire runs to the opposite corner of the bridge to a datalogger placed on the East abutment face

allowing for connection to a solar panel on the south face of the structure to provide power. Initial readings from all sensors were taken to verify proper function. All sensors provided readings indicating that damage resulting in failure had been avoided during construction.

5.3 Jasper County 118 Data Collection and Processing

Data was collected from the datalogger by traveling to the bridge site and downloading the data to a .DAT file. The data recording began on August 30th, 2018 and was retrieved on January 4th and May 8th, 2019 providing over 8 months of data. The logger recorded measurements every hour, resulting in over 6000 data recordings for each of the thirty-two sensors in the bridge.

5.3.1 Jasper Instrumentation Results

Data processing began by examining trends in the data for each sensor type to verify proper operation. As mentioned previously, each sensor contains a thermistor to measure temperature. Measurements taken by the sensors are much more valuable when compared with temperature than time due to the long-term nature of the project and relatively long time between measurements. In order to determine the ambient air temperature at the bridge location, the temperature data from each sensor not embedded in concrete or soil nor exposed to the sun was averaged for the entire time history. For example, the displacement transducers on the East end of the bridge were not included since they are able to receive direct sunlight from the South, especially during the winter. Air temperatures for the monitoring period ranged between 88.2° F in September and -19.4°F in January. The largest difference between minimum and maximum temperatures of 24.2°F on a single day occurred on October 3rd when maximum and minimum temperatures reached 62.1°F and 37.9°F respectively.

The week of September 9th-15th was chosen for in-depth analysis to narrow the amount of data used in plots and further examine trends. The plot of daily maximum and minimum air temperatures (Figure 5.8) shows a large discrepancy in the minimum temperature compared with the maximum temperature. This means there was a large daily temperature range during the entire week with high temperatures more than 10° higher than low temperatures. This time period also shows a general increasing trend over the course of the week with both high and low temperatures increasing steadily by 15°. This seven-day period captures both the daily cyclic loading and long-term trends in seasonal temperature.

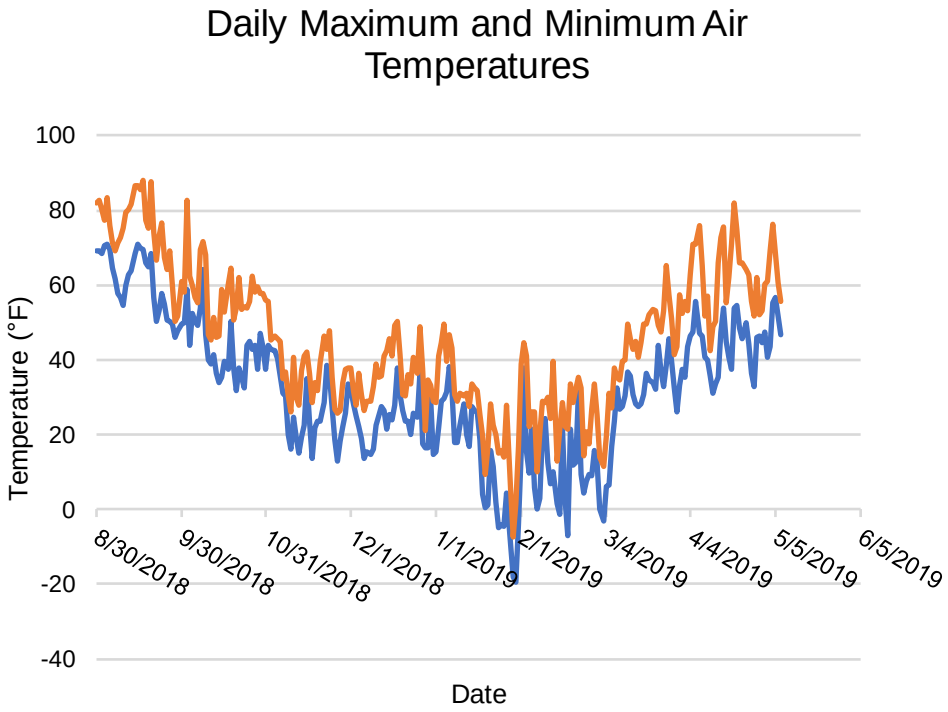

Figure 5.8. Jasper - Daily Maximum and Minimum Air Temperatures 8/30/2018-5/08/2019

5.3.2 Jasper Bridge Longitudinal Expansion

Displacement transducers were installed on the bridge with the intent to measure expansion for comparison to theoretical calculations per Iowa DOT LRFD Bridge Design

Manual 5.8.3.1.2, illustrate changes in expansion over long time periods, and examine the effect of the 45° skew angle on transverse displacement. The displacement of the East and West ends of the bridge over the full monitoring period can be seen in Figure 5.9 and Figure 5.10 which shows their cyclical nature and relationship with temperature.

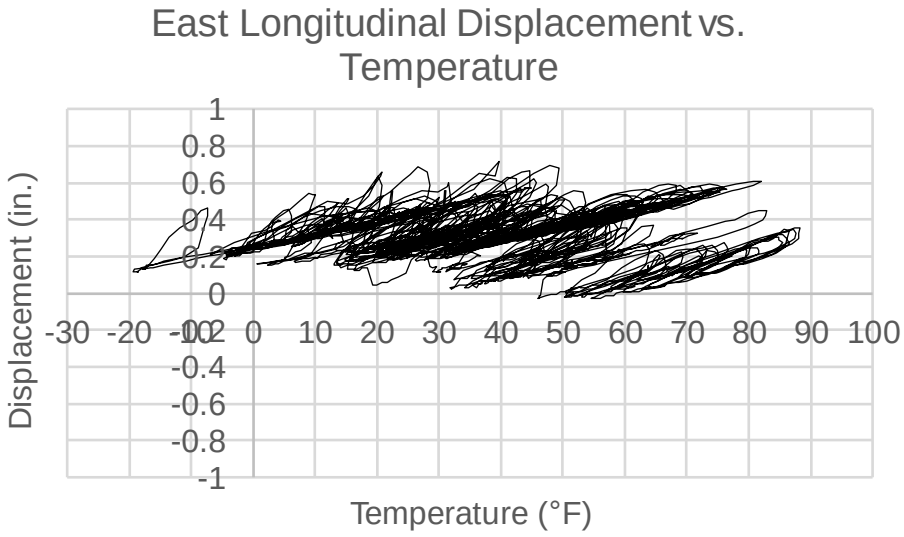

Figure 5.9. Jasper - East Longitudinal Displacement

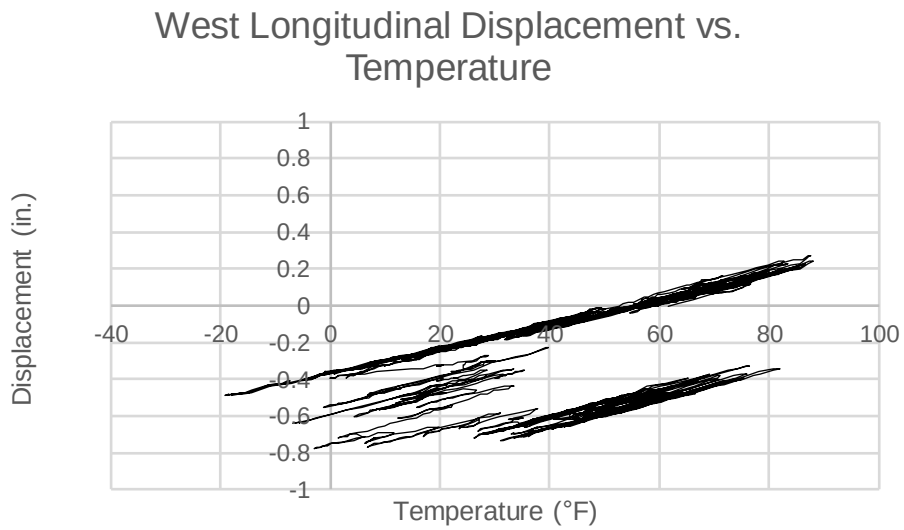

Figure 5.10. Jasper - West Longitudinal Displacement

In order to compare measured expansion with calculated values, the total longitudinal bridge expansion was plotted versus time in Figure 5.11. Total expansion includes both the East and West ends of the bridge corrected for the change in length of the steel cables attached to the transducers. The Jasper semi-integral abutment conversion was designed for zero displacement at the West end; however, the data shows a significant amount of movement over the entire four-month period similar to the east end. A temperature range of 75° produced a total displacement range of 0.66 inches. The total longitudinal expansion compared with theoretical expansion show nearly identical trends, with daily ranges for calculated values underestimating measured values by 52.7% on average (Table 5.1). The bridge is expanding and contracting more than expected. The discrepancy could be a result of many different factors including the true coefficient of thermal expansion for the structure as a whole, the effect of skew angle on expansion, limited accuracy of the sensor setup, or temperature gradient through the depth of the structure due to sunlight. In order to better account for the effect of bridge skew, a new modified expansion was calculated using the principle that skewed bridges expand and contract along an axis between the two acute corners (Aktan and Attanayake 2011). The modified theoretical expansion, which was calculated using the longitudinal component of expansion considering a modified bridge length of 212.5', is also included in Figure 5.11. The modified theoretical expansion is 15% larger than the standard calculated value, which more closely resembles the measured values.

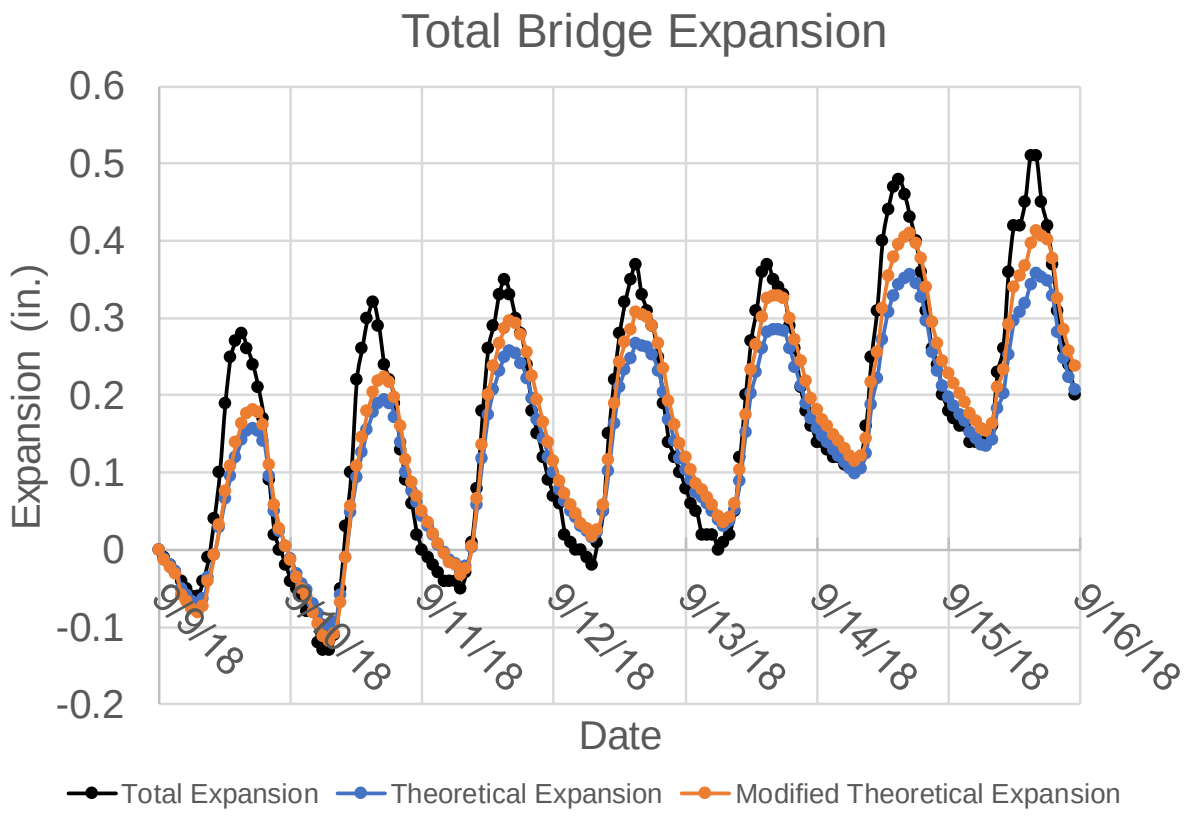

Figure 5.11. Jasper - Total Measured, Theoretical, and Modified Bridge Expansion

Table 5.1. Peak Total Expansion Values and Range Percent Difference

Measured Maximum (in.)	Measured Minimum (in.)	Measured Range (in.)	Theoretical Maximum (in.)	Theoretical Minimum (in.)	Theoretical Range (in.)	Range Percent Difference
0.28	-0.06	0.34	0.16	-0.07	0.23	49.2
0.34	-0.13	0.47	0.19	-0.10	0.30	58.2
0.35	-0.05	0.40	0.26	-0.03	0.29	40.2
0.37	-0.02	0.39	0.27	0.02	0.25	54.7
0.37	0.00	0.37	0.28	0.03	0.25	45.6
0.48	0.09	0.39	0.36	0.10	0.26	52.0
0.53	0.14	0.39	0.36	0.13	0.23	69.0

Calculated longitudinal expansion underestimates expansion more as time increases, shown especially from 9/14/2018 onward where minimum expansion values show a gap between calculated and theoretical, where previously only positive peaks showed a similar

gap. The displacement data shows no lag between the measured data and the theoretical values based on air temperature. This illustrates that the expansion of the bridge reacts to changes in temperature within one hour which is the time between data points. The steel girders of the Jasper bridge do not show any thermal inertia when considering thermal expansion of concrete girder bridges. Concrete girders take time for heat transfer through the entire cross section, so expansion lags behind air temperature changes. This concept can be observed by comparing temperatures in the concrete approach slab with air temperatures. Figure 5.12 shows temperatures for both the East and West approach slabs along with air temperatures over the 7-day period 9/9/2018-9/15/2018. Concrete temperatures show peaks roughly three hours after air temperatures and daily air temperature ranges are 50% larger than those of the 10” concrete slab. Temperatures within the slab reach a higher peak value on 9/9/201 for which weather records show sunny conditions without cloud cover. The roadways exposure to sun resulted in a temperature higher than the air temperature not only on the road surface, but through the depth of the slab.

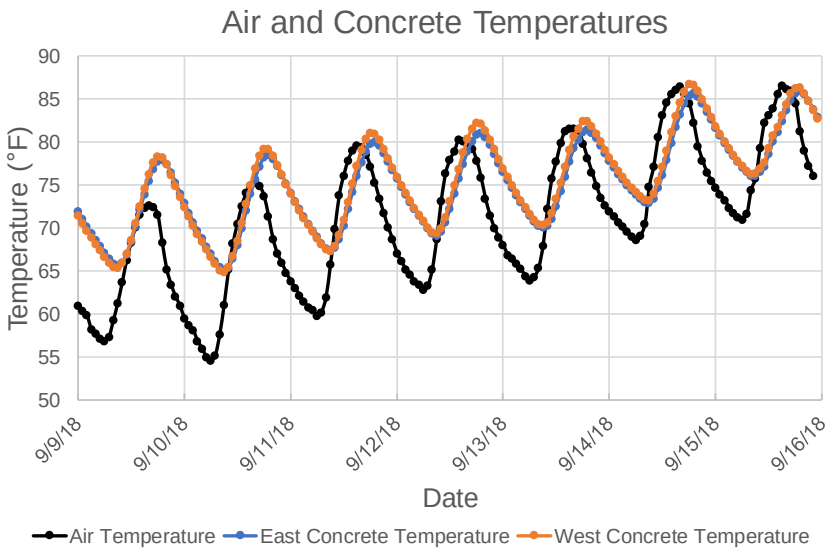

Figure 5.12. Jasper - Air and Concrete Temperatures over Time

Crackmeters installed on the Jasper bridge were intended to measure the relative movement between the bridge and the approach slabs. The data taken from all four crackmeters is similar to each other but does not match the expected trends. West end joints show minimal movement (Figure 5.13, Figure 5.14) with ranges of 0.08” and 0.061” respectively. This is reasonable given the expectation that the West approach slab is tied to the abutment. Zero expansion corresponds to the joint condition at the time datalogger began recording. Even if the abutment moves despite its intended design, the approach slab would be pulled with it and the crackmeters would measure limited opening of the tied joint. East crackmeter movements (Figure 5.15, Figure 5.16) are on the same magnitude as the West, but they should be an order of magnitude higher and more in line with displacement data. Ideally, East crackmeters would match East displacement data due to the abutment moving independently of a separated approach slab. Two possible explanations include malfunctioning of the crackmeters, or incomplete separation of the approach slab from the abutment.

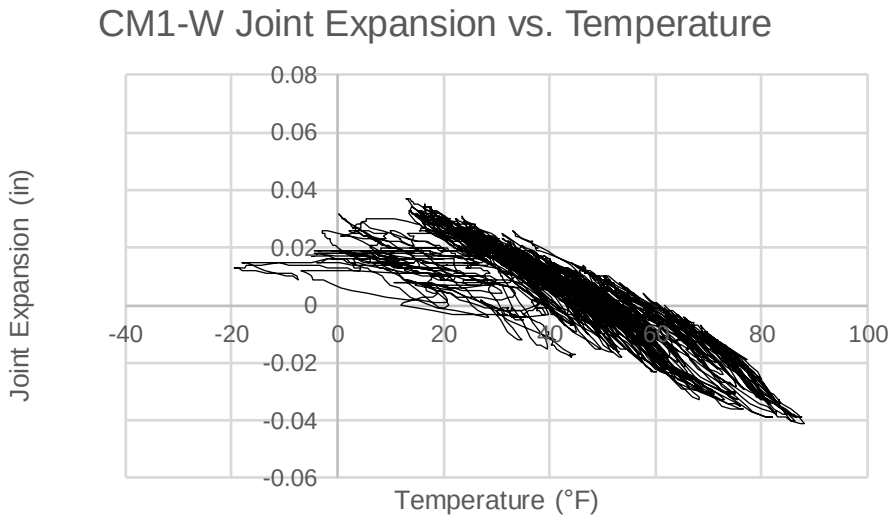

Figure 5.13. Jasper - West End Joint Expansion (Southwest Bridge Corner)

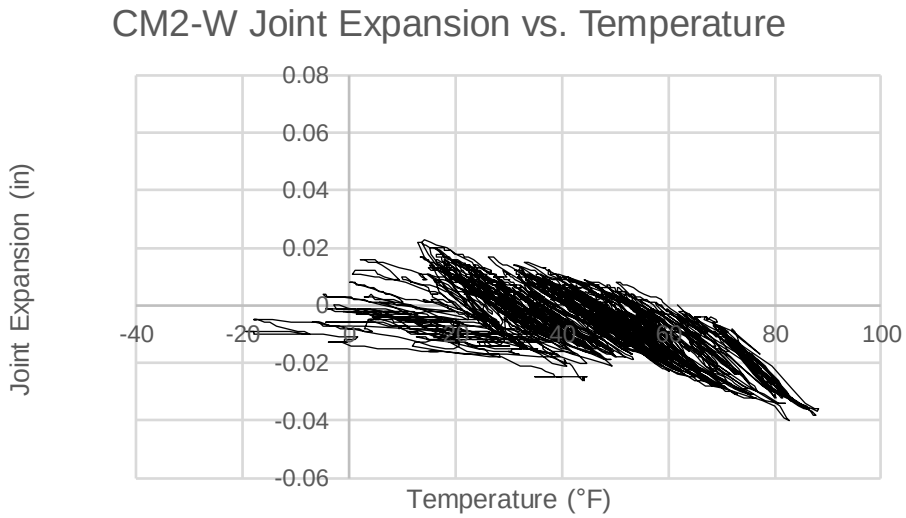

Figure 5.14. Jasper - West End Joint Expansion (Northwest Bridge Corner)

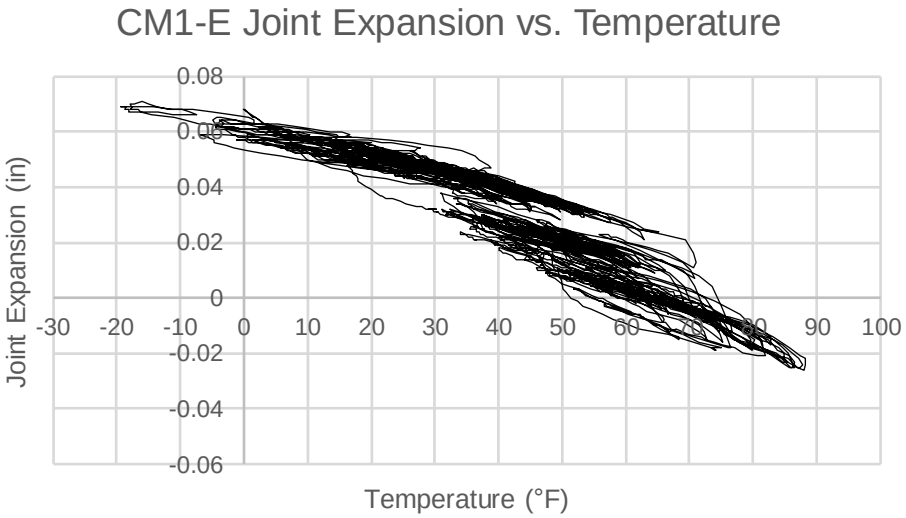

Figure 5.15. Jasper - East End Joint Expansion (Northeast Bridge Corner)

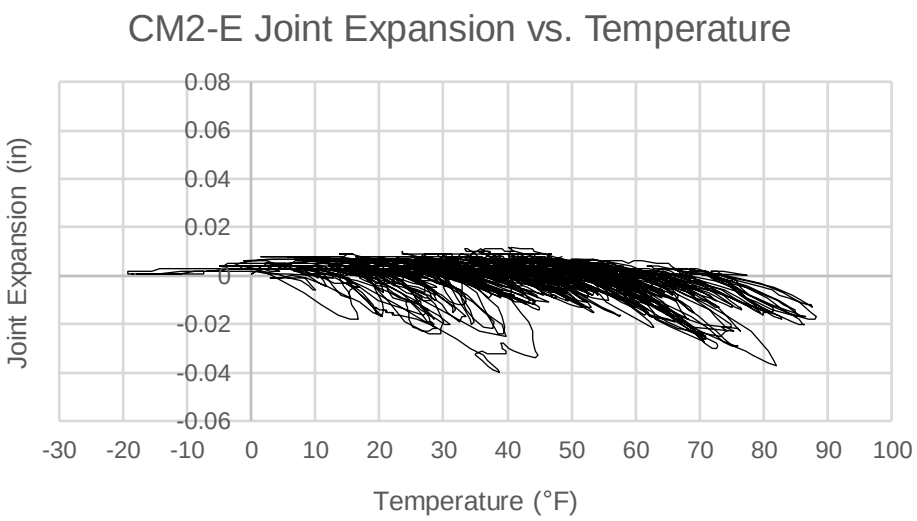

Figure 5.16. Jasper - East End Joint Expansion (Southeast Bridge Corner)

5.3.3 Jasper Bridge Transverse Expansion

One of the reasons skew is so problematic for moveable abutment bridges is the transverse displacement that arises as a result of earth pressures normal to the skewed abutment backwall. Longitudinal expansion leads to a rotation of the entire bridge structure as both ends tend to move perpendicular to the bridge centerline in the direction of the acute bridge corners. Transverse displacement can be on the same magnitude as longitudinal displacement (Arenas et al. 2013). Transverse displacement for the East and West end of the bridge was plotted against temperature in Figure 5.17 and Figure 5.18. The two directions of displacement were plotted against each other to see their relationship (Figure 5.19) during the period of 9/9-2019 to 9/15/2019. Through seven daily temperature cycles the two variables show a linear relationship with the line of best fit showed on the plot with an R^2 value of 0.95. The relationship shows that for the Jasper bridge the transverse displacement is equal to 81% of longitudinal displacement. This value is in line with expectations considering the 45° skew. At lower skew angles earth pressures are more aligned with the bridge centerline that

don't result in a large rotational force. A similar relationship exists for the West end of the bridge with transverse displacement equaling approximately 120% of longitudinal values (Figure 5.20).

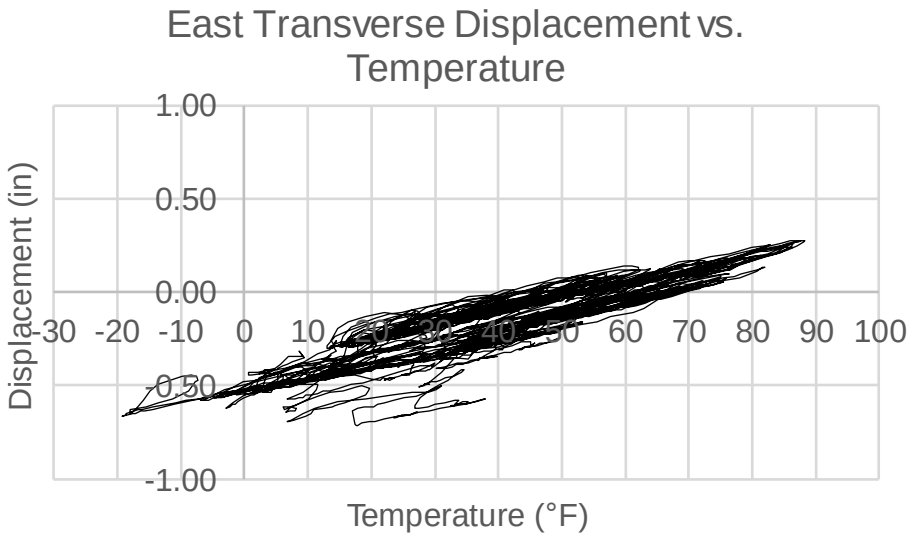

Figure 5.17. Jasper - East Abutment Transverse Displacement

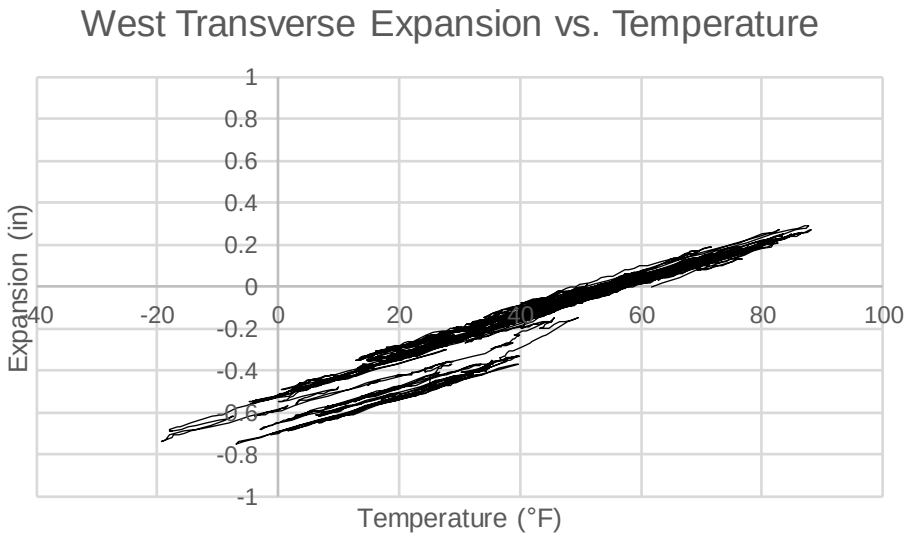

Figure 5.18. Jasper - West Abutment Transverse Displacement

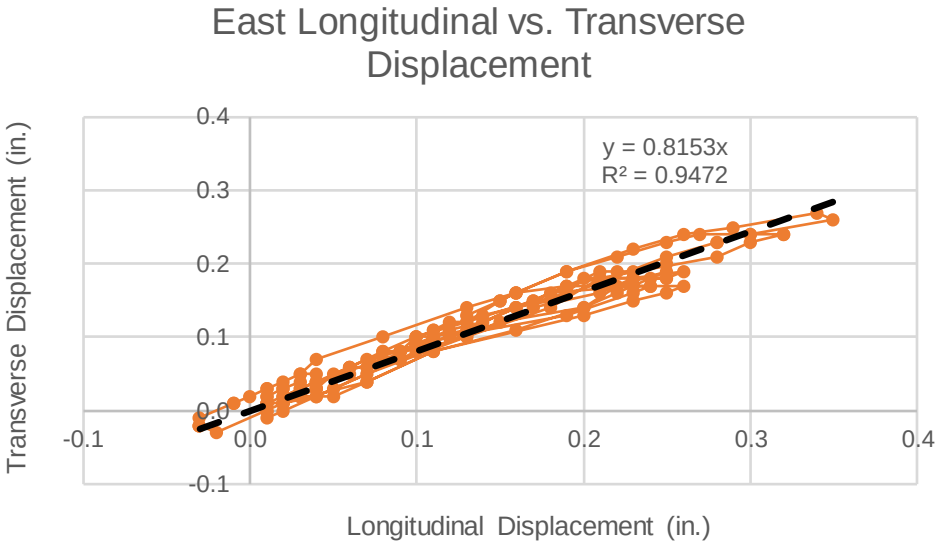

Figure 5.19. Jasper - East Longitudinal and Transverse Displacement Relationship

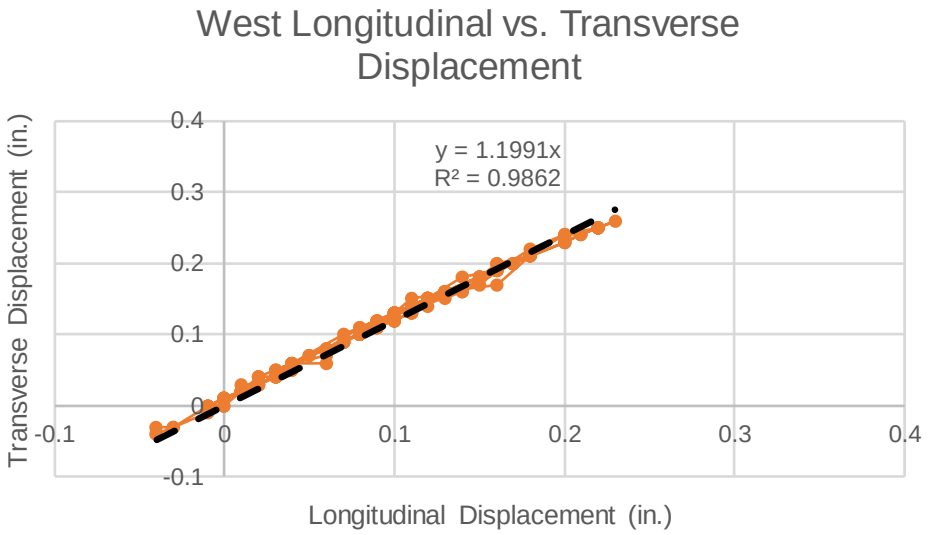

Figure 5.20. Jasper - West Longitudinal and Transverse Displacement Relationship

5.3.4 Jasper Abutment Backwall Earth Pressures

Two earth pressure sensors were installed on each abutment backwall directly below the approach slab. Unfortunately, it is apparent that EP1-E is not functioning correctly due to the extreme results it has produced. The other three sensors show pressures on the magnitude

of 100 psf, but EP1-E shows pressures averaging 19 ksf. Given the depth of the sensor and the surcharge loading above it, it can be concluded that the sensor is not functioning correctly. Discussion will cover the remaining sensors EP2-E, EP1-W, and EP2-W. Immediately after construction and before any abutment movement, earth pressures should match the at-rest earth pressure given below (Das 2016):

$$\sigma_h = K_o \sigma_o' + u$$

$$\sigma_h = K_o (q + \gamma H_1) + u$$

$$K_0 \approx 1 - \sin \varphi'$$

In the case of the Jasper bridge pore water pressure (u) is assumed to be zero due to the porous backfill used and design of the bridge drainage. The surcharge loading is equal to 125 psf based on the approach slab weight and the sensor is located at a depth of 0.625'. The active earth pressure coefficient is calculated to be 0.357 using an assumed friction angle of 40° based on correspondence with Iowa DOT. At-rest earth pressure is calculated to be 75.9 psf for the given conditions. Another value of note is Coulomb's passive earth pressure (Das 2016):

$$\sigma_p' = \gamma z K_p$$

Passive pressure is calculated to be 402.5 psf using the same soil depth as the previous calculation and using K_p equal to 4.6 for a friction angle equal to 40°, wall angle equal to 90°, and backfill angle equal to 0° since the approach slab lies on a flat surface. Earth pressure data for each of the three sensors for the entire eight month monitoring period is shown below in Figure 5.21, Figure 5.22, and Figure 5.23. The Geokon earth pressure sensors used provide a resolution of 0.025% of their maximum pressure of 14.6 ksf which is why data appears discretized, especially for the West end. They are more suitable for

measuring large bearing pressures under foundations; however, they can still provide useful data for low pressure ranges such as the ones seen below the Jasper approach slab. EP1-W located at the bridges obtuse corner shows lower magnitudes of pressure compared to the two sensors located at the bridge's acute corners (EP2-W, EP2-E). This is opposite the findings of Hassiotis et al. (2006) which state that pressures are higher in the obtuse corner for skew bridges. One possible explanation may be the difficulty of compaction in the obtuse corner which corresponds to the acute approach slab corner. Space to install the sensors was limited due to the high skew and it was anticipated that compaction would be difficult around the sensors. Zero pressure corresponds to the sensor's initial condition in before any backfill was placed against the face of the sensor. A large portion of measurements are for a negative pressure indicating the abutment pulling away from the soil. Over the first four months from September to January during a period of generally decreasing temperatures EP2-E and EP2-W show maximum pressures of 324 and 134 psf respectively. A higher pressure at the East end of the bridge where expansion is designed for is expected since the abutment should push further in into the soil due to a larger displacement resulting in a larger pressure. Both sets of data show interesting trends related to temperature. On a small scale, for a temperature change of around 10° pressures increase greatly and decrease with approximately the same slope. If this relationship were consistent over time, all data would fall in a single line. This is not the case, since there are multiple peaks visible at different temperatures. For example, EP2-E shows a peak pressure of 324 psf at 88° during September after initial construction, and maximum of 1274.4 psf at 30.2°. This peak value is a spike almost twice the magnitude of all other data recorded so it may be the result of point loading by a piece of aggregate; however, there are many consistent spikes in pressure at lower temperatures than the highest

recorded value of 88°. One possible explanation for this behavior is a ratcheting effect on the abutment. As the abutment pulls away from the soil when temperature decreases, soil falls into the void left by the abutment. When the abutment expands into the soil during a temperature increase the resulting pressure is larger at a lower temperature than before. Overall, the general shape of the curves suggests higher temperatures are associated with higher pressures which matches the expected trend. Half of the Jasper data set that was analyzed covered a period in the fall and winter which generally experienced bridge contraction. The second half shows much bridge expansion with increasing temperatures and generally higher pressures than recorded at the same temperatures during the cooling period. Peak pressures for EP2-E did surpass the calculated passive pressure value multiple times over a single daily cycle before pressure reduced drastically during bridge cooling overnight. It is anticipated that additional trends will become apparent once monitoring has been completed for an entire yearly cycle.

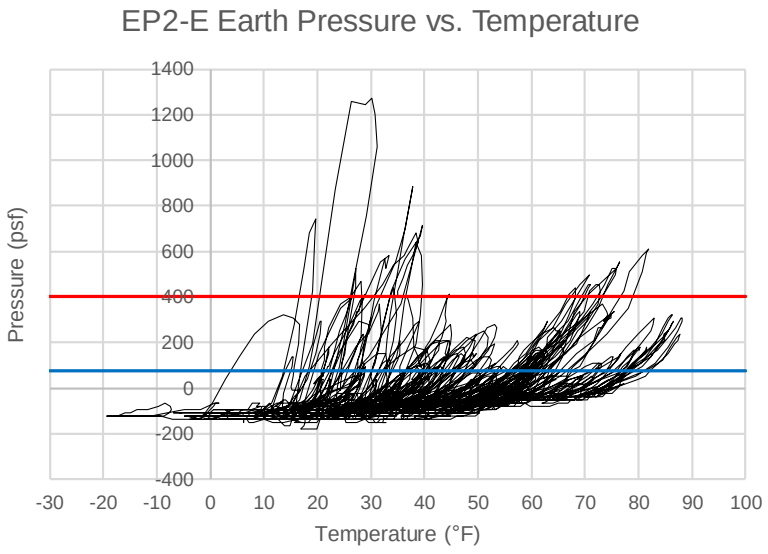

Figure 5.21. Jasper - EP2-E Earth Pressure for Full Monitoring Period

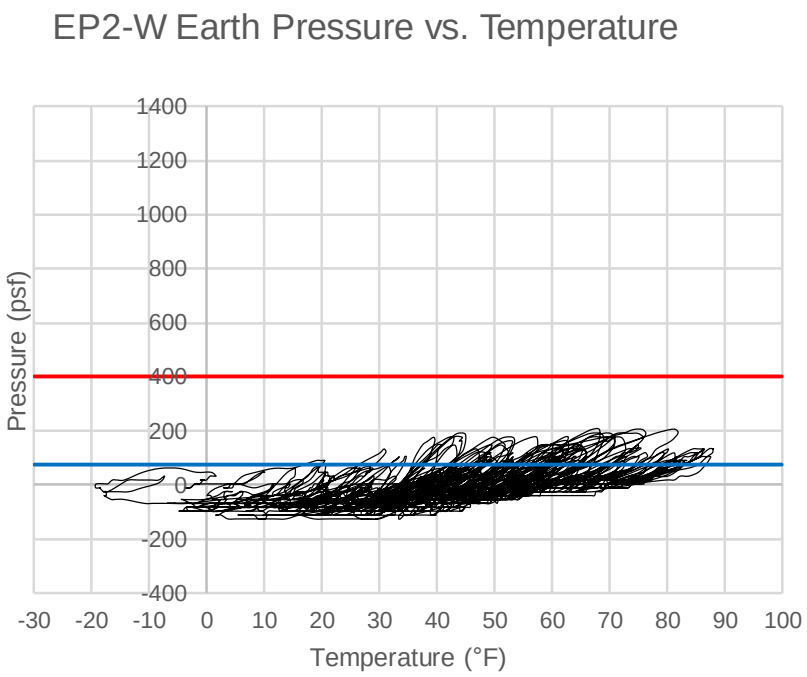

Figure 5.22. Jasper - EP2-W Earth Pressure for Full Monitoring Period

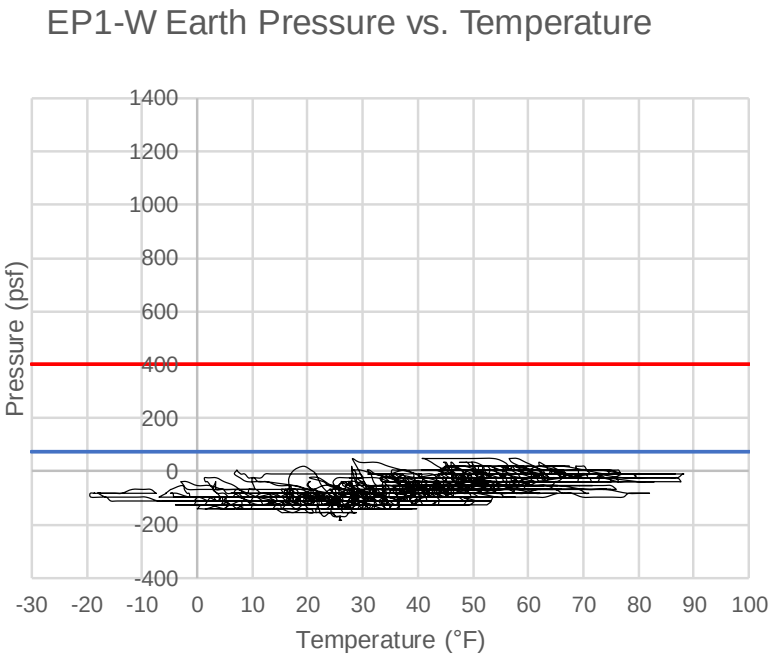

Figure 5.23. Jasper - EP1-W Earth Pressure for Full Monitoring Period

5.4 Story County 118

Story County 118 (Story) is a new construction bridge located near Ames, Iowa chosen for monitoring due to its tied approach slabs. The bridge is 374.5’ x 60’ and carries two lanes of northbound traffic on I-35 over the Skunk River using four spans. The bridge uses integral abutments at both ends with approach slabs attached using inclined tie bars. Approach slabs are supported by inverted-T sleeper slabs at the other end (Figure 5.24). Sleeper slabs exist to support the end of the approach slab away from the deck and minimize the effects of settlement of fill below the slab. The instrumentation plan can be seen in Figure 5.25. Both the North and South end of the bridge were outfitted with identical sensors. Due to the symmetric nature of the bridge, it is expected that behavior will be identical. In the event of any sensor malfunctions there will be no loss of critical data. Strain gauges were placed throughout the slab across the width and at both ends near the abutment and the sleeper slab. These gauges should capture axial strain and force in the slab due to temperature effects, along with any bending. Three strain gauges were also placed on the tie bars connecting the approach slab to the abutment in an attempt to capture the axial forces in those bars. A total of twelve strain gauges were placed in each approach slab. Four crackmeters were installed at each bridge end to measure joint movement of both the abutment-to-approach joint and the approach-to-sleeper joint.

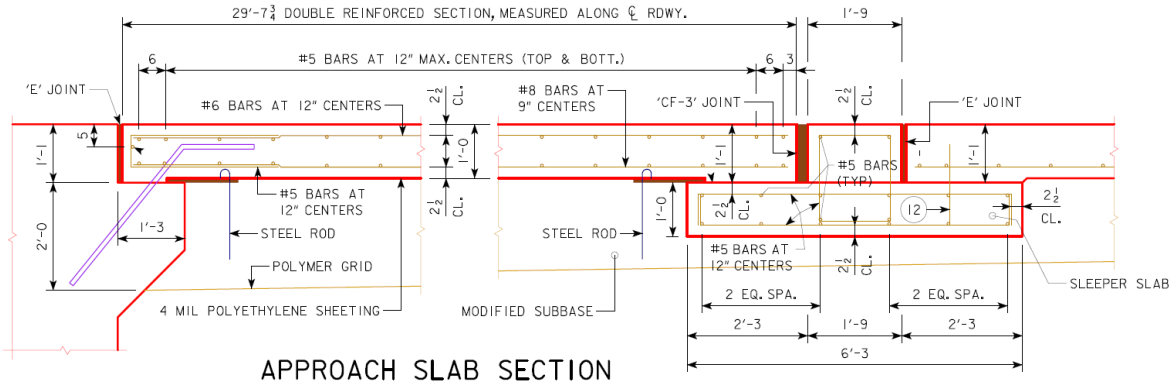

Figure 5.24. Story - Approach Slab Section and Dimensions (Iowa DOT)

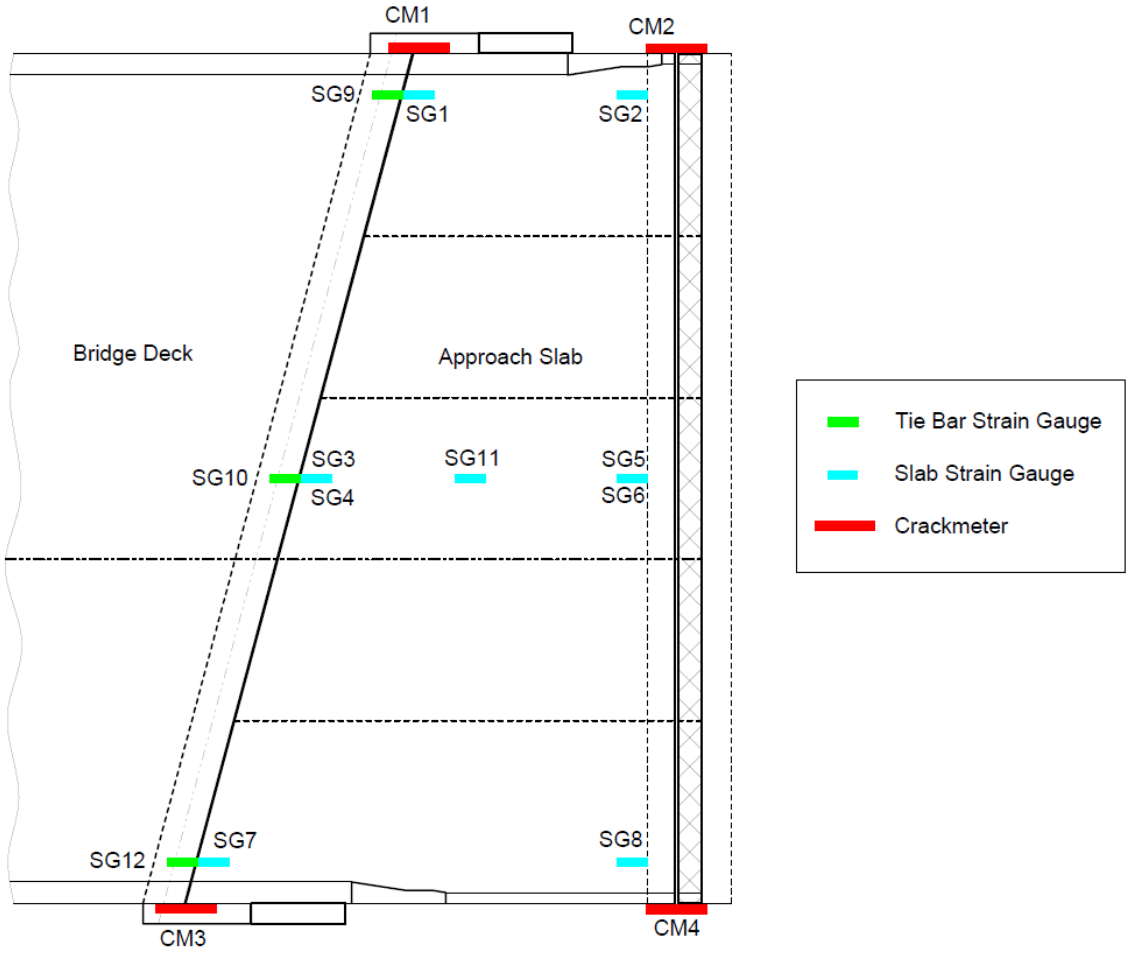

Figure 5.25. Story - Approach Slab Instrumentation Plan

5.4.1 Story Strain Gauge Installation Process

Strain Gauges were installed in a similar layout to the previous bridge, Jasper County 118. Nine strain gauges were ziptied to longitudinal bars to measure strains in the longitudinal direction. Three gauges were placed on the bars tying the approach slab to the bridge abutment. The tie bars are inclined where they exit the abutment and strain gauges were attached as close to the joint as possible to measure axial strains in the bars (Figure 5.26). Approach slabs were poured in 2 sections and wires were run to a single location before exiting the slab.

Figure 5.26. Story - Strain Gauges Installed on the Longitudinal Rebar and Tie Bars

5.4.2 Story Crackmeter Installation Process

Four crackmeters were placed over joints in the concrete barrier rail (Figure 5.27). The majority of the barrier is continuous with the bridge deck while the end portion rests on the approach slab. Any movement at the roadway joint will match the movement between the

barrier segments. Placing the crackmeter on the exterior protects it from any potential impacts or debris. One crackmeter was placed at each of the 4 corners of the bridge. Joint measurements on either side should be extremely similar if not identical; however, due to the 15° skew of the bridge both sides were measured to monitor any variations. The installation process consisted of placing one anchor, determining the location of the other anchor by reading the sensor output using a VW reader, placing the second anchor, installing the sensor, and installing a metal cover. The crackmeters were installed at 25% of their total 2" range since temperatures were between 25° and 30° F. Since the maximum expected movement at any one joint is only 1.2", there was adequate room for movement in both expansion and contraction of the joint.

Figure 5.27. Story - Crackmeter Installation across the Barrier Rail Joint

Four additional crackmeters were placed to measure the approach slab to sleeper slab joints. For the crackmeters to avoid interfering with the road surface, they were placed on the sides of approach slabs (Figure 5.28). Wooden blocks were placed at the corners of the slabs where they overlap with the sleeper slab before pouring concrete, so they could be pried out after curing to reveal a space for crackmeters. This location and method allowed for the installation to be flush with the side of the slab and avoid interference with any posts driven into the soil to support the metal barrier railing. Accessing the "blockout" locations required digging large holes in two locations and breaking through a large amount of excess concrete in another. This excess concrete was leftover as a result of the placement of the concrete barrier rail and had buried a bundle of strain gauge wires at one corner of the bridge. Fortunately, the concrete was broken up with no visible damage to the wires.

Figure 5.28. Story - Crackmeter Approach Slab Side Blockout Location

5.4.3 Story Datalogger Installation

Delays in the construction of the Story County 118 bridge on I35 resulted in the final crackmeters being installed in January. The winter temperatures in Iowa during the month of January rarely reach above freezing making installation of a datalogger all but impossible due to the fine motor skills necessary to strip and attach the sensor wires to the logger itself. The wires from all sensors were tacked to the bridge to organize them and lengths were cut at a central location which would be the future location of the logger. Temperatures through the winter remained too low for the installation of the logger since it requires fine motor skills to correctly organize and connect the tiny wires. The datalogger was installed on March 21st, 2019 in reasonable temperatures and without any precipitation.

5.4.4 Story County 118 Data Collection and Processing

Data was retrieved from the logger on May 7th, 2019, eight days after installation. The logger records measurements every hour providing 942 data points for 32 different sensors. Records for crackmeter CM4-S were deemed unusable even after wiring was checked after initial problems upon datalogger installation. Temperatures over 190° F and expansion readings over 4” are not consistent with the other sensors of the same type. All other sensors appeared to be functioning correctly.

Analysis of the Story bridge instrumentation data begins with examining the temperatures experienced by the bridge over the weeklong time period from March 22nd to March 30th, 2019. Air temperatures were taken by the datalogger itself which is placed on the abutment face, protected from sunlight. The crackmeters may see sunlight depending on the time of day and season due to their locations at each of the four corners; however, each crackmeter was installed with a steel angle cover which blocks any direct sunlight. Even though the ends of the covers were left open they may see minimal amounts of indirect

heating from sunlight on the cover. The minimum air temperature reached was 25.8° F on 3/31/2019 and the maximum of 85.2° was reached on 4/21/2019 (Figure 5.29). Concrete temperature taken by averaging strain gauge temperatures is also included in the plot with air temperature. The same relationship between the two from the Jasper bridge can be seen. Concrete has a thermal inertia due to its insulation properties and does not react to changes in air temperature immediately. The maximum and minimum concrete temperatures also are smaller in magnitude. Maximum concrete temperature was 72.6° F, 12.6° less than the maximum air temperature. The minimum concrete temperature of 35.6° is 9.8° higher than the minimum air temperature. Relatively cloudy weather during the monitoring period prevented concrete temperatures from reaching higher peaks due to direct sunlight.

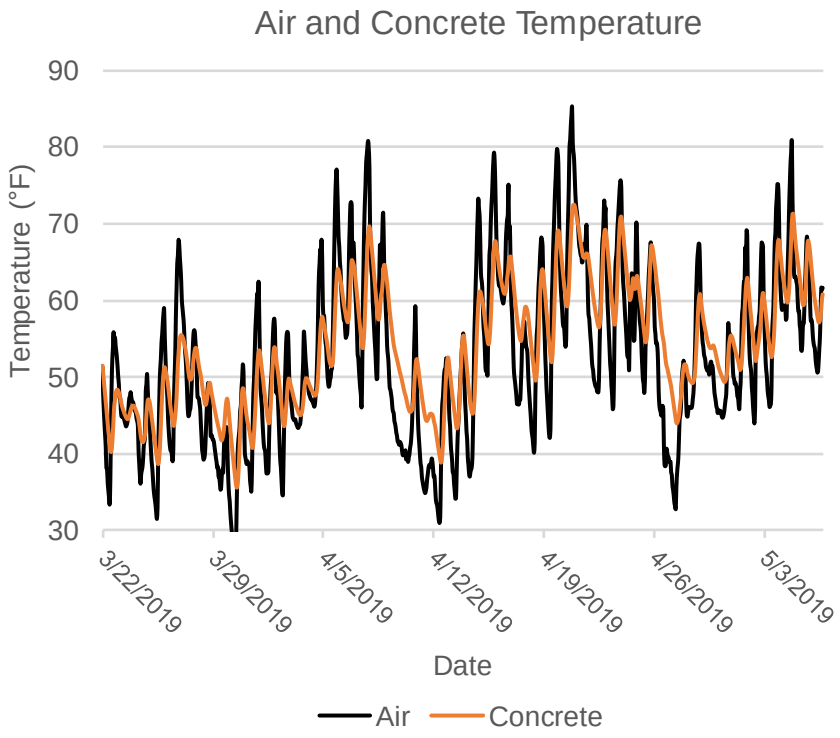

Figure 5.29. Story - Air and Concrete Slab Temperatures

Placement of crackmeters on both joints at either end of the bridge approach slabs allows for calculation of relative and absolute displacement of the bridge super structure and both approach slabs. The sleeper slabs at either end of the bridge are assumed to be stationary. Using displacements and theoretical expansion of the approach slab, the total expansion of the superstructure can be determined (Figure 5.30). Expansion is plotted using the start of the monitoring period as zero displacement. Crackmeter data from the East side of the bridge (CM3-N, CM4-N, CM1-S, CM2-S) was used since CM4-S did not function correctly. Approach slab expansion was calculated in the same manner as bridge expansion using a coefficient of thermal expansion of 6e-06 /°F. Due to the 15° skew of the Story bridge, total approach slab length on each side of the bridge is 56'11". The sum of expansion in crackmeters minus the theoretical expansion of approach slabs leaves the amount of expansion that can be attributed to the superstructure. Theoretical bridge expansion is calculated in the same manner as for the Jasper bridge using a length of 375'. Temperatures for expansion calculations used average concrete temperatures from the slabs instead of air temperature. The temperature of the precast prestressed concrete girders used for construction of the story bridge more closely match the temperatures of the slab for the same reason that a lower temperature range is used for calculating maximum expansion. The relationship between temperatures within concrete members and the air temperature has been discussed previously.

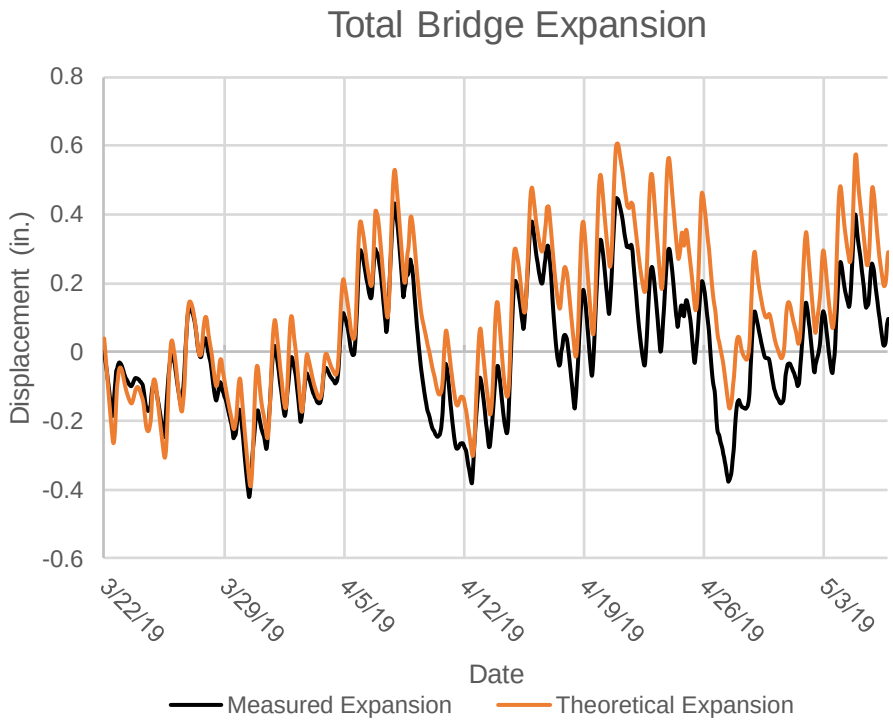

Figure 5.30. Story - Measured and Theoretical Longitudinal Bridge Expansion

Discussion of crackmeter data begins with the three operational crackmeters placed between the approach slab and sleeper slab (CM2-N, CM4-N, CM2-S). Figure 5.31, Figure 5.32, and Figure 5.33 show joint expansion against concrete temperatures to envision joint movement with expansion and contraction of the bridge. Positive values correspond to bridge contraction in which the approach slab pulls away from the sleeper slab. Generally negative values are expected since crackmeters were installed during temperatures lower than the monitoring period so the bridge would have expanded and pushed the approach slab towards the sleeper slab. CM2-N and CM4-N show a strong linear relationship with temperature indicating the joint opens and closes depending on expansion of the bridge. CM3-N shows similar behavior minus a flat portion at its most negative expansion. It is possible the sensor bottomed out at a lower limit due to installation issues with the slab pushing the anchorage

hardware used to attach to the sleeper slab. CM3-N was not used for calculation of bridge expansion. Overall the joints between approach slabs and sleeper slabs appears to be functioning correctly in terms of the movement that is supposed to be accommodated at that location. Physical condition of the CF-3 joints at those location should be monitored for performance and ability to prevent surface water intrusion.

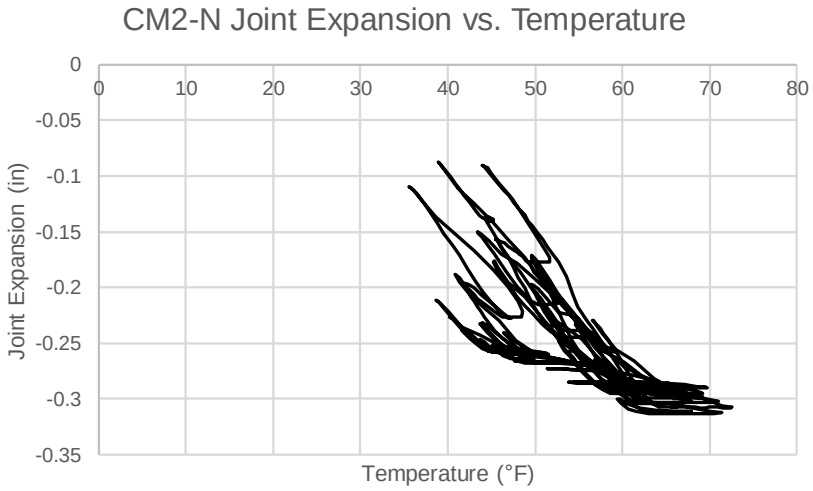

Figure 5.31. Story - Approach Slab to Sleeper Slab Joint Expansion

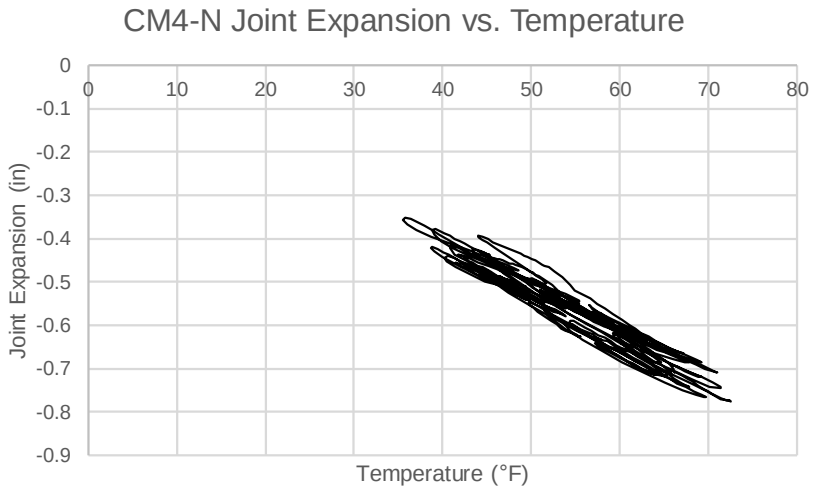

Figure 5.32. Story - Approach Slab to Sleeper Slab Joint Expansion

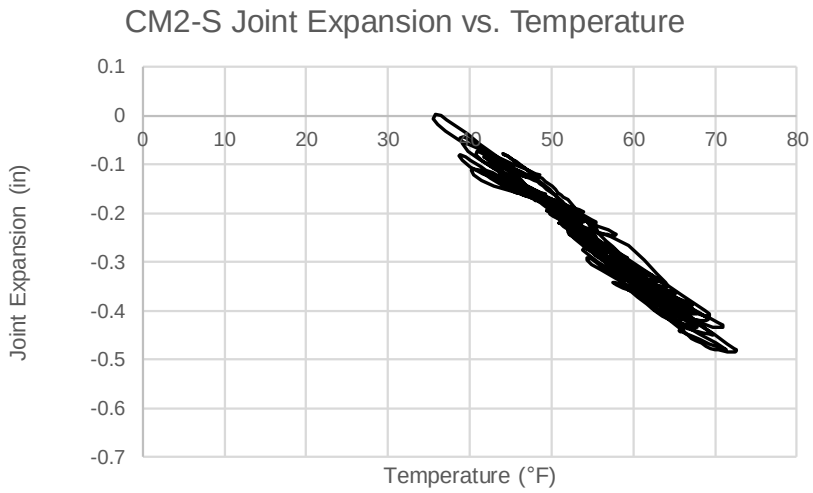

Figure 5.33. Story - Approach Slab to Sleeper Slab Joint Expansion

Crackmeters placed between the main bridge barrier rail and approach slab rail section will continually provide extremely valuable data on the tied approach slab joint over the entire long-term monitoring period of the bridge. These crackmeters directly measure an aspect of the bridge that contributes greatly to overall service life by preventing or allowing infiltration of water from the bridge surface into the embankment behind the bridge abutment. In a perfect scenario, the tie bars would not allow any relative movement between the approach slab and the abutment. The data recorded by each of the four crackmeters shows that is not the case (Figure 5.34, Figure 5.35, Figure 5.36, and Figure 5.37). All four crackmeter plots for CM1-N, CM3-N, CM1-S, and CM3-S have been corrected to use zero expansion for the joint condition at the time of installation and are plotted with the average concrete temperatures on the X-axis. CM3-N and CM1-S were installed on 12/13/2018 when temperatures reached a high of 38° F. CM1-N and CM3-S were installed on 1/17/2019 when temperatures reached a high of 29° F. All four crackmeters share two common trends and show similar behavior and shape in the curves where temperatures reached a maximum of

over 72.6° within the concrete approach slabs. The first is that joint expansion appears to be related to temperature which is apparent by the general negative slope of each of the four curves. As temperature decreases, the bridge contracts and pulls on the approach slab inducing tension. This behavior is not unexpected and should not cause a problem for the joint as long as stresses in the bars are not high enough to cause yielding and permanent deformation. Generally, the joints close when temperatures increase, and bridge expansion releases the force on the joint created by contraction. If the joints acted in a purely elastic fashion, the curves would only cross the X-axis at the temperature for which the crackmeters were installed. This is not the case and a zero reading at a higher temperature may indicate the fact that the ¼" joints may reach a limit where increasing temperature only serves to push the approach slab and further closure of the joint is not possible. Further monitoring through the summer will shed more light on long term behavior. The second trend shared by all crackmeters is that in the short period of data that was collected, all four crackmeter curves show a looping behavior in contrast with the linear behavior of the other set of four crackmeters. As the bridge switches from expansion to contraction or vice-versa the joint will open or close before the slab begins to slide in either direction. If repeated cycles result in increasing measurements at the joint the gradual opening of the joint could be seen over time. CM1-S especially seems to be exhibiting increasing joint widths over time as the looping behavior creeps in the positive direction with increasing temperature. A year of joint expansion data would prove very valuable in examining trends such as this.

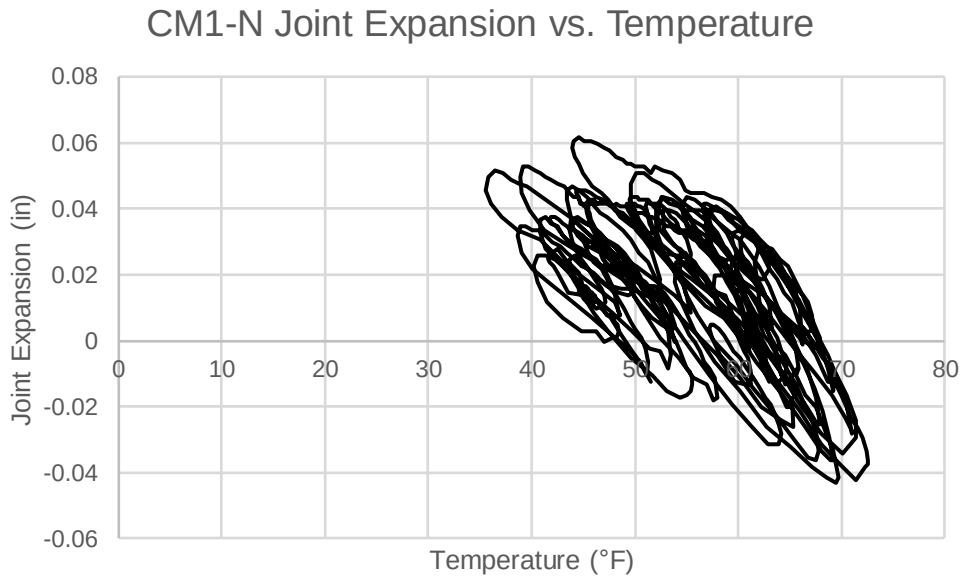

Figure 5.34. Story - Bridge Barrier to Approach Slab Barrier Joint Expansion

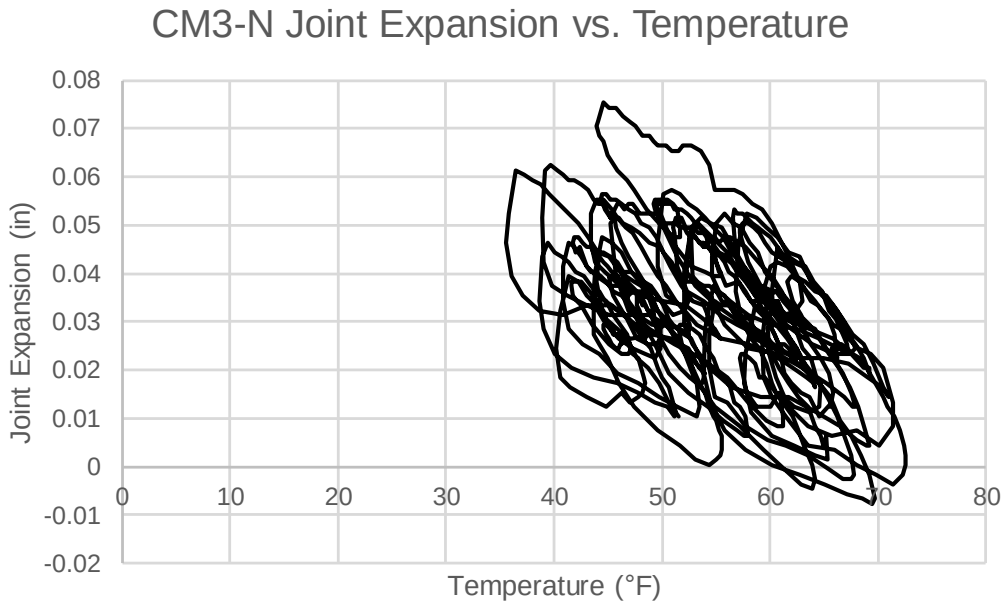

Figure 5.35. Story - Bridge Barrier to Approach Slab Barrier Joint Expansion

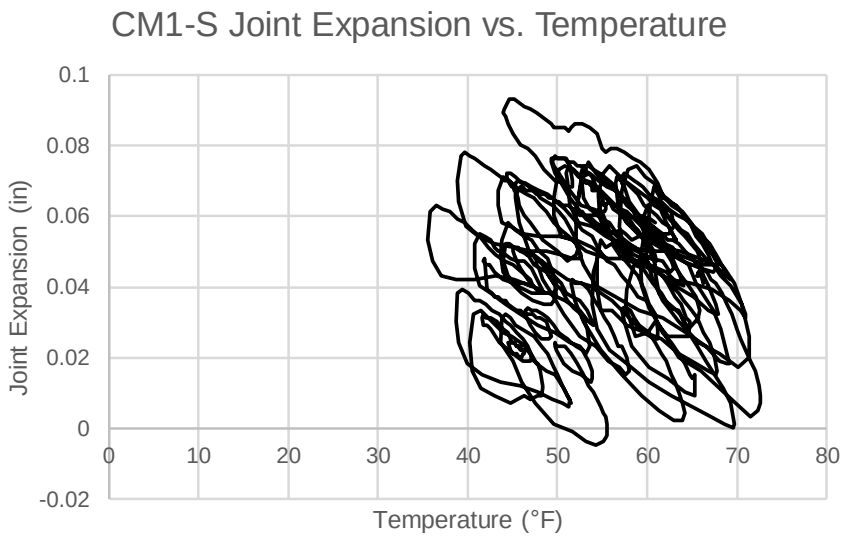

Figure 5.36. Story - Bridge Barrier to Approach Slab Barrier Joint Expansion

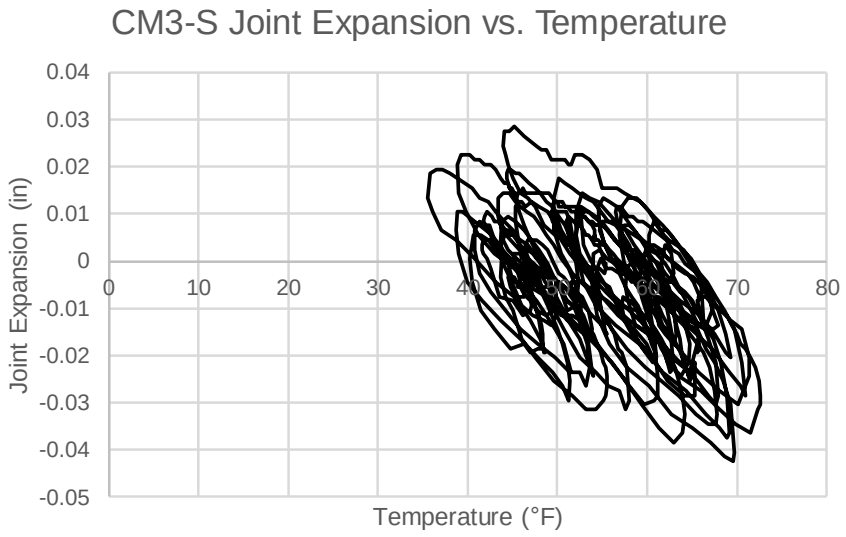

Figure 5.37. Story - Bridge Barrier to Approach Slab Barrier Joint Expansion

Initial lab strains show similar behavior for almost all the gauges embedded in the Story bridge approach slabs. Gauges show an expected response to temperature changes with a linear relationship. Slopes of trendlines vary from -1.5με/°F to -4.5με/°F depending on the gauge location. Plots of data from each gauge are not included for the sake of brevity, but a

representative set of data from SG3-N can be seen in Figure 5.38. A large set of strain data over a larger time period would prove beneficial and allow for more in-depth analysis. Five of the six strain gauges attached to the stainless-steel tie bars connecting the bridge abutment and approach slab do not appear to be functioning as intended. The gauges do not capture any trends in strain other than thermal expansion, like the gauges placed longitudinally in the slab. SG10-S is the exception and is located on the center tie bar of the South approach slab. A plot of strains in SG10-S versus temperature in Figure 5.39 show a curve very similar in shape to the one produced by crackmeter joint measurements seen previously. This point towards the fact that SG10-S may correctly be measuring strain in the tie bar. A comparison with strain taken from finite element modeling activities is available in Chapter 6. Based on the fact that the other five strain gauges (SG9-N, SG10-N, SG12-N, SG9-S, SG12-S) are not providing the desired measurements, the type of strain gauge used with tie bars should be changed for anticipated future monitoring plans for the other two bridges planned by Iowa DOT, Polk County 120/419 and Butler County 118.

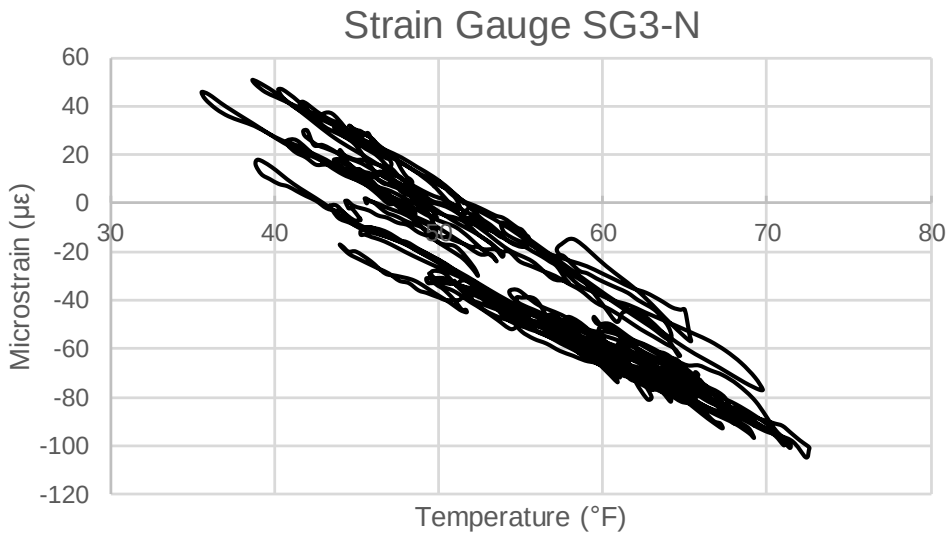

Figure 5.38. Story - Representative Slab Strain Gauge Behavior

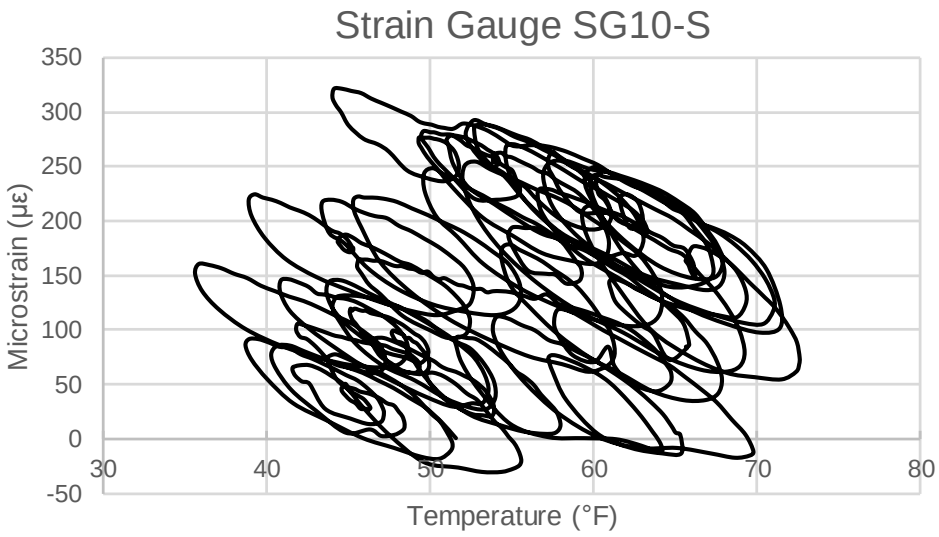

Figure 5.39. Story - SG10-S Measured Strains

5.4.5 Story Construction Issues

Several issues arose during the construction of the Story bridge that were observed while installing sensors both during construction and after opening of the bridge. The many issues apparent during construction of the bridge give credence to claims that poor approach slab performance when considering settlement is commonly due to poor construction (Yasrobi 2016, Dupont and Allen 2002). Improperly constructed bridge elements are not something that develops over time; they are present from the very beginning and can impact service-life immediately. In the case of Story County 118, a section of the concrete barrier rail was placed on the approach slab to allow for drainage continuity and direct water away from the bridge abutments and deck joints. Plans show the concrete curb formed up to the end of the barrier to create a continuous vertical surface; however, it appears formwork used for the barrier end has left a gap in the curb where it meets the barrier at each of the four corners of the bridge (Figure 5.40). Water will run through this gap into the embankment closer to the abutment than desired and avoid erosion control measures.

Figure 5.40. Story - Curb Gap at the Barrier End (Typical)

The Story bridge was opened for traffic with an open joint lacking joint filler at each end of both barriers shown in Figure 5.41; however, bridge plans indicate an ”E” joint in the concrete barrier wall between the main section and approach slab section (Figure 5.42);. Crackmeters were installed since it was apparent no further work would be completed. The open joints will allow snow and ice to fill the gaps possibly expanding and damaging the surrounding concrete. Longitudinal rebar in the barrier appeared to be continuous across the joint in multiple locations likely due to shifting during forming of the barrier. Vertical cracking appeared 1 month after bridge opening in the barrier near the joint location.

Figure 5.41. Story - Open Barrier Joint (Typical)

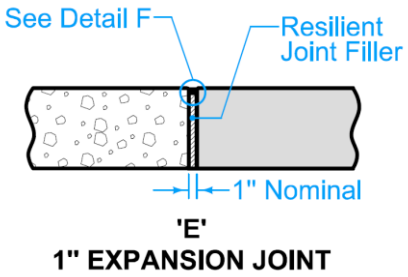

Figure 5.42. Iowa DOT "E" Joint (Iowa DOT)

Approach slabs were poured directly on the modified subbase fill without the use of the 4-mil polyethylene sheeting specified in the approach plans (Figure 5.43). Due to the large aggregate used for the modified subbase, there is a concern the concrete has penetrated the voids around the individual pieces and will cause an interlocking effect when the slab attempts to slide. This potential issue will become more apparent as time goes on and the tied approach connection is forced open by a slab that will not move as it was designed.

Figure 5.43. Story - Approach Slab Modified Subbase Condition Immediately before Concrete Pouring

The cause for most concern was a large void under the South abutment discovered in January while attaching wires to the bridge exterior (Figure 5.44). A large portion of soil

support under the Northwest corner of the South abutment had eroded leaving a large space many feet deep in the abutment footprint and at least one foot tall. Rebar was clearly visible protruding from the bottom of the abutment along with one of the foundation piles (Figure 5.45). A ribbed drain pipe ended directly at the void location, but it was unclear where it came from or if it was the reason for the erosion. Iowa DOT was notified of the issue and inspected the area of concern.

Figure 5.44. Story - Large Void under the South Abutment Corner

Figure 5.45. Story - Visible Exposed Rebar and Foundation Pile

CHAPTER 6. FINITE ELEMENT MODELING

Finite element (FE) models of Jasper County 118 and Story County 118 were created using Abaqus FEA software. The purpose of the models is to represent the behavior of the bridge approach slabs and their response to bridge thermal movement and allow for a parametric study by changing different model attributes. The models were limited to only the first section of the approach slab, the soil beneath the slab, and a portion of the abutment. The goal of the study does not include accurately modeling the thermal expansion of the bridge deck. The objective of the FE analysis is to take theoretical expansion of the bridge and apply that displacement to the abutment, simulating the bridge pushing/pulling on the approach slab while simultaneously including the appropriate temperature change that corresponds to the maximum bridge movement. Results are focused on the behavior of the approach slab itself and steel tie bars in response to thermal movement. Ideally, a FE model would be able to capture every aspect of approach slab behavior, but unfortunately simplifications must be made due to computational requirements and idealized material models. Concerns were raised at the outset of the project by Iowa DOT about the performance of approach slabs with regards to skewed bridges or other bridges not currently allowed to use tied approaches. It is clear that when performing properly, tied approach joints act less like a joint and more like a continuation of the deck. They can prevent water and deicing solution from leaking into the bridge embankment and help to avoid the associated issues. The FE models will help to illustrate how friction force is carried by the tie bars and give some insight into how bar type and skew affect behavior. Improvement in the performance of the tied approach joint is anticipated to improve bridge service life.

A three-dimensional model was chosen to allow for skew of the approach slab. 3D solid C3D8R elements were used for both the concrete approach slab and the soil below to allow for frictional contact between the two surfaces. A 2D model allows for modeling of a deeper depth of soil under the approach slab and more accurate soil behavior and interaction with the abutment; however, a two-dimensional model does not in any way allow for bridge skew other than 0°. It was also determined that replacing the soil with properly calibrated spring elements would not provide the same effects as a solid element with frictional contact, since friction is a nonconservative force.

6.1 Jasper County 118 FE Model

Model formation began with geometry taken from the Jasper Co 118 plans. The approach slab and abutment are 28’ wide to match the lane width of the bridge. A 10” thick trapezoidal shape approximates the geometry of the approach slab. A large soil block was created in the same shape, and the cut geometry function removed any overlapping volumes between the soil and both approach slab and abutment to simulate good compaction against all surfaces with no voids. The model geometry can be seen in Figure 6.1. All models align the centerline of the bridge roadway with the X-axis, vertical direction with the Y-axis, and the transverse direction with the Z-Axis.

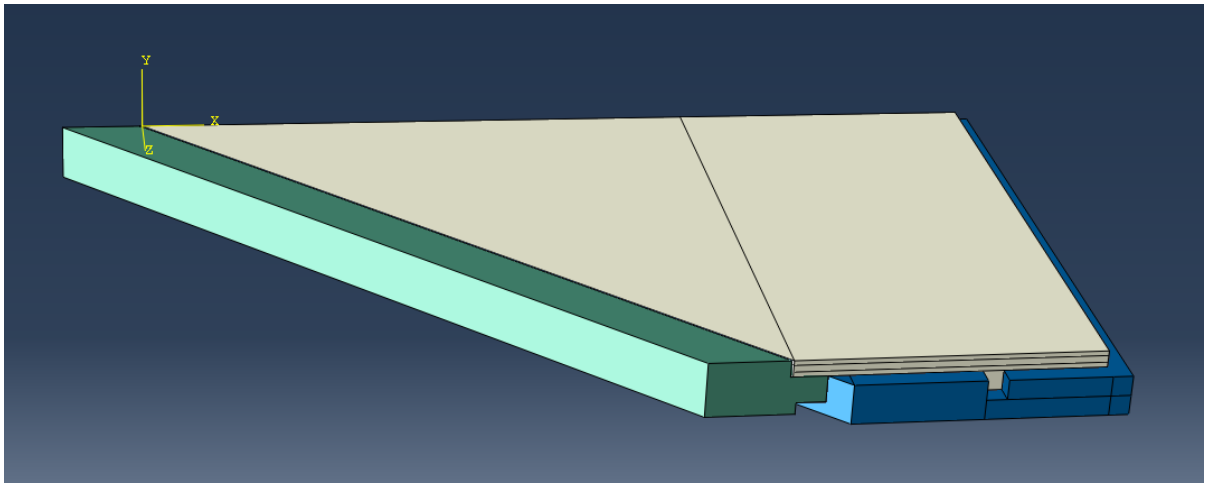

Figure 6.1. Jasper - Finite Element Model Geometry

6.1.1 Material Properties

A standard 4 ksi compressive strength concrete was created per the Jasper Co 118 bridge plans and applied to the approach slab and abutment. Young's Modulus of 3605 ksi and Poisson's ratio of 0.3 were used for linear elastic behavior. Concrete stresses are expected to remain low and given the scale of the model, the use of a "concrete damaged plasticity" model in Abaqus was deemed unnecessary and unattainable. Soil properties represent typical values for the "modified subbase" used by Iowa DOT under approach slabs. Correspondence with Iowa DOT provided a compacted unit weight of 140 pcf. A gradation table per Iowa DOT Article 4109.02 is provided in Table 6.1. Figure 6.2 shows the limits provided by the gradation table plotted on a grain size distribution chart. Classification using the Unified Soil Classification Chart (ASTM D2487) determines the modified subbase is a coarse-grained soil. Based on the fact that the curves provided fall mostly below the point included in red that corresponds to the #4 sieve and 50% passing, it is likely most subbase material would be classified as a well-graded gravel (GW) or poorly graded gravel (GP). Modulus of elasticity was taken to be 20 ksi after finding a range of values from 14-30 ksi in

available literature for compacted gravel (Kaniraj 1988), along with 0.35 for the gravel Poisson's ratio. Soil behavior was limited to linear elastic due to the nature of the analysis being performed and the desired results. The 3D soil elements are present only to provide the frictional surface to interact with the bottom of the approach slab simulating the friction between the approach slab and the soil beneath. The bearing capacity of the soil is of no concern nor is the soil properties effect on the expansion of the bridge, since the expansion displacement is applied to the model as input. The vertical loading consists only of self-weight of the slab and the 3D solid elements chosen for representation of the soil provide minimal settlement of the approach slab.

Table 6.1. Iowa DOT Modified Subbase Gradation

Sieve	Size (in)	Size (mm)	Percent Passing
1 1/2"	1.5	38.1	100
3/4"	0.75	19.1	70-90
#8	0.093	2.38	10-40
#200	0.0029	0.074	3-10

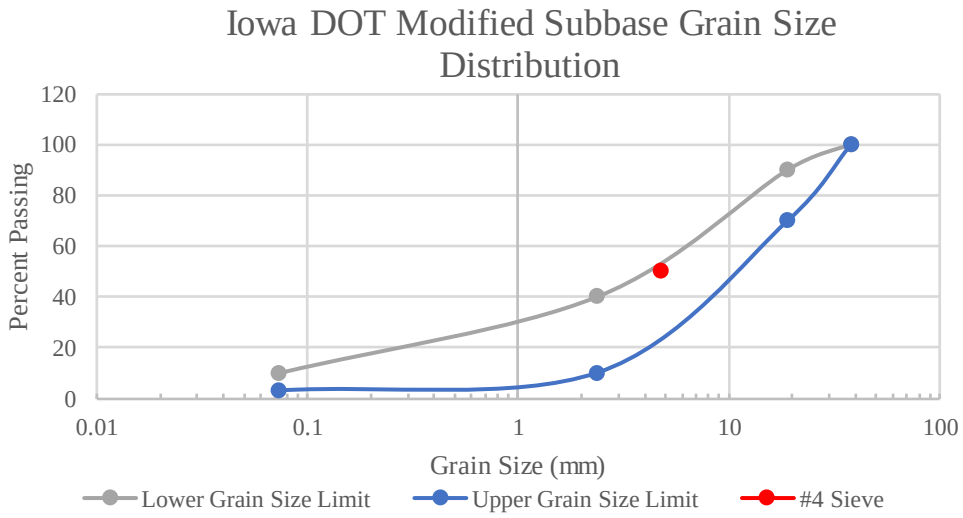

Figure 6.2. Iowa DOT Modified Subbase Grain Size Distribution

6.1.2 Element Meshing

Element meshing was completed part by part (Figure 6.3). Due to the 45° skew it was extremely difficult to maintain properly shaped elements and avoid poor element shapes. Approach slab and soil meshing proved to be more difficult than that of the abutment. Partition planes were used to divide the parts into segments. For the approach slab, partitions were used to split the part into a large triangular piece and several long rectangular pieces. The soil part was split up in a similar fashion. A size control applied after partitioning resulted in the desired mesh. Some elements produced warnings of poor shape; these elements occurred in the triangular portions of the parts and an effort was made to adjust them. The approach slab and soil mesh sizing were chosen to be the same size in order to provide better contact simulation results.

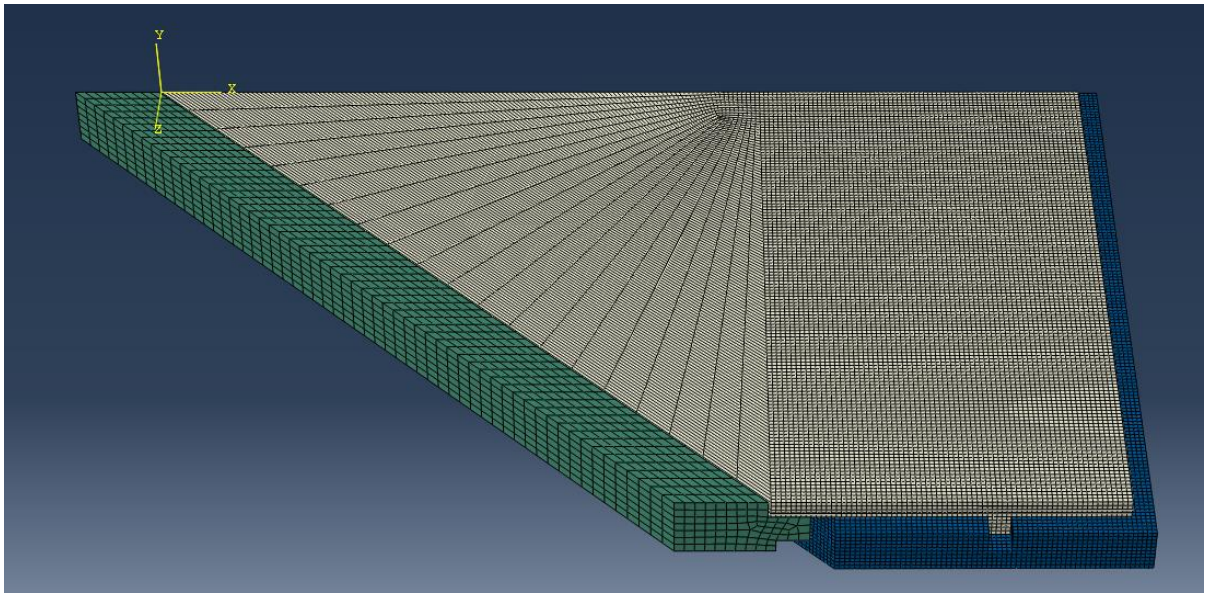

Figure 6.3. Jasper - Finite Element Model Mesh

6.1.3 Boundary Conditions

Boundary conditions applied to the model aim to replicate the real-life support conditions of the bridge (Figure 6.4). The base of the soil was fixed for all translation, and

the sides of the soil not in contact with the abutment or footing were fixed in translation in X or Y to “contain” the soil within an imaginary box. No boundary conditions were placed on the approach slab itself; however, the soil lug held the approach slab in place and prevented translation in the X direction.

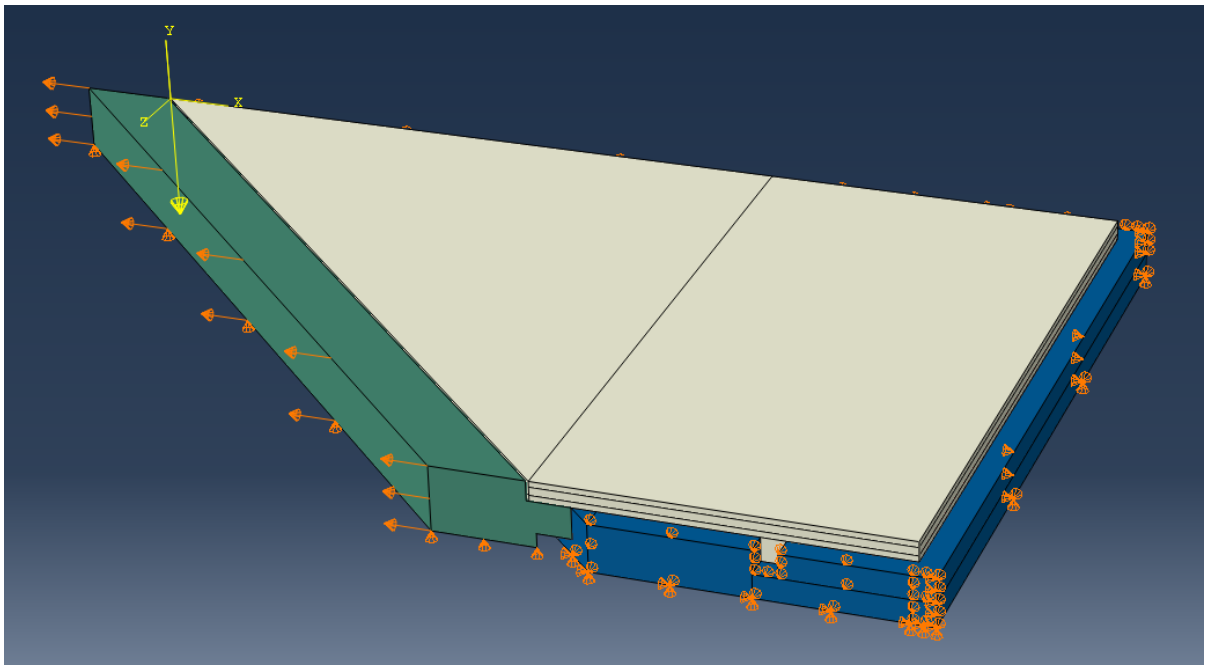

Figure 6.4. Jasper - Finite Element Model Boundary Conditions

6.1.4 Loading

Loading began with Step 1 of the model introducing gravity loads. Since Abaqus is unitless, verification was required to check that gravity was working as intended. The material density for concrete was set to 0.087 and the gravity set to -1 in the negative Y direction, so that when multiplied together they produce a unit weight of 0.87 pounds per cubic inch, equaling 150 pounds per cubic foot. As a test, a non-skewed 10” thick concrete slab was simply supported along 2 edges with gravity loading applied. The support reactions at either end matched the expected values and the deflection in the center of the slab matched the expected value for a beam to within 5%. The second loading step applied is a temperature

change applied to make the slab shrink or expand. The same test slab shrunk as expected based on calculations using the concrete coefficient of thermal expansion of $6.0x10^{-6}$ /°F. Loading applied to the full-scale model included both contraction and expansion with full temperature changes applied to the concrete elements. Negative temperature loading is applied with simulated bridge contraction, and positive thermal loading with simulated bridge expansion. Full longitudinal movement was calculated as 2.16" per Iowa DOT LRFD Bridge Design Manual 5.8.3.1.2 for the Jasper bridge using a 184.5' length. Typically, only half the length would be used for a symmetrical bridge, but Jasper is designed to accommodate all expansion at the East end. Spring elements were added in the Z direction to the ends of the Abutment and calibrated to provide the correct Z displacement per unit X displacement. The Jasper bridge instrumentation data indicated that for that bridge, transverse (Z) displacement equals 81% of longitudinal (X) displacement. Live loading was not included in analyzing approach slab movement. Temperature changes at an extremely low rate with one cycle per day. Live loading does not have any effect on bridge expansion which is determined only by material properties and geometry. Vehicular loads were not apparent in the instrumentation data from the bridges used to calibrate the models since data is taken hourly. The models are not intended to capture the vertical load carrying capacity of the approach slab or soil.

Bridge expansion loading provides conservative tie bar and concrete stress results due to the behavior of the soil block. The limited depth of the soil block and Y support conditions used mean that any vertical expansion of the soil block due to Poisson's effect is upward. The upward deflection lifts the approach slab upwards creating additional force on the tie bars not seen in the bridge contraction case. The models show similar behavior through the

first increments of expansion or contraction as full friction force is realized and the slab begins to slide. Results diverge between the two cases as displacement reaches its maximum. Ideally, the full depth of abutment and soil would be modeled allowing for better stress distribution which is possible in a 2D analysis but not feasible for a 3D analysis such as this one. The type of loading simulated by the expansion case is as if a bridge were to be constructed during the coldest day of the year and experience increasing temperatures only until the warmest day of the year. This is not the case as temperatures have been shown to not only experience seasonal cycles, but shorter daily cycles as well (Greimann et al. 2008). Section 5.7.2.4 of the Iowa DOT LRFD Bridge Manual dictates that design of expansion joints should consider a construction temperature of 25 to 75°F. The perfectly mated contact surfaces of FE models simulate perfect compaction, which becomes especially difficult near the abutment face and when corbels are present to support approach slabs. Ignoring the lifting effect of compressed soil on the approach slab, bridge expansion serves to close the tied approach joint which is a desirable outcome. Lateral opening of the joint is the primary concern and thus higher importance is placed on various results for the bridge contraction case with negative thermal loading.

6.1.5 Surface Contact

Contact surface pairs were identified between the approach slab and soil, approach and abutment, abutment and soil, and abutment and footing. Two different contact properties were created for concrete-to-concrete friction and concrete-to-soil friction. The general contact function of Abaqus provided a satisfactory method due to the simple geometry of the contact surfaces of the model. A coefficient of 0.6 was assigned to concrete-to-concrete contact per ACI 318-14 Table 22.9.4.2, and a coefficient of 0.55 for concrete-to-soil was used to represent concrete on gravel or coarse sand (Potyondy 1961). Abaqus contact

behavior was tested using a simple rectangular member placed onto another member of the same size. After gravity was applied to initiate contact between the two surfaces, the top member was displaced laterally a distance of 1". The theoretical friction force was calculated as the weight of the member, 1250 lbs, multiplied by the friction coefficient of 0.5. The load-displacement data for the incremented displacement showed a force nearly identical to the calculated value of 625 lbs after ramping up almost immediately from zero which was maintained through the rest of the movement (Figure 6.5). This behavior show the Abaqus "penalty" frictional behavior used works as intended by maintaining a constant force after slippage occurs.

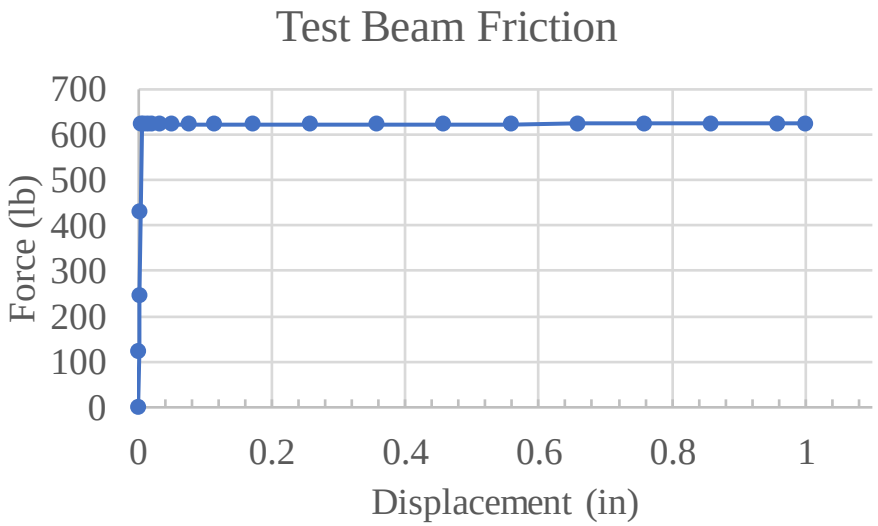

Figure 6.5. Abaqus Friction Behavior Verification

6.1.6 Slab Rebar

Abaqus allows for the modeling of rebar using multiple different methods. Elements can be embedded within others to constrain their translational degrees of freedom. The embedded elements must lie completely within the host elements, as rebar does within concrete. The element type chosen for the slab was a SFM3D4 surface embedded within 3D

solid elements. The surface section properties allow for input of a rebar material, area per bar, bar spacing, and bar orientation. The inputs convert the bar inputs into shell elements of an equivalent thickness of steel spread over the surface area. Using bar orientations of 0° and 90° allows for specification of longitudinal and transverse bar layers according the local part coordinates. A simple test beam confirmed the effect of layer orientation where displacement and stress results matched plain concrete with bar orientation set to 90°, and both stress and displacement decreasing with orientation set to 0°. Two different surfaces were used, one for the upper layers of bars and one for the lower layers of bars per the Jasper County 118 plan set. Surface depths within the set were determined by the clear cover given in the plans and the longitudinal bar diameter to result in surfaces placed at the centroid of the longitudinal bars.

6.1.7 Model Calibration

Strain gauge data was used for calibration of FE models using temperature changes and corresponding strain values to determine appropriate coefficients of thermal expansion. The use of air temperature values was deemed inappropriate since the temperature of the slab does not match the air temperature due to thermal inertia. The temperature of the slab lags slightly behind the air temperature since it takes time for heat to transfer through the depth of the 10” approach slab where the strain gauges are located. For this reason, an average temperature of both the East and West approach slabs was calculated using an average of the thermistor values for all strain gauges embedded in the slabs.

Strain values in the X direction were extracted from the model results for the locations of strain gauges placed in the instrumented Jasper County 118 bridge. The temperature ranges for each month of instrumentation along with the single daily highest temperature change were extracted from the thousands of data points available. Data for all

ten strain gauges provided a corresponding strain value, and the temperature change was used to back-calculate an equivalent α value for each strain gauge. Alpha (α) values generally agreed with each other, except for SG9-E which exhibited extremely low strains no matter the time period or temperature change that was examined. In general, back-calculated α values were on the order of $2x10^{-6}$ /°F for the day with the largest temperature change. These numbers did not match the initial model results of strains corresponding to α values of $6x10^{-6}$ /°F. The same back-calculation of α done for the model output results produced values very similar to the material property input value, indicating the model slab expands and contracts freely, with no discernable impact from friction with soil. The instrumentation data shows that there may be other factors influencing expansion that cannot be captured in the model, which is to be expected given the scope of the model and simplifications made for modeling. Different time periods for strain gauge data were examined by calculating a running α value based on the strains for the last 24 hours at each hourly data point. Alpha (α) values for each strain gauge reached a maximum of $7.77x10^{-6}$ for SG5-E with typical maximums around $6.0x10^{-6}$ for the other gauges, minus SG9-E which did not appear to be performing correctly. The Federal Highway Administration (FHWA) provides a range of expected thermal coefficients of thermal expansion for different materials including aggregate, cement, and concrete. Since concrete composition varies greatly between batches and even within a single slab, the FHWA gives a typical range of 4.1-7.3 10^{-6}/°F for concrete. An α value of $4.1x10^{-6}$ was adopted for use in the model since it was clear the slab was expanding and contracting on the lower end of the FHWA range. A comparison of all measured and FE α values is available in Figure 6.6. Other properties like surface friction coefficients cannot be calibrated

correctly with the data provided from instrumentation, so they must be taken from literature and can be varied as part of a parametric study.

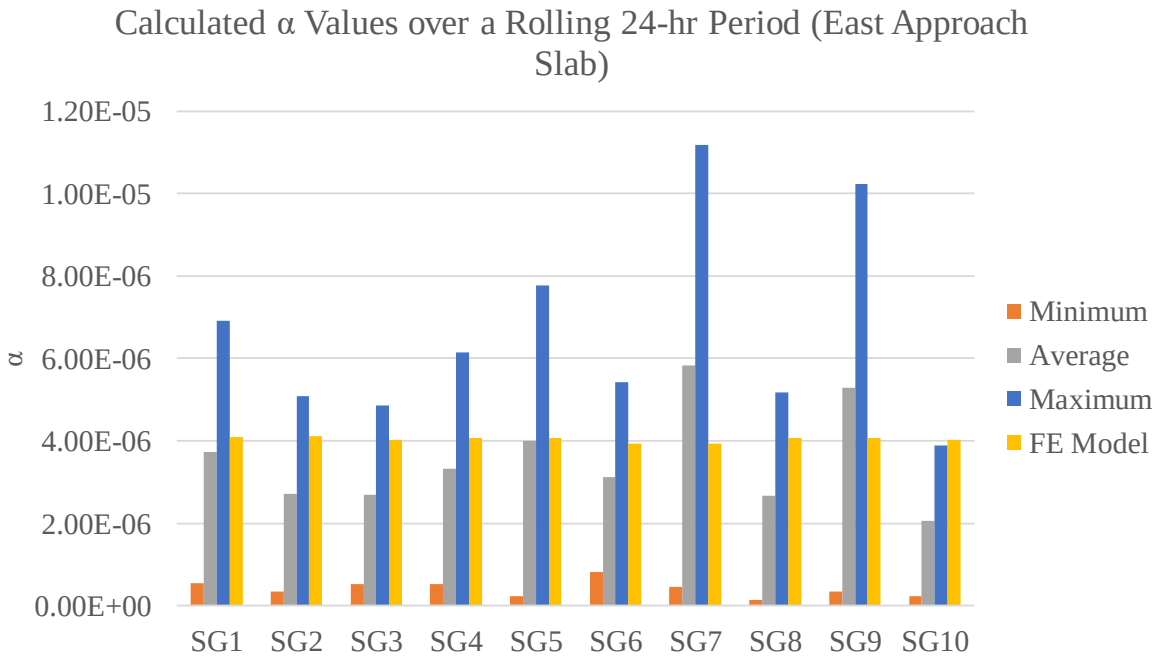

Figure 6.6. Jasper - Equivalent Thermal Coefficient of Expansion

6.1.8 Jasper County 118 FE Results

In order to study the effect of a tied connection on the slab in combination with a 45° skew, a second model was made to include a tied connection (Figure 6.7). The soil block dimensions are 1' wider than the slab on each side to allow for frictional sliding without loss of contact. The soil lug on the bottom of the slab was eliminated to create a smooth surface to allow sliding. In order to simulate a tied connection, the embedded element function was used again, in this case wires meshed with beam elements approximated the individual bars. The tie bar size, shape, and spacing was adopted from the Story County 118 plans resulting in angled #8 bars spaced 14.8" apart resulting in 23 bars across the joint width. The beam

elements were embedded in both the abutment and approach slab host elements (Figure 6.8). Applying a displacement in the negative X direction to the abutment pulled the slab with it as expected confirming the bars were working as intended tying the abutment and approach slab together.

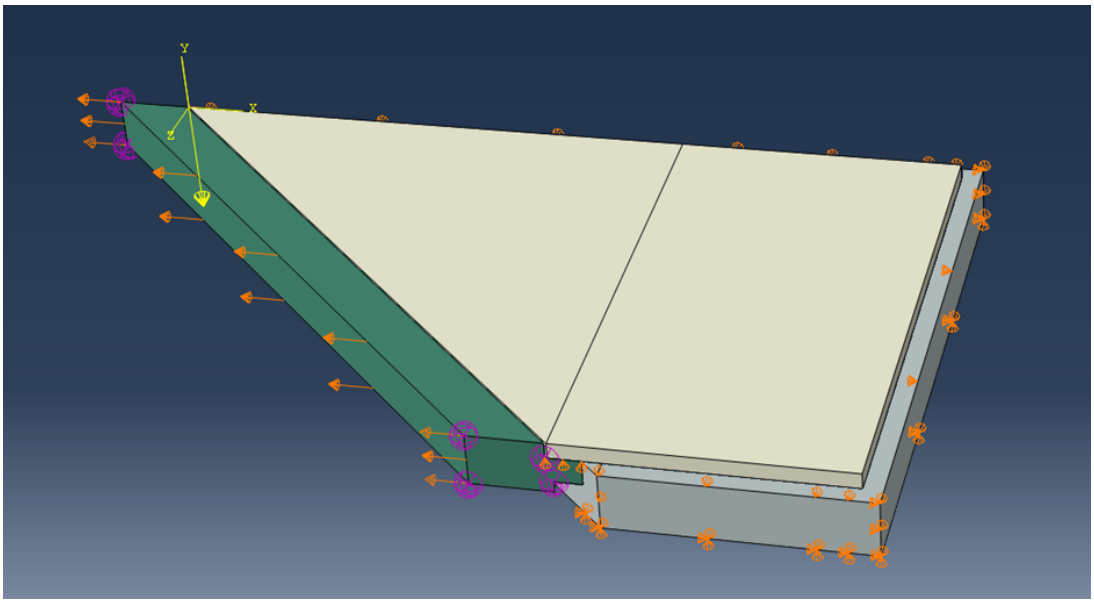

Figure 6.7. Jasper - Modified (Tied) Finite Element Model Boundary Conditions

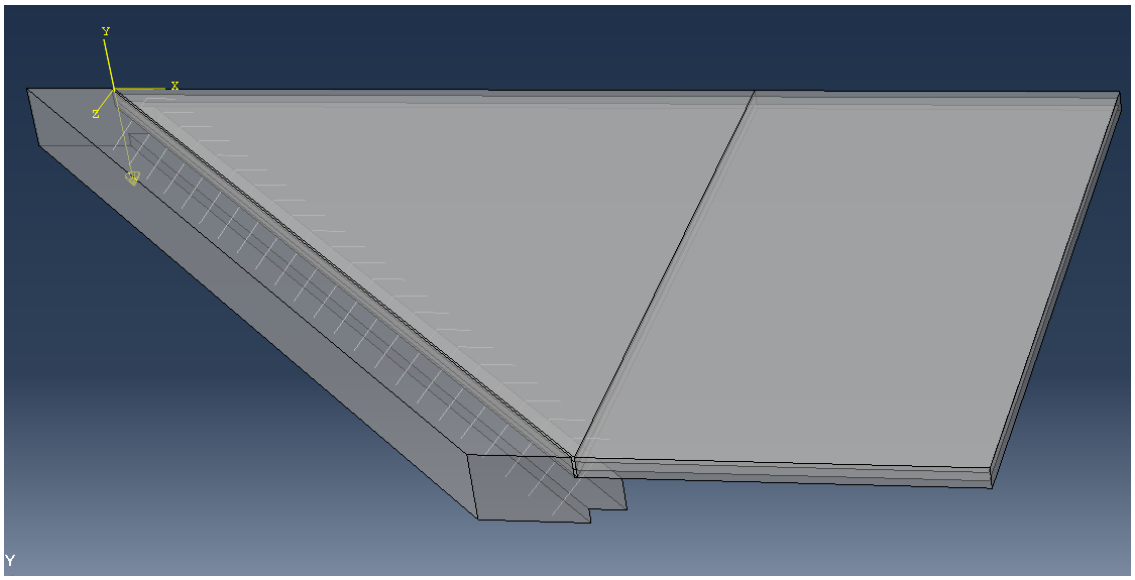

Figure 6.8. Jasper - Modified (Tied) Finite Element Model with Tie Bars

Since the tie bars and sleeper slab used in this modified model were not specifically designed for construction with the Jasper approach slab, they are not suitable for examination of any stresses of forces. They exist solely for the investigation of the displacement of a tied approach slab with 45° skew. The Jasper slab itself including thickness and rebar were not designed to be tied to a moveable abutment either; however, stress contours are extremely valuable for identifying critical locations and seeing trends that would not otherwise be present if not for the high skew.

Two different loading scenarios were applied to both the original (free) and modified (tied) models (Table 6.2). A positive thermal loading condition applied a temperature change of +100°, and a corresponding displacement of 2.16” in the positive X-direction to simulate expansion of the bridge superstructure which was calculated using a temperature change of +150° for steel girders. The opposite loading was applied to simulate bridge superstructure contraction under negative thermal loading.

Table 6.2. Jasper - Finite Element Model Load Cases

Load Case	Model	Abutment Movement	Thermal Loading
1	Free	Expansion	Positive
2	Free	Contraction	Negative
3	Tied	Expansion	Positive
4	Tied	Contraction	Negative

The high skew angle of the Jasper bridge results in the bridge displacements being of particular interest. The tied approach slab connection leads to the investigation of corresponding approach slab displacements. The same loading scenario and abutment movements for the two different models produced different approach slab movements. Free contraction loading in Case 2 show the slab’s soil lug works as intended by holding the slab in place and pulling the outer edges of the slab to a centroid located roughly in the center of

the slab width at the soil lug (Figure 6.9). Expansion Case 1 mirrors this behavior with the slab edges moving away from the same central location.

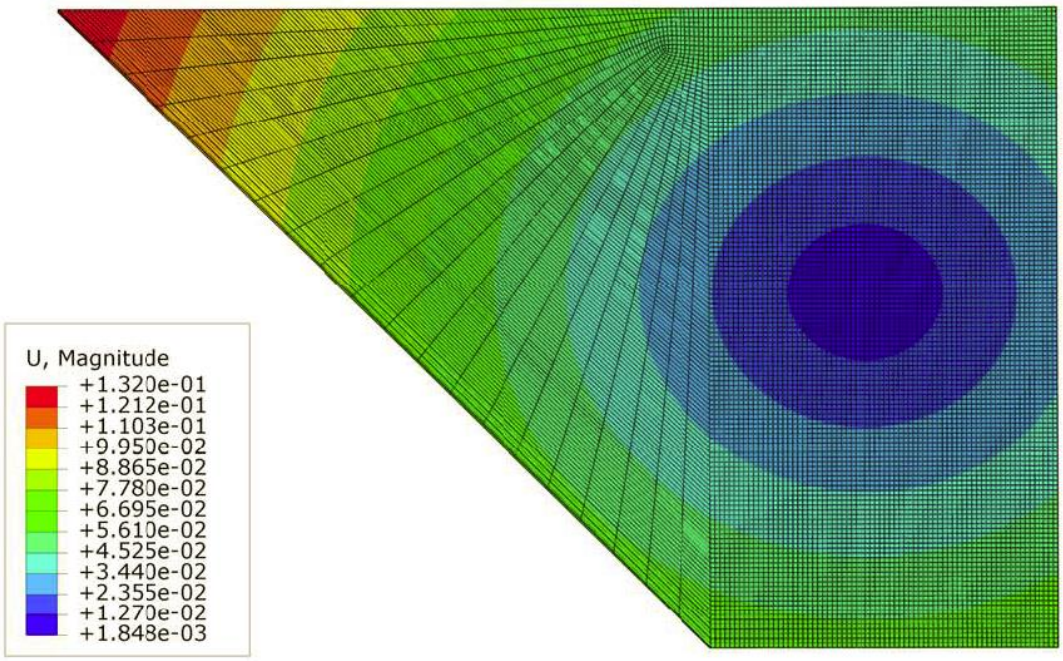

Figure 6.9. Jasper - Case 2 Displacement Magnitude

Displacement contour plots help to illustrate how the slab moves in response to both an applied displacement to the abutment and a temperature change. X-displacement for Case 3 shown in Figure 6.10 shows a range of 2.103” to 2.257”. The difference can be attributed to the expansion of the slab itself. The further reaches of the slab are pushed away from the joint indicated by the maximum magnitude located in the corner. Case 4 X-displacement values show a similar pattern (Figure 6.11) with values ranging from -2.159” to -2.325”. Contours are angled differently to Case 3 since Case 4 does not include a large transverse displacement at the abutment.

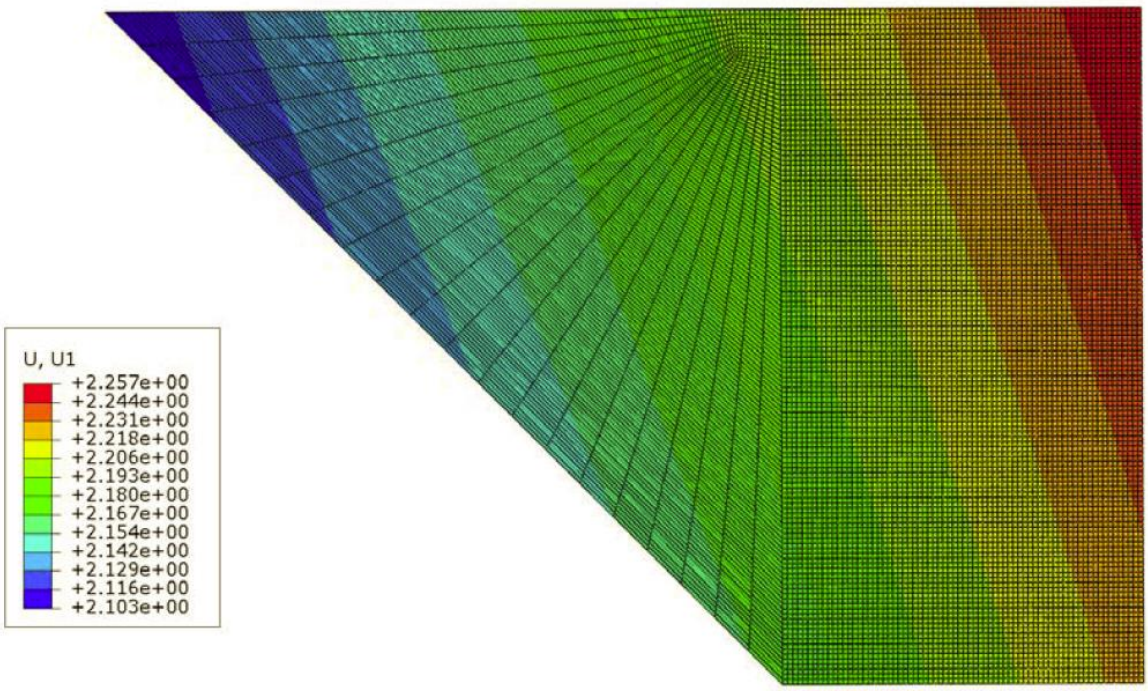

Figure 6.10. Jasper - Case 3 X Displacement

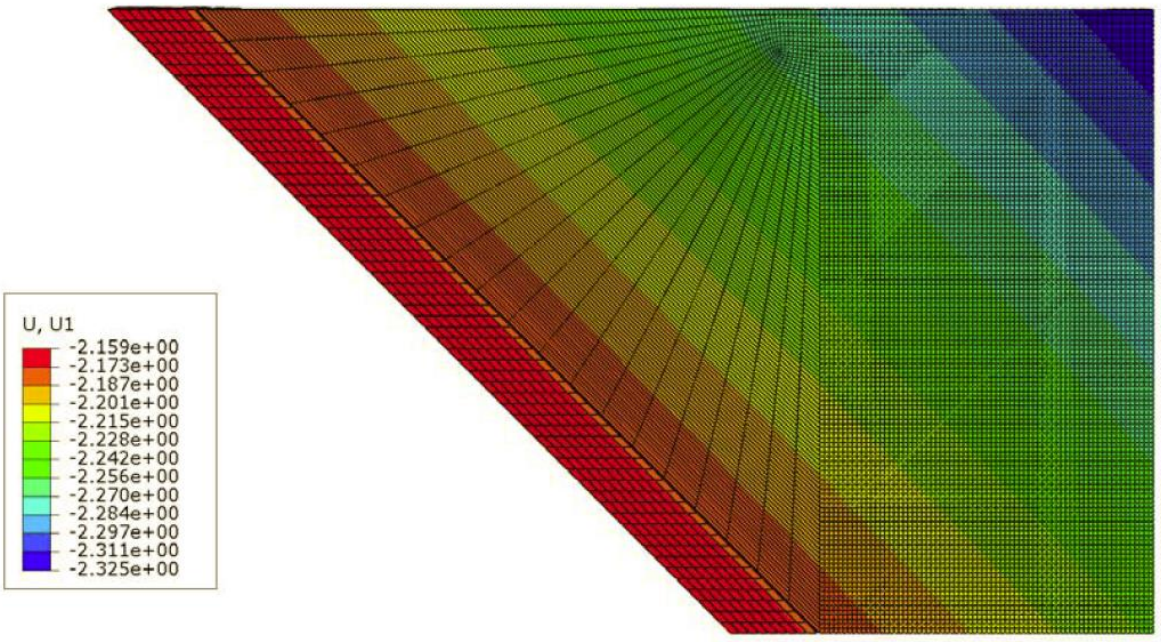

Figure 6.11. Jasper - Case 4 X Displacement

The displacements for all four load cases can be seen in Table 6.3. Figure 6.12 shows the free expansion and contraction of the slab with displacements amplified by a 100x scale for clarity. The deformed shapes are all concentric about the center. Compare with the Load Case 3 and 4 displacements when are shown in Figure 6.13 with a much lower 10x scale amplification. A similar shape change occurs due to temperature change, but global displacements are much larger. Load Case 3, which captures expansion of the slab, drags the slab transversely while Load Case 4 does not have nearly as much transverse deflection. Slab rotations were calculated using the position of the two points located on the slab edges along the road centerline, and at the joint itself using two points at either end of the joint. Rotation for Case 3 is -0.0071° about the Y-axis at the abutment-approach joint and only -0.0055° along the slab centerline. A frictional force located at the centroid of the slab acting in the opposite direction of transverse displacement would cause a positive rotation about the joint end of the slab, possibly accounting for the discrepancy. Similarly, rotation at the abutment-approach joint is 0.0161° for Case 4 and 0.0174° measured at the slab centerline. Using the same logic described previously, it follows that the slab rotation would be lower than at the joint.

Table 6.3. Jasper - Approach Slab Corner Displacements

Point	Base Coordinates (in)		Displacements (in)							
			Tied				Non-Tied			
			Expansion		Contraction		Expansion		Contraction	
			Case 1		Case 2		Case 3		Case 4	
	X	Z	X	Z	X	Z	X	Z	X	Z
Pt 1	0	0	2.108	1.865	-2.175	0.105	-0.122	-0.052	0.120	0.052
Pt 2	516	0	2.256	1.916	-2.324	-0.041	0.028	-0.047	-0.030	0.048
Pt 3	516	336	2.224	2.026	-2.230	-0.150	0.026	0.062	-0.028	-0.061
Pt 4	336	336	2.170	2.010	-2.177	-0.101	-0.027	0.062	0.025	-0.061

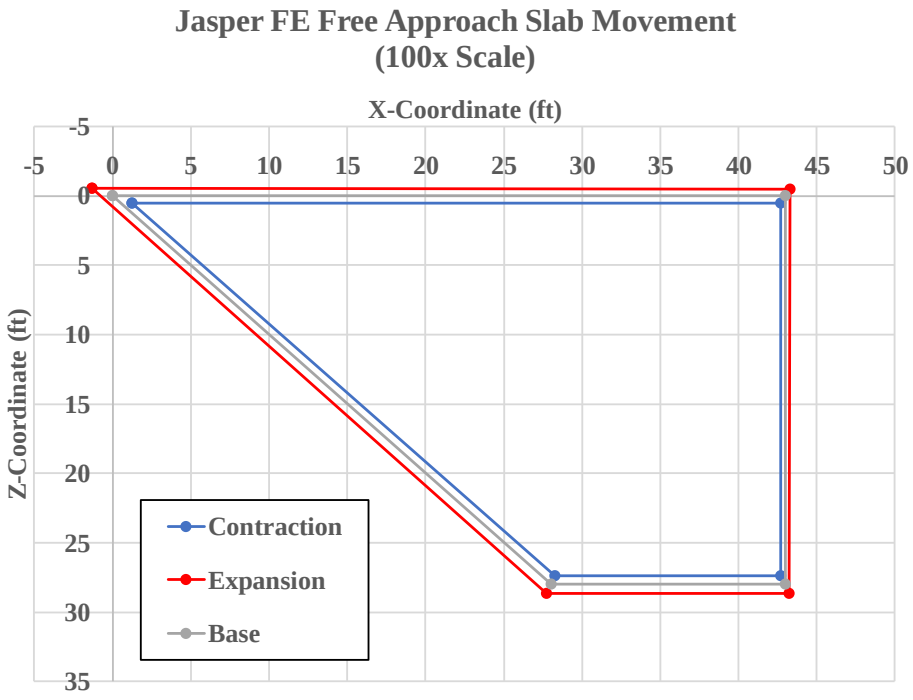

Figure 6.12. Jasper - Case 1 & 2 Approach Slab Movement

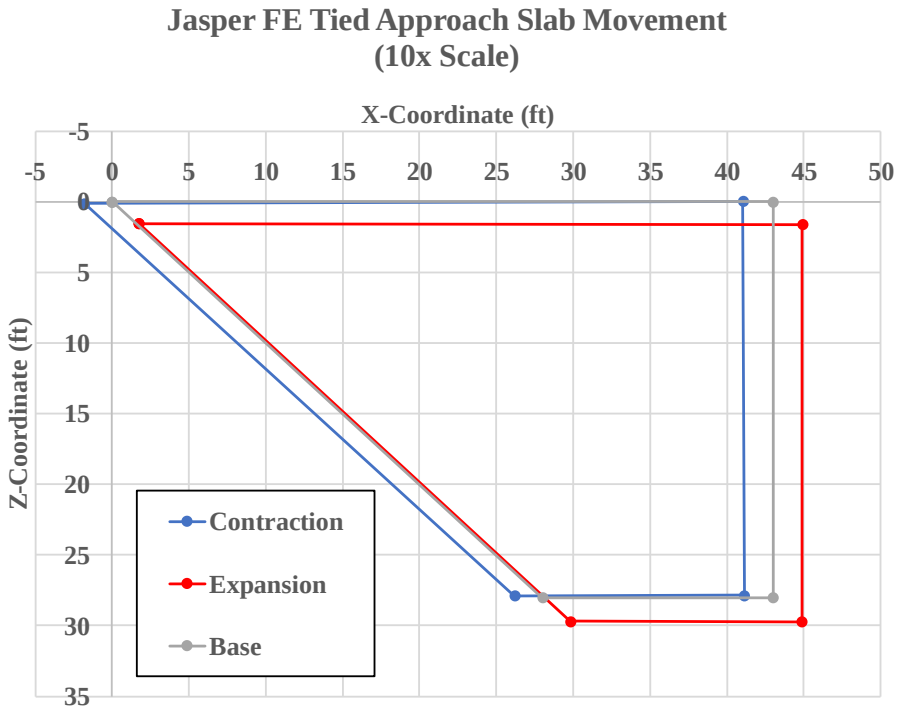

Figure 6.13. Jasper - Case 3 & 4 Approach Slab Movements

Friction force (F) between the approach slab and soil is determined by the normal force between the two surfaces (N) and a coefficient of friction (μ) given a fiction model of $F=\mu N$. Abaqus displays the contact pressures in Figure 6.14 and Figure 6.15 for Cases 3 and 4, respectively. The two profiles show very different behavior due to the effect of the abutment movement. Case 4 shows a contact shape similar to the approach slab shape indicating the slab generally has a low, even contact pressure across its entire surface. Contact for Case 3 is extremely high near the abutment-approach joint and comparatively low enough elsewhere that it becomes difficult to distinguish due to the contour colors used. The abutment movement pushes into the soil creating a small upward deflection due to the Poisson effect. The upward movement of soil is resisted by the slab and results in high contact pressure; thus, high contact shear resisting slab sliding. This behavior is not unexpected given the boundary conditions applied to the soil; however, it represents a worst-case scenario that is unlikely to occur. Settlement of the soil beneath approach slabs would likely mean that even with the bridge expansion, the soil would not result in a net upward deflection of the approach slab of the magnitude seen in the analysis. True loading also occurs in many small cycles due to daily temperature swings, alternating between expansion and contraction. Ratcheting of the soil or erosion occurring near the abutment would create a void and space for soil to deflect upwards at the abutment backwall without creating additional upward pressure on the approach slab. Both Case 3 and 4 showed a peak soil pressure at the acute approach slab corner which corresponds to the obtuse bridge corner.

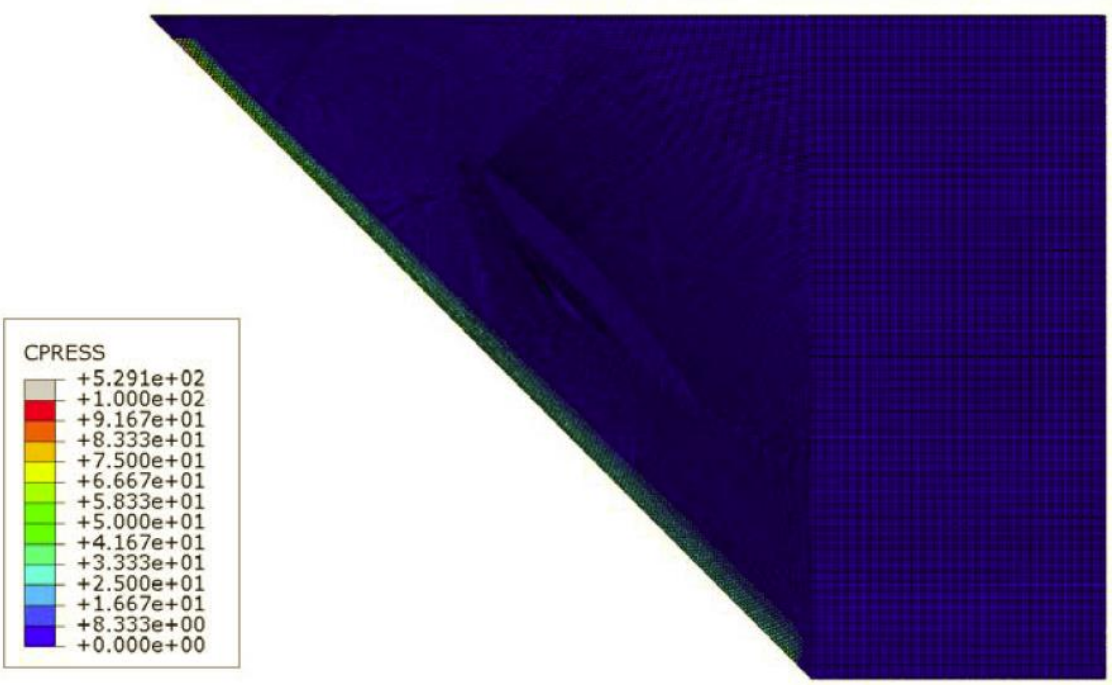

Figure 6.14. Jasper - Case 3 Soil Contact Pressure Contour Plot

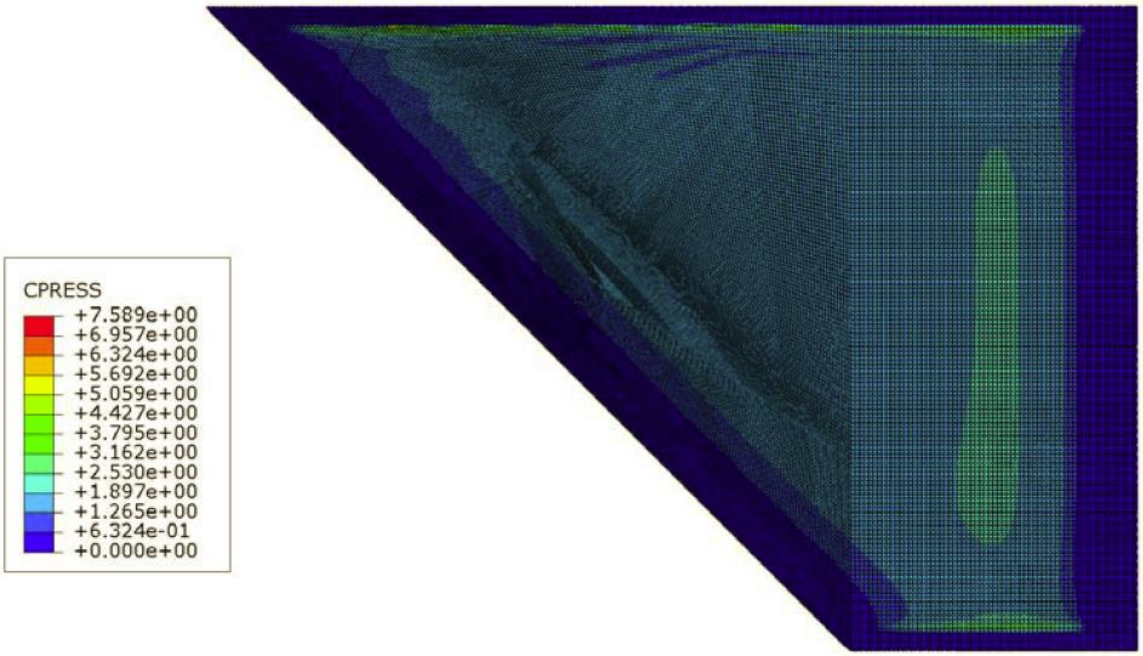

Figure 6.15. Jasper - Case 4 Soil Contact Pressure Contact Plot

Soil pressures translate directly to shear forces, given the frictional behavior chosen for modeling. Contact shear profiles match the contact pressure profiles shown above. Summing all contact shear force on the surface of the slab gives the total force required to move the slab. The same results can be reached by extracting forces from the tie bars connecting the abutment and approach slabs. Expansion and contraction show two different behaviors seen in the load-displacement plot for the Jasper bridge (Figure 6.16). Case 4 (negative displacement) shows an ideal friction curve similar to the test beam. Once the peak friction force is reached the slab slides with a constant force value of around 78 kips. Case 3 (positive displacement) shows a slight dip in force before increasing steadily to a maximum value of 99 kips. The changing force value can be attributed to the changing contact surface shape. The positive slope in force may be a result of the upward deflection of the soil near the abutment-approach slab joint. The lateral movement of the abutment creates the upward deflection of the soil. The approach slab is tied to the abutment and resists the upward deflection increasing contact pressure and contact shear. As the abutment moves further the effect is amplified and overall friction force increases. A load-displacement curve for longitudinal and transverse force is shown in Figure 6.17. Recall that for bridge expansion the Jasper bridge experienced transverse displacement equal to 81% of longitudinal displacement. The plot shows the total transverse shear force taken from the tie bars during bridge expansion compared with longitudinal force. The forces are similar magnitudes since the approach slab is moving in both directions and is resisted by a contact shear force in both directions.

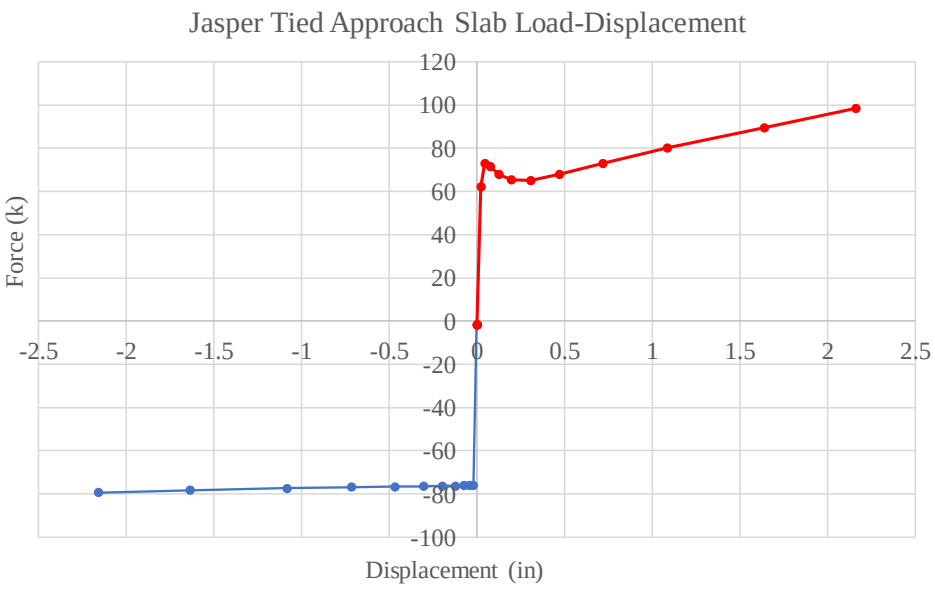

Figure 6.16. Jasper - Tied Approach Slab Load-Displacement (X-Direction)

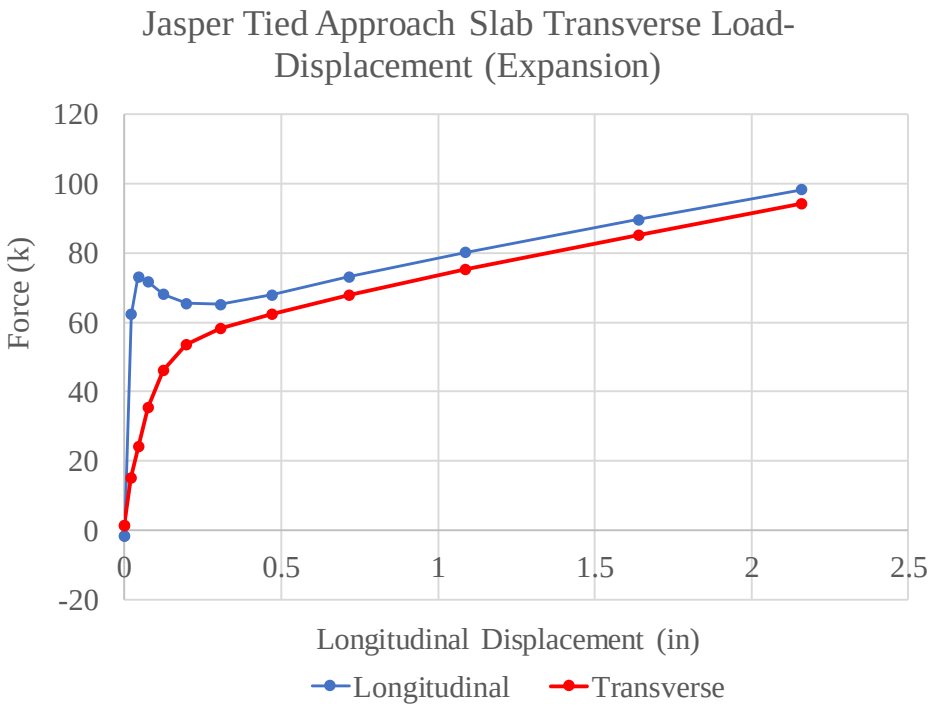

Figure 6.17. Jasper - Tied Approach Slab Transverse Load-Displacement (Expansion)

6.2 Story County 118 FE Model

A finite element model was created to replicate the Story County 118 bridge that was instrumented with sensors similar to Jasper County 118. Model formulation began with the same techniques employed for the Jasper model. The model consists of a two-foot-deep soil block matching the depth of "modified subbase". An equal depth portion of the abutment is tied to the approach slab using 53 inclined paving notch dowels placed per the Story bridge plans. The approach slab is 63.2' wide to accommodate a 60' roadway and a length at the longer edge of 36.5'. The soil and sleeper slab extend 1' beyond the edges of the approach slab to provide a continuous surface for sliding. The dowels are Grade 75 stainless steel to match those installed per Iowa DOT. The stainless-steel material is modeled with plastic behavior at 75,000 psi. Other material properties match those seen in the previous analysis for Jasper County 118. Boundary conditions are similar to the Jasper model as well. Z-direction restraint is only present on the sides of the soil for a 12' length extending away from the abutment to simulate confinement from wingwalls. Concrete barrier loading was placed on the approach slab using an equivalent pressure and 14" width for a length of 19' on each side. The pressure loading was applied to a partitioned section of the approach slab matching the footprint of the barriers. Soil boundary conditions vary slightly from the previous analysis. Since the Story bridge utilizes integral abutments the backwall deforms the soil at all depths, so modeling a thicker depth of soil than abutment to allow for a pinned condition is not possible. Therefore, a roller condition supports the soil. A loss of relative displacement between the slab and soil occurs but is extremely minimal and occurs after full friction is realized.

6.2.1 Mesh Density Study

A study was completed on the mesh sizing of both the approach slab and soil beneath it. Mesh sizes were applied using a size control to both parts, since it is recommended to maintain similar sizes between surfaces for optimal contact simulation. Sizes began with 12" allowing for one element through the full depth of the slab and decreased to 3". The axial stress in the X-direction in the approach slab after application of only gravity loads is shown in Table 6.4 and plotted versus mesh size in Figure 6.18. The time taken for computation of the gravity step is also displayed. A mesh size of 4" was chosen to provide proper result accuracy and minimize run time.

Table 6.4. Story - Approach Slab Mesh Sensitivity Results

Mesh Size (in)	Axial Stress (X-Direction)	Gravity Step Analysis Time
12	0.109	4:59
8	0.327	16:54
6	0.314	12:54
5	0.342	33:37
4.5	0.506	53:58
4	0.508	36:36
3.5	0.513	1:05:12
3	0.508	1:42:17

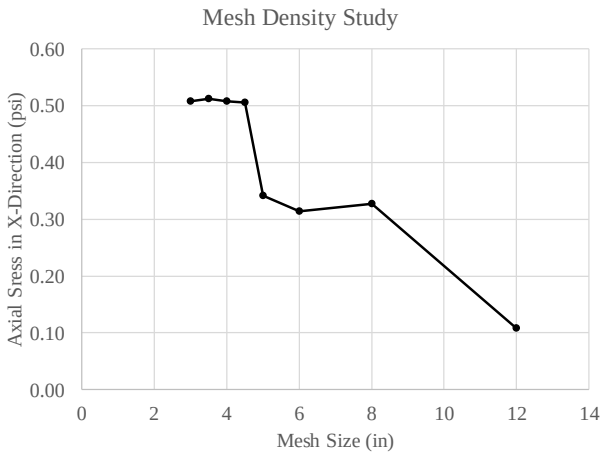

Figure 6.18. Story - Approach Slab Mesh Density Sensitivity

6.2.2 Comparison with Field Results

FE results were compared with field monitoring data to examine how accurately the FE model captures the true performance of the bridge. A short period of bridge contraction and negative thermal loading for chosen for study. Beginning 3/25 at 7:00 PM the bridge underwent a temperature decrease until 3/26 at 8:00 AM. The associated 8.1° temperature drop and 0.074" abutment displacement were applied to the Story bridge base model. Figure 6.19 shows measured strains of all 9 slab strain gauges for both the North and South approach slabs. Also included is the measured strains from the same locations in the FE model slab. Strains from the North and South slabs are consistent with each other but show much more variation between gauges than the FE model results. Overall, strains are all in the correct direction and on the same magnitude. A longer time scale and larger temperature range would provide a better comparison, especially for extremely high temperatures during maximum bridge expansion, since FE results for the expansion case are anticipated to be highly conservative.

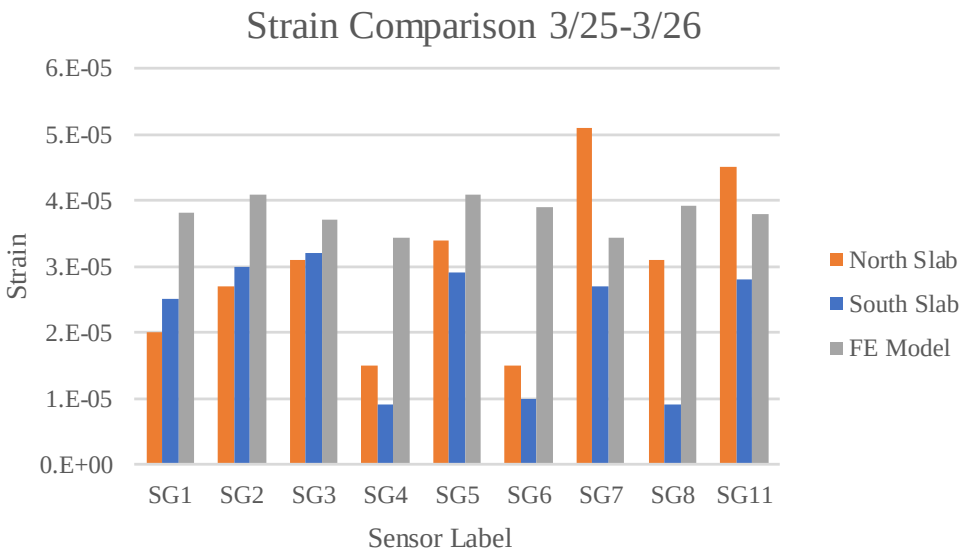

Figure 6.19. Story - Approach Slab Strain Comparison

Figure 6.20 shows strain in SG10-S for the same 13 hour period plotted with strain extracted from the FE model from the center tie bar at the location of SG10-S. SG10-S is the only recorded strain included since it was the only tie bar strain gauge determined to be capturing strain in the bar to which it was connected. Final results were 62 με and 60 με for the field results and FE model respectively. The shape of the two curves differs with the model showing a linear increase in strain initially with a plateau after the slab begins to slide. The strains in SG10-S show a consistent increase in strain throughout the temperature change.

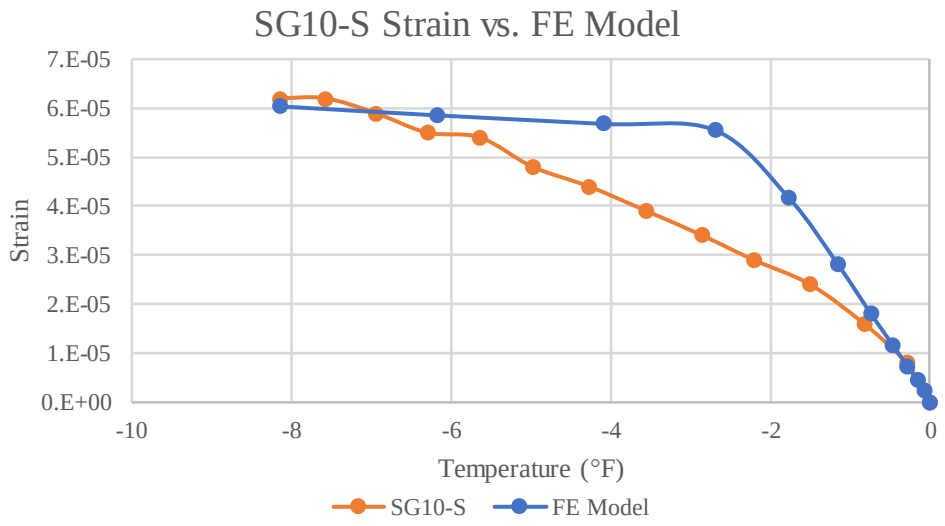

Figure 6.20. Story - Tie Bar Strain Comparison

Comparisons of model approach slab displacement at the sleeper slab and tied approach expansion are provided in Figure 6.21 and Figure 6.22 respectively. Both model and field results show the same increasing displacement with decreasing temperature; however, the model overestimates displacement by 30%. Peak model displacement is 0.10” compared to the field results of 0.08”. The only two factors contributing to the displacement at the approach slab end are the tied approach slab joint and change in length of the approach

slab itself. Joint expansion was determined from the FE model results by subtracting the approach slab edge displacement from the abutment edge displacement to find the relative displacement between the two parts. The comparison model and true joint behavior in Figure 6.22 shows two different pictures. Model expansion increases slowly and reaches a maximum plateau of 0.004". Crackmeter data shows the joint expansion increases steadily to a maximum value of 0.018", over four times the model value. The difference between the two values, 0.014", is similar in magnitude to the difference between approach slab displacement results in Figure 6.21. An underestimation of joint expansion by the model would show up in an overestimation of approach slab displacement at the sleeper slab. Overall the model generally captures thermal behavior of the approach slab. However, it does have limitations and does not appear to capture a continuous opening of the approach slab to abutment joint. The joint doesn't seem to be limited by a plateauing frictional force. Possible explanations include a force present at the approach slab to sleeper slab joint, or a more complicated frictional behavior that cannot be represented with the frictional behavior used in this model.

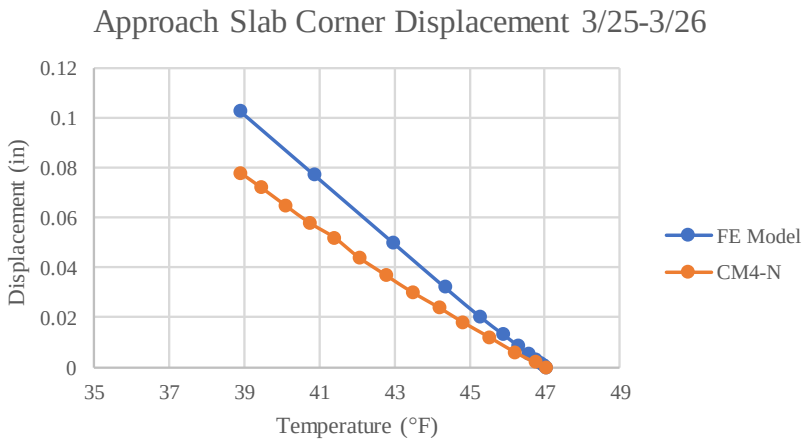

Figure 6.21. Story - Approach Slab Corner Displacement Comparison

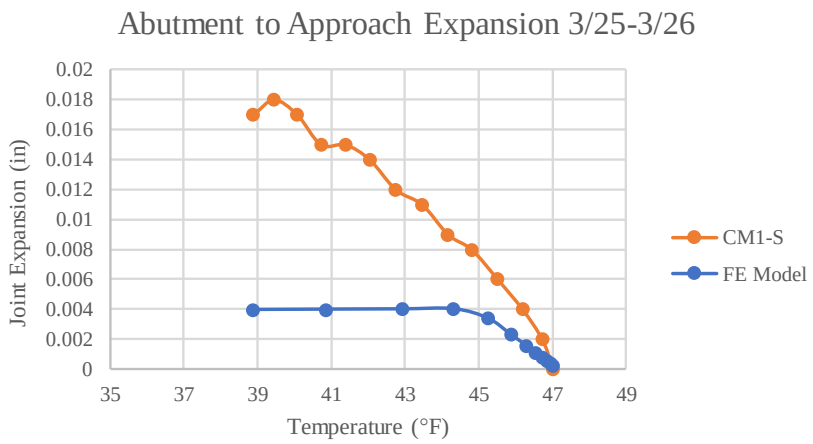

Figure 6.22. Story - Tied Approach Expansion Comparison

6.2.3 Parametric Studies

In order to study the effect of input parameters on the model behavior, parametric studies were completed on the coefficient of friction between concrete and soil, approach slab tie bar type, and bridge skew. The base model parameters and variations made in each study are seen in Table 6.5. Each study was completed independent of each other and included one full cycle of expansion and contraction. Loading included a temperature change of positive or negative 100° F along with an abutment movement of 1.35" in either direction. Expansion and contraction were run as separate analysis simulating a worst-case scenario in which the bridge experiences full expansion or full contraction. As discussed previously, true temperature cycles induce expansion and contraction daily accompanied by a general seasonal trend; however, simulation of these numerous reversing cycles would prove to be computationally unreasonable. Important results taken from the parametric studies include load-displacement plots, contact pressure distributions, tie bar stresses and slab stresses.

Table 6.5. Parametric Study Model Variations

	Simulation Scenario	Friction Coefficient	Soil Stiffness	Tie Bar Angle	Skew
Base	1	0.55	20 ksi	40°	15°
Friction Study	2	**0.4**	20 ksi	40°	15°
	3	**0.55**	20 ksi	40°	15°
	4	**0.7**	20 ksi	40°	15°
	5	**1**	20 ksi	40°	15°
Soil Study	6	0.55	**13.9 ksi**	40°	15°
	7	0.55	**20 ksi**	40°	15°
	8	0.55	**27.8 ksi**	40°	15°
Tie Bar Study	9	0.55	20 ksi	**40°**	15°
	10	0.55	20 ksi	**20°**	15°
	11	0.55	20 ksi	**0°**	15°
Skew Study	12	0.55	20 ksi	40°	**0°**
	13	0.55	20 ksi	40°	**15°**
	14	0.55	20 ksi	40°	**30°**

6.2.4 Parametric Study of Soil to Concrete Coefficient of Friction

Four different values were used for the coefficient of friction to determine what effect, if any, a changing coefficient of friction has on the slab and tie bar behavior other than simply increasing the force required to pull the approach slab. Increasing the coefficient of friction will directly increase friction force, but a more in-depth look is required to determine if the increased force is carried in different ways or if the contact surface is affected. Values of 0.4, 0.55, 0.7 and 1.0 were input in the Story bridge base model as described above. A coefficient of friction will vary from bridge to bridge depending greatly on the materials used, condition of the soil, and construction of the slab. The amount of friction between the slab and soil beneath it is difficult to measure due to the large contact surface of the slab and the fact that it must be indirectly measured through strains in the slab. Placing instrumentation on each tie bar is simply not reasonable due to the cost and effort it would require. Predicting the amount of friction a slab will experience is difficult, and this study aims to check slab and tie bar behavior as a result of varying amounts of friction. If force is

distributed in the same manner no matter the magnitude, a design can be completed under the expectation that locations of maximum tie bar or concrete stresses will not shift.

Load-displacement curves for each case are visible in Figure 6.23. Increasing the coefficient of friction increases the total amount of force necessary to pull the slab as expected. Contraction maximum forces are 172, 236, 299, and 452 kip for coefficients of friction equal to 0.4, 0.55, 0.7, and 1.0 respectively. The shape of curves is maintained, and forces are amplified. von Mises stresses and maximum principal stresses in the approach slab surface are provided in Table 6.6. Overall, stresses in tie bars and concrete are larger for bridge expansion due to the compression of soil and subsequent vertical displacement of the approach slab. Both stresses for all four cases show increasing magnitudes with increasing friction which is an expected result. Incremental increases in von Mises stress for contraction and expansion are similar magnitudes. The maximum principal concrete stress in the approach slab increases only 25 psi from the lowest friction to the highest friction. A visual representation of tie bar stresses for bridge contraction is provided in Figure 6.24. Stresses increase linearly with increasing friction, but a coefficient of friction between soil and concrete equal to 0 would not eliminate all stress in the tie bars since some friction remains between the approach slab and sleeper slab. If more data points were available for μ between 0 and 0.4 the curve reach a small amount similar to the stress after only gravity loading.

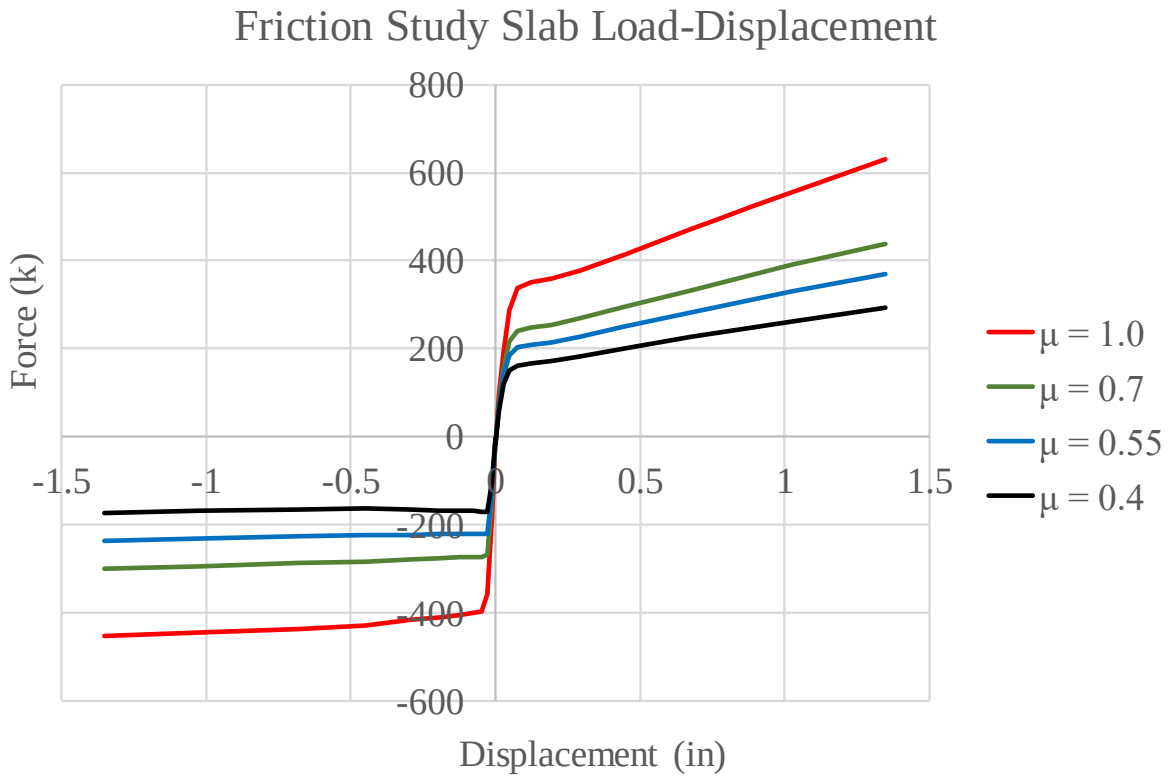

Figure 6.23. Story - Soil Friction Load-Displacement Comparison

Table 6.6. Story - Friction Study Tie Bar and Concrete Stress Results

Friction (μ)	Tie Bar von Mises Stress (ksi)		Concrete Maximum Principal Stress (psi)	
	Contraction	Expansion	Contraction	Expansion
0.4	8.4	41.4	191	468
0.55	13.1	43.0	197	482
0.7	16.3	43.2	203	474
1	22.7	42.7	216	442

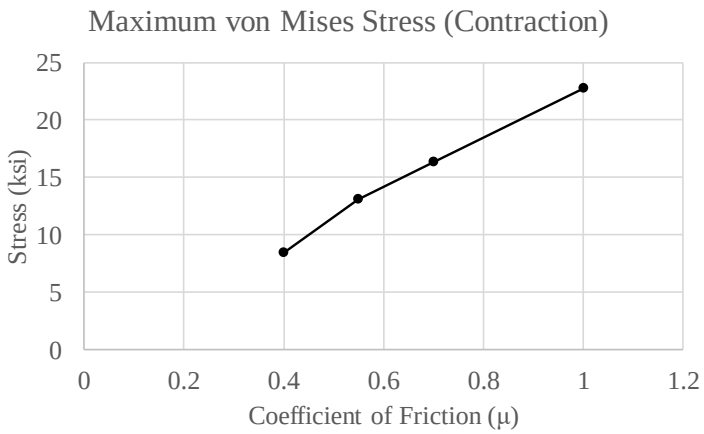

Figure 6.24. Story - von Mises Stress for Varying Coefficients of Friction (Contraction)

6.2.5 Parametric Study of Soil Stiffness

Three different soil stiffness values were used to determine the sensitivity of the model to changing soil stiffness and the effect on important results. The Story base model uses a modulus of elasticity of 20 ksi for the soil material. This value was taken from literature as an average for dense gravel, since no material testing was completed on modified subbase material. The modulus of elasticity values for loose and stiff soil were taken as 13.9 and 27.8 ksi respectively, the typical upper and lower limits for the same soil. The varying soil stiffness had extremely little effect on both approach slab stress and tie bar stress when considering the bridge contraction load case. This is an expected result since the approach slab is being pulled over the surface which remains relatively flat. Approach slab maximum principal stress increased only 2 psi for the contraction case (Table 6.7). Concrete stresses for both contraction and expansion are compared in Figure 6.25. Trends for the two loading cases are different where soil stiffness had minimal effect during bridge contraction, concrete stresses increase by 140 psi over the range of soil stiffness values. Upward deflection of the soil at the obtuse approach slab corner creates an upward pressure

underneath the approach slab and induces a negative bending moment in the slab. This results in a more positive principal stress in the approach slab surface. A stiffer soil provides a larger upward pressure thus a larger maximum principal stress. Maximum von Mises stress in the tie bars increased only 0.2 ksi and the range between minimum and maximum stresses in any one bar increased only 0.5 ksi (Table 6.8). This is also an expected result for the same reasons that concrete stresses were expected to have minimal changes in response to soil stiffness during bridge contraction. In the same way soil stiffness effects concrete stress during bridge expansion, tie bar stresses are also increased. Both behaviors result from the same upward deflection of soil.

Table 6.7. Story - Soil Stiffness Study Approach Slab Concrete Stresses

Approach Slab Maximum Principal Stress (psi)		
Soil	Contraction	Expansion
Loose	196	402
Medium	197	482
Stiff	198	558

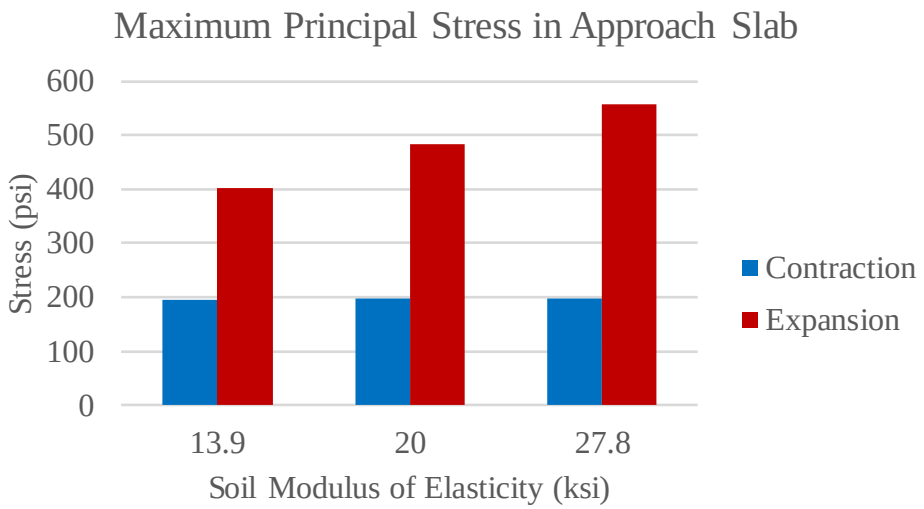

Figure 6.25. Story - Soil Stiffness Study Approach Slab Concrete Stresses

Table 6.8. Story - Soil Stiffness Study Tie Bar von Mises Stresses

Tie Bar von Mises Stress at Joint (ksi)					
Soil		Contraction	Range	Expansion	Range
Loose	Maximum	13.2	10.4	36.2	34.9
	Minimum	2.8		1.3	
Medium	Maximum	13.1	10.1	43.0	42.3
	Minimum	3.0		0.6	
Stiff	Maximum	13.0	9.9	49.7	48.5
	Minimum	3.1		1.2	

6.2.6 Parametric Study of Tie Bar Orientation

Variation exists in the types of dowels used to connect approach slabs to abutments and bridge decks. For example, Iowa DOT uses vertical bars in the BR-205 approach slab standard (Figure 6.26). Alternatively, the dowels used in the construction of Story 118 are inclined at approximately a 40° angle from vertical. Inclined bars are recommended for semi-integral abutments (Aktan et al. 2008) and abutment to approach slab connections should be designed to allow rotation (Hassiotis 2006, Weakley 2005). A continuous connection using horizontal bars can be redesigned as a deck-over-backwall concept in which the deck is made continuous and a backwall exists only to hold back the soil embankment. In this configuration the design is made to accommodate a connection which transfers moment.

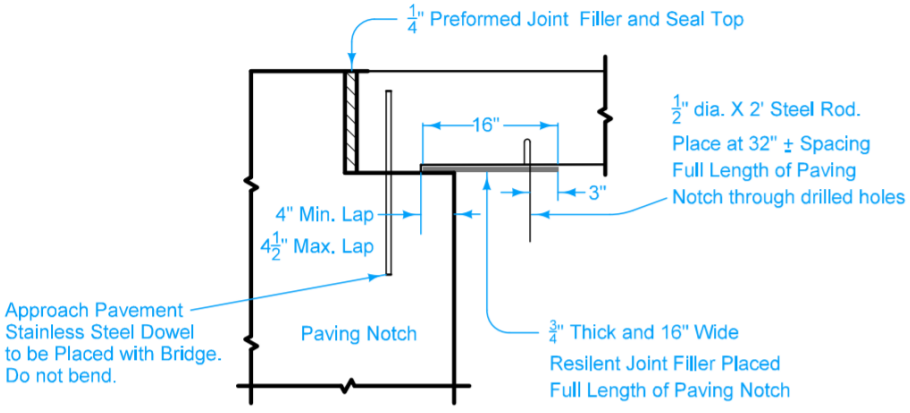

Figure 6.26 Iowa DOT BR-205 Standard Tied Connection (Iowa DOT)

Three different bar orientations were analyzed to compare the responses to identical loading. A set of vertical bars, inclined bars per Story County 118 plans, and third orientation with an inclination angle of 20°, which can be considered the median between the other cases, were modeled in Abaqus. All three bars were the same size #8 and grade 75 stainless steel. The bars were placed exiting the abutment at the same location, 8" from the vertical face of the paving notch. Bar styles were the only change applied to the base model with identical loading to the base model. Load-displacement plots are not included since all three cases show the same behavior, which is to be expected.

Discussion of the results begins with concrete stress. Table 6.9 shows the maximum principal stress in the approach slab surface for each load case and bar orientation. Vertical bars result in the lowest concrete stress of 176 psi, and 40° bars produce a stress of 197 psi. The median orientation bars produce a concrete stress only 2 psi less than the more inclined bars. There does not appear to be any clear trend in resulting concrete stress. Expansion loading also does not show a clear increasing or decreasing trend in stresses for changing bar orientation (Figure 6.27). The maximum stress of 530 psi occurs with the median bars. Maximum principal stresses in the approach slab surface occur in locations not coinciding with the bars and seem to be more dependent on friction force and soil stiffness in the case of bridge expansion.

Table 6.9. Story - Tie Bar Study Approach Slab Concrete Stresses

Approach Slab Maximum Principal Stress (psi)		
Bar Angle (°)	Contraction	Expansion
40	197	482
20	195	530
0	176	455

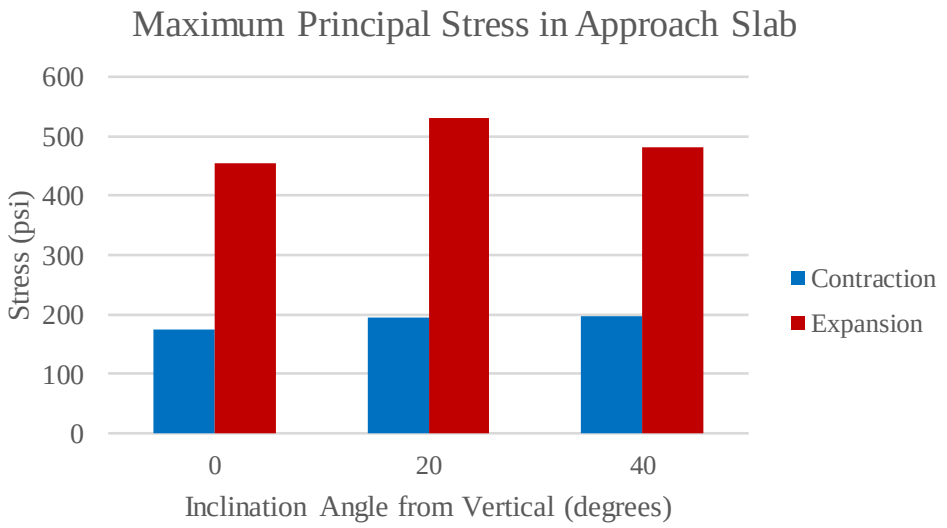

Figure 6.27. Story - Tie Bar Study Approach Slab Stresses

Maximum and minimum von Mises stresses for any single bar across the tied approach joint are listed in Table 6.10. The lowest maximum and minimum stresses respectively for bridge contraction of 13.1 and 3.0 ksi respectively are both for the most inclined bars, the type used in the story bridge. Stresses increase as bars are made more vertical until the highest stresses are seen in the vertical tie bars (Figure 6.28). Bridge expansion does not show a similar trend as stresses are almost identical for the two inclined bar types and increase for the vertical bars. Minimum Von Mises stresses in the two inclined bar cases were extremely low reaching less than 100 psi in one case. This behavior was seen in individual tie bars as loading progressed as vertical slab movement reversed the axial force in the bars from compression to tension. Bridge expansion pushes the slab and induces compression in the inclined tie bars, but as the abutment moves soil pushes the approach slab upwards inducing tension in the tie bars. No clear trend can be identified in the expansion load case with regards to reducing stress by changing tie bar orientation (Figure 6.29).

Rotation at the abutment occurs due to settlement of the approach slab and creates an upward displacement of the approach slab due to the paving notch edge acting like a fulcrum for the slab. As noted previously, horizontal tie bars that resist this movement only result in cracking of the slab, and an inclined connection is preferred to accommodate rotation. It follows that when examining the connections response to a horizontal movement, as in this analysis, that a more horizontal orientation would perform better. Maximum von Mises stresses decreased with increasing inclination angle from vertical.

Table 6.10. Story - Tie Bar Study Tie Bar von Mises Stresses

Tie Bar von Mises Stress at Joint (ksi)					
Bar Angle (°)		Contraction	Range	Expansion	Range
40	Maximum	13.1	10.1	43.0	42.3
	Minimum	3.0		0.6	
20	Maximum	18.7	11.9	44.6	44.5
	Minimum	6.7		0.0	
0	Maximum	22.6	15.8	59.5	19.6
	Minimum	6.8		39.9	

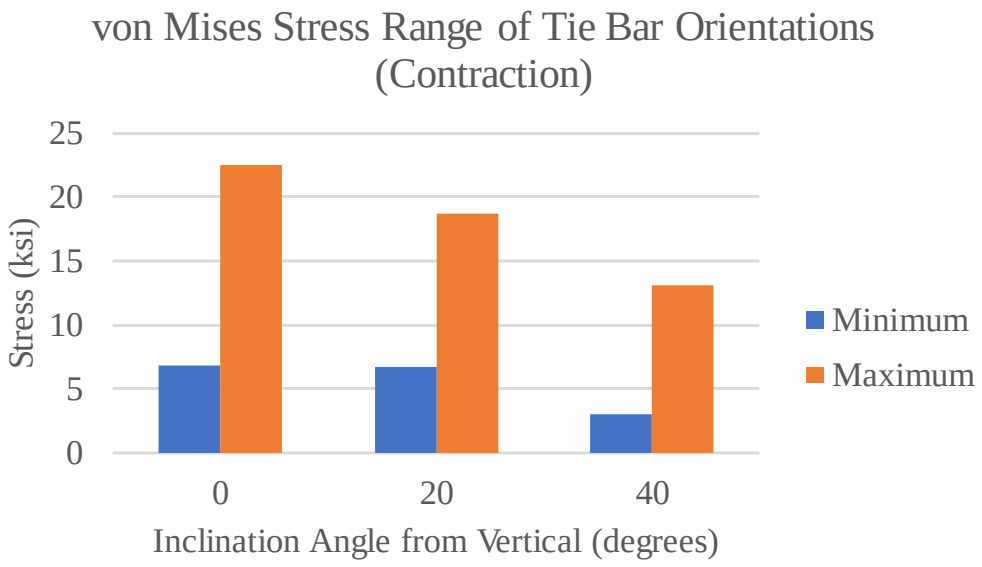

Figure 6.28. Story - Tie Bar Study von Mises Stresses (Contraction)

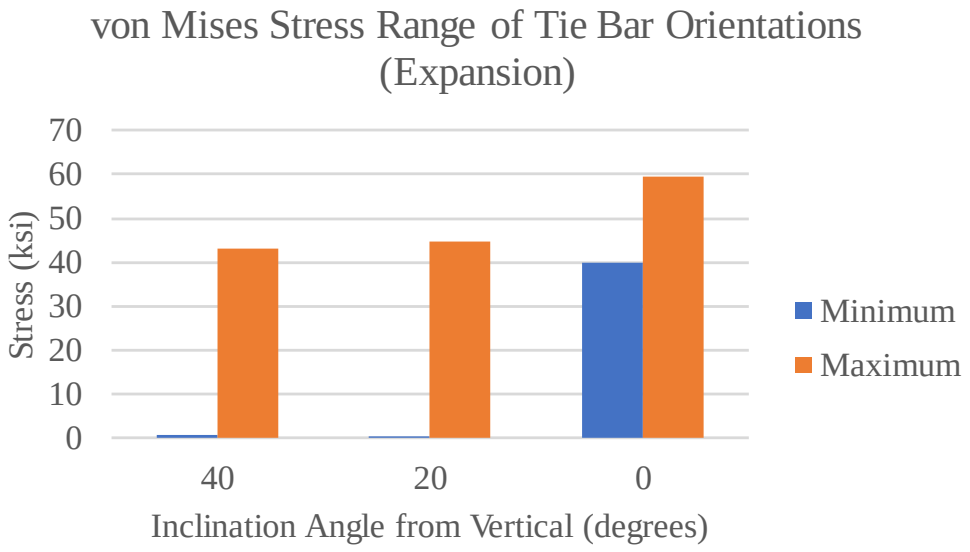

Figure 6.29. Story - Tie Bar Study von Mises Stresses (Expansion)

6.2.6 Parametric Study of Skew Angle

The most important aspect of the finite element analysis of these bridge approach slabs is the investigation of the effects of bridge skew on the stresses in approach slabs and tie bars. Currently there are limitations placed on the use of different types of bridges and details including integral abutments, semi-integral abutments, and tied approach slabs. Increasing skew angle creates unknown consequences in many cases that must be investigated through the use of finite element analysis to avoid the risks associated with constructing new details that may perform extremely poorly. A bridge with 0° will have the entire force of the approach slab carried by the tie bars in one direction bridge movement should be limited to one axis aligned with the bridge centerline. The approach slab will have a constant length across the width of the bridge and it can be assumed that tie bars can be spread across the joint with regular spacing to carry an equal amount of force by attributing a tributary width. Increasing the bridge skew angle not only changes the shape of the approach

slab making it longer at one side than the other, it also change the stress distribution across the abutment to approach slab joint.

Three different skew angles were used for analysis including 0°, 15°, and 30° (Figure 6.30). The slab length at the short side was kept at 20’ to accommodate the barrier rail used for Story 118 which has a length of 19’. Increasing slab size results in an increased slab weight (Table 6.11) and friction force (Figure 6.31). It would follow that forces and stresses in the tie bars, along with stress in the approach slab would generally increase. These values will be discussed in more detail.

Figure 6.30. Story - Approach Slab Plan View for Changing Skew Angle from 30 to 0 degrees (left to right)

Table 6.11. Story - Skew Angle Study Slab Weights

Skew (°)	Obtuse Side Length (ft)	Acute Side Length (ft)	Slab Area (ft^2)	Slab Weight (k)
0	20.0	20.0	1263.4	189.5
15	20.0	36.9	1798.0	269.7
30	20.0	56.5	2415.3	362.3
45	20.0	83.2	3258.6	488.8

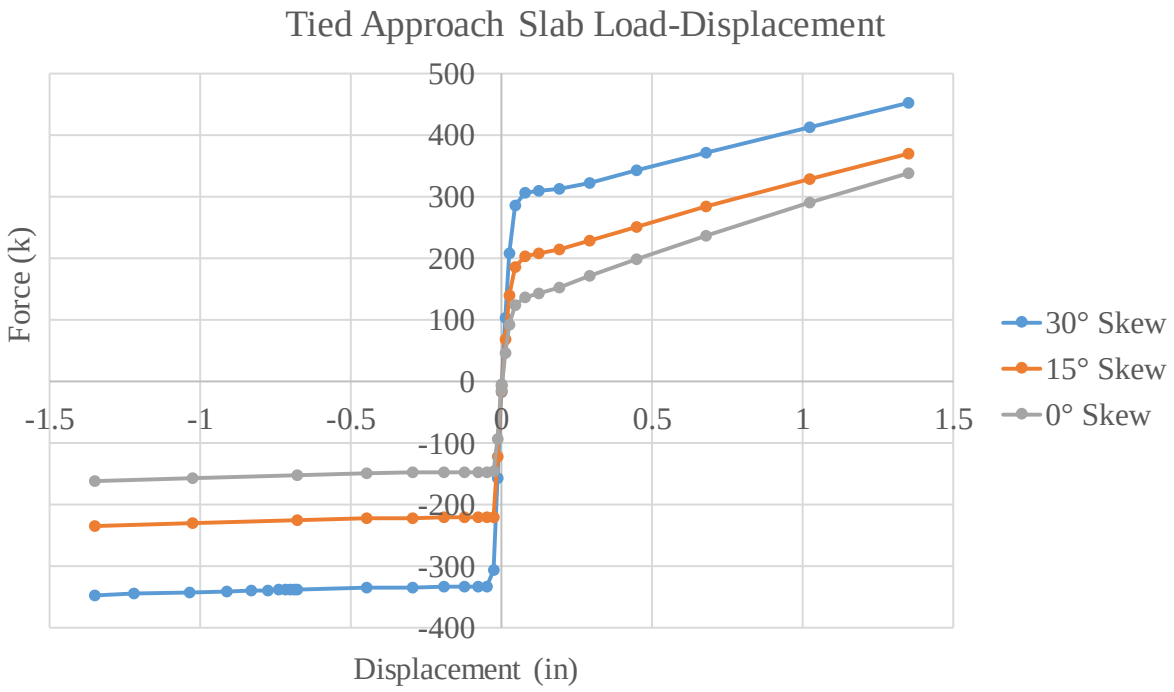

Figure 6.31. Story - Skew Angle Study Load-Displacement

Identical loading was applied to each model consisting of an abutment movement of positive or negative 1.35" and temperature change of positive or negative 100° F. Maximum principal stresses in concrete in the top surface of the approach slab are shown in Figure 6.32. Concrete stresses for bridge contraction increase by a relatively small amount of 27 psi between 0° skew and 30° skew. Maximum values were located near the acute slab corner (Figure 6.33) which corresponds to the longer side of the slab. This location is expected since there is a larger amount of contact surface between the slab and soil, thus a larger total friction force. All stresses in the contraction case including the maximum of 210 psi for the 30° skew slab remain below the modulus of rupture of 480 psi per AASHTO 5.4.2.6. Approach slab surface stresses are higher for every bridge expansion case than for even the maximum value for contraction. The maximum approach slab principal stress of 482 psi

occurs in the 15° slab. The maximum stress occurs on the side opposite the maximum stress during contraction, on the short slab slide near the obtuse approach slab corner (Figure 6.33). Contraction forces the soil under the slab upwards creating a tension force in the top of the slab. As discussed previously, the expansion load case is conservative assuming no soil settlement, no void formation near the abutment, and a rigid boundary condition at a reasonably shallow depth.

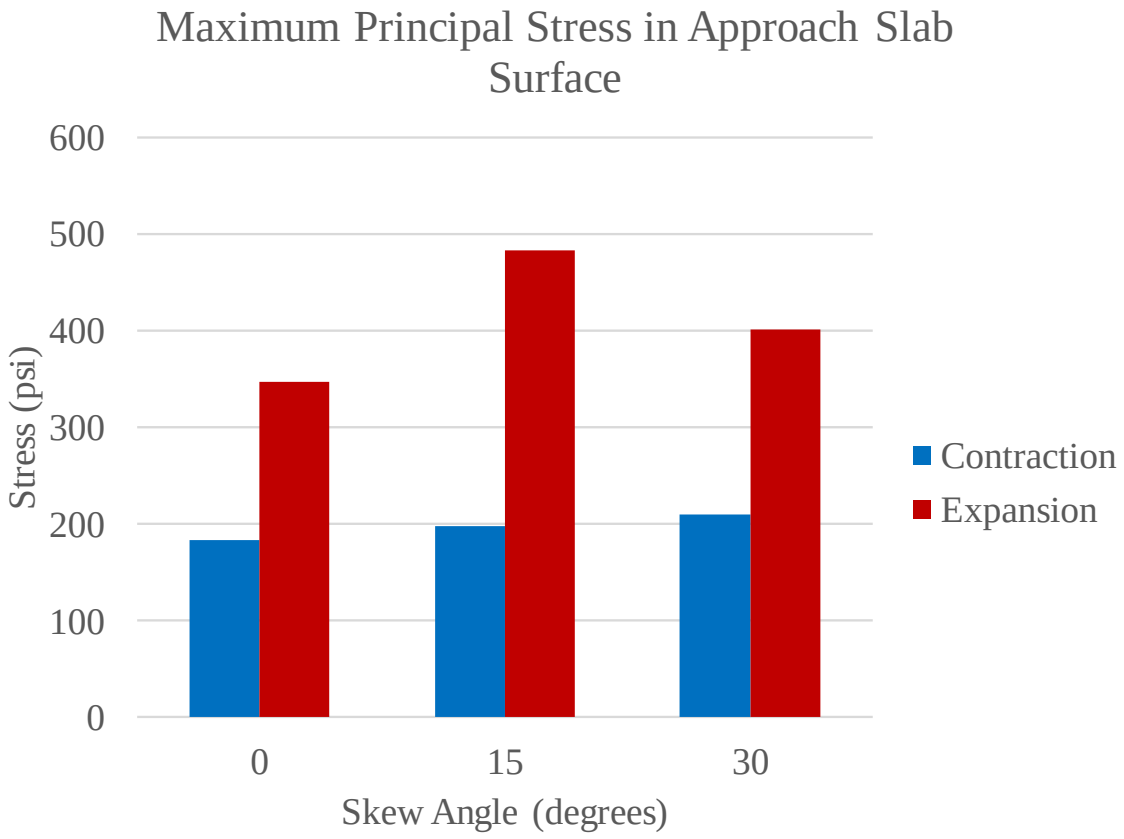

Figure 6.32. Story - Skew Angle Study Concrete Stresses

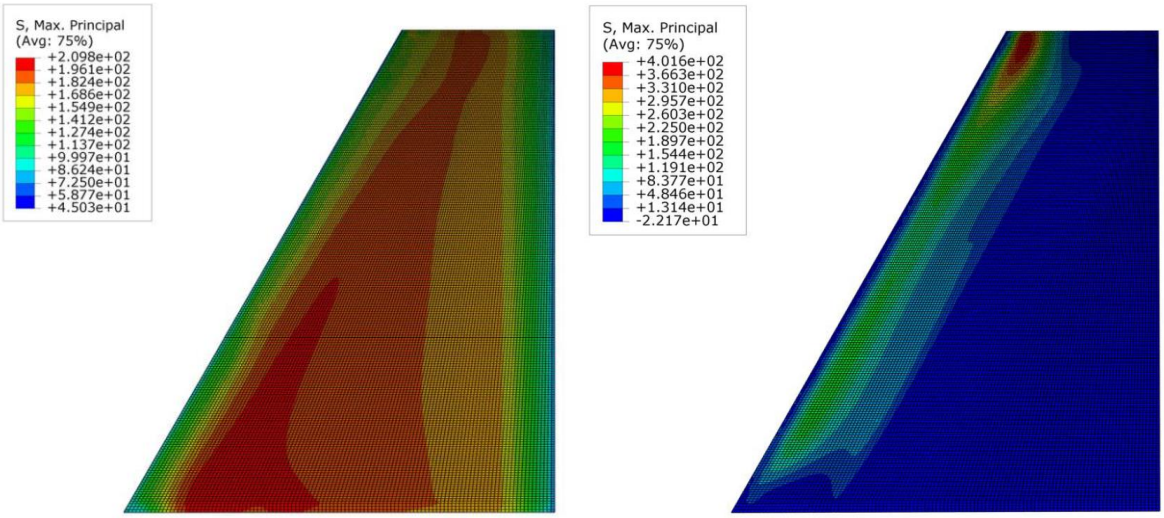

Figure 6.33. Story - Concrete Stress Contours for 30-degree Skew for Contraction (left) and Expansion (right)

Tie bar stresses, much like concrete stresses, also vary with increasing bridge skew angle. As seen previously, increasing skew angle increases the total size of the slab and force required to move it; however, tie bar stresses do not increase evenly in response. Figure 6.34 shows the maximum and minimum von Mises stress in the set of 53 tie bars across the joint. Maximum values increase from 5.4 ksi to 17.3 ksi with increasing skew from 0° to 30°. Minimum von Mises stress values decrease from 3.8 ksi to 0.3 ksi. The range increases from 1.6 ksi to 17.0 ksi. The stress distribution in bars across the joint changes greatly due to the changing skew angle. The distribution in stresses for all 53 tie bars can be seen for each case in Figure 6.35, Figure 6.36, and Figure 6.37. Stresses increases slowly over the course of the first step as gravity is applied, then increase greatly at the beginning of step 2 as the slab begins to slide. The increase in stress range is very apparent as skew increases and the maximum values increase as well with changing Y-axis between the plots. Using the Abaqus visualization module, a clear gradient can be seen across the joint where high stresses occur in bars closer to the acute slab corner and lowest stresses occur in the obtuse approach slab

corner. The same behavior is present in the contraction case minus the 2 or 3 highest stresses in bars at the obtuse corner where approach slab uplift is highest. The increase in stress in the bars is not as a direct result of the increase in slab size. If that were the case, stresses in the obtuse slab corner bars would remain the same instead of decreasing. The change in slab shape due to increased skew angle is shifting force towards the acute slab corner. This result is especially important considering that tie bars are currently distributed evenly across the tied approach slab joint no matter the skew in Iowa DOT's J40 standard bridge plans. The standards are available for bridges of 0°, 15°, 30°, and 45° and all abutment plans indicate ties use the same spacing.

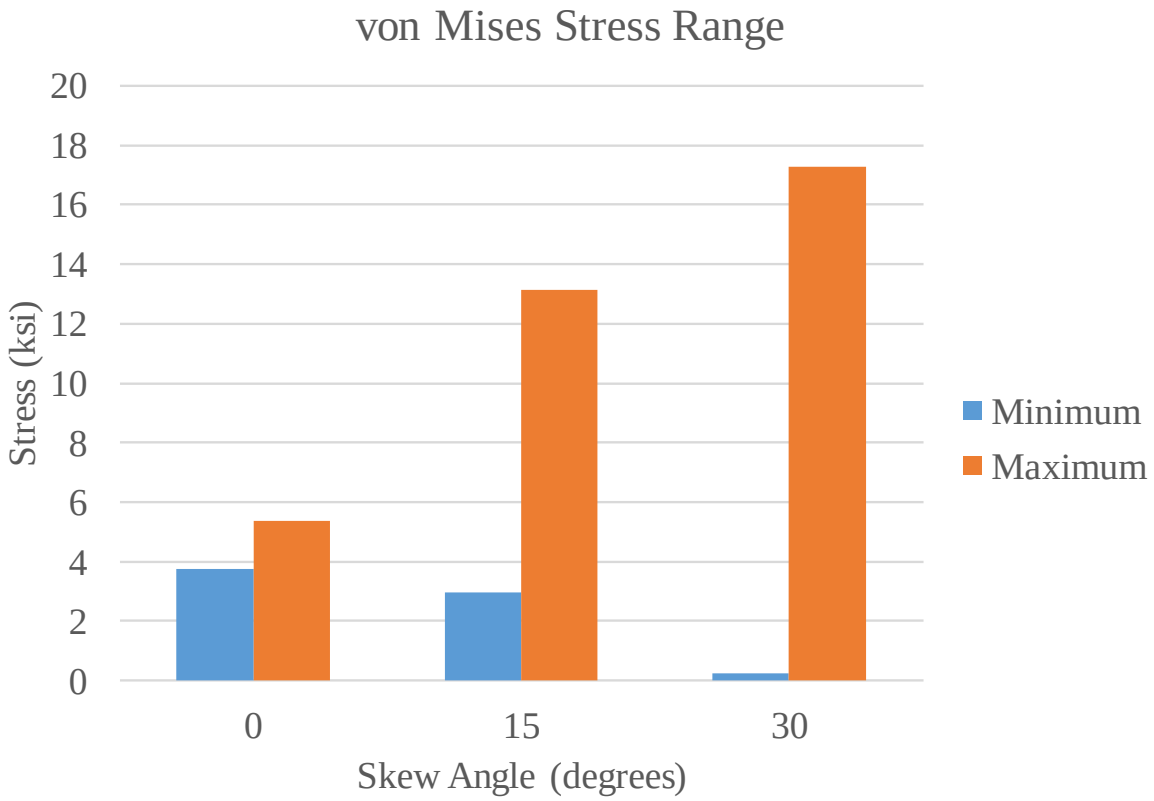

Figure 6.34. Story - Skew Angle Study von Mises Stress Range (Contraction)

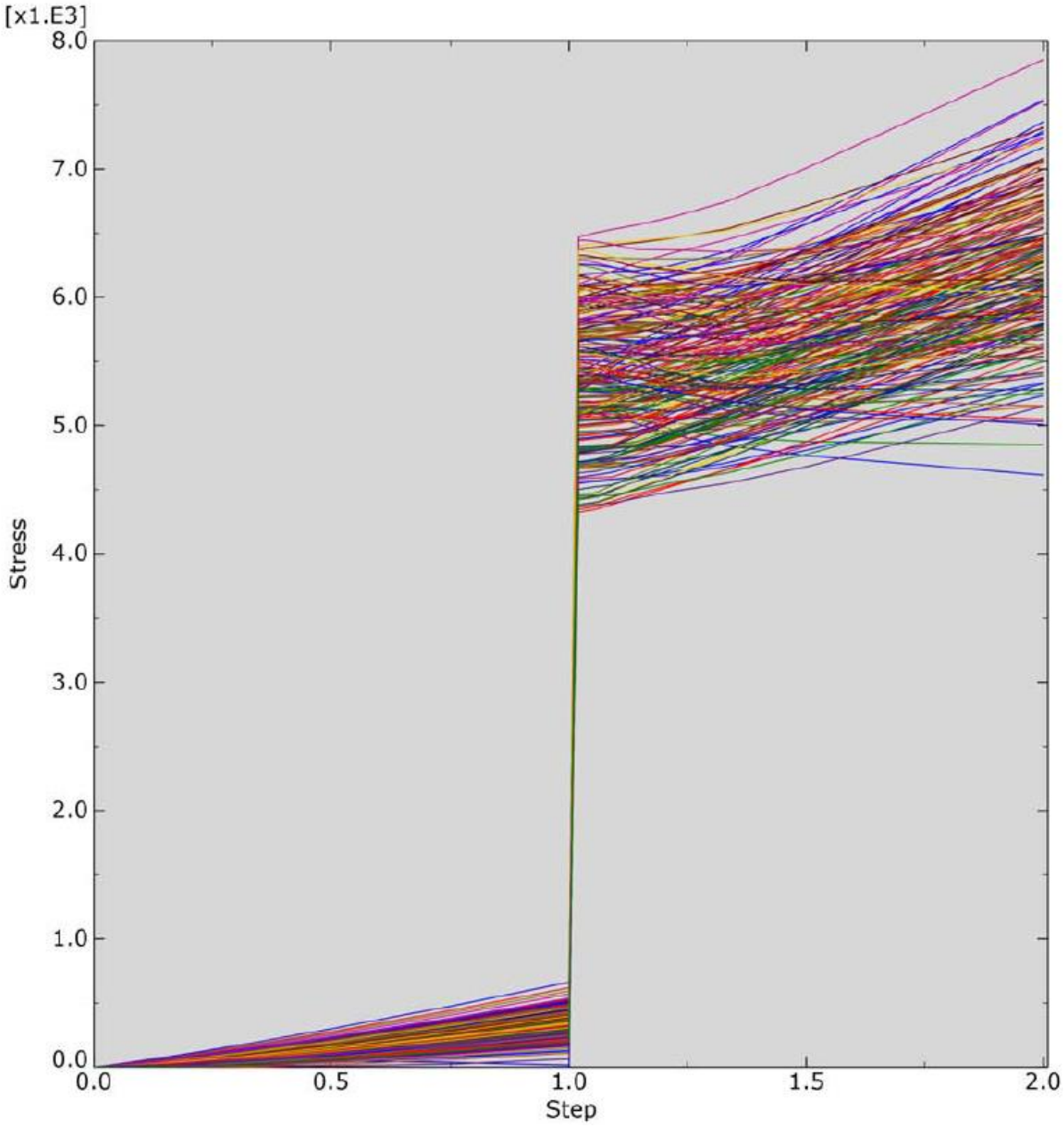

Figure 6.35. Story - von Mises Distribution for 0 Degree Skew

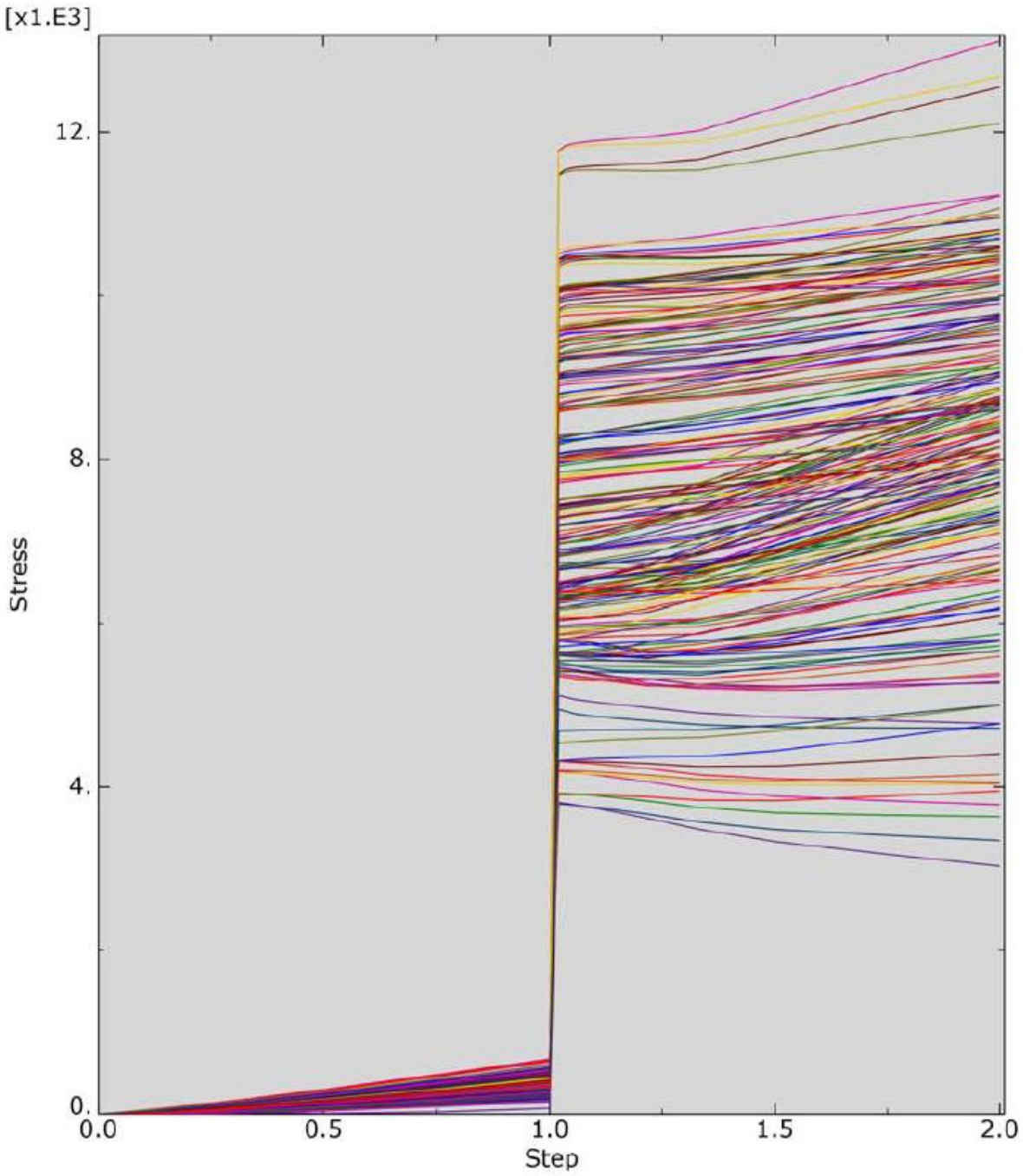

Figure 6.36. Story - von Mises Distribution for 15 Degree Skew

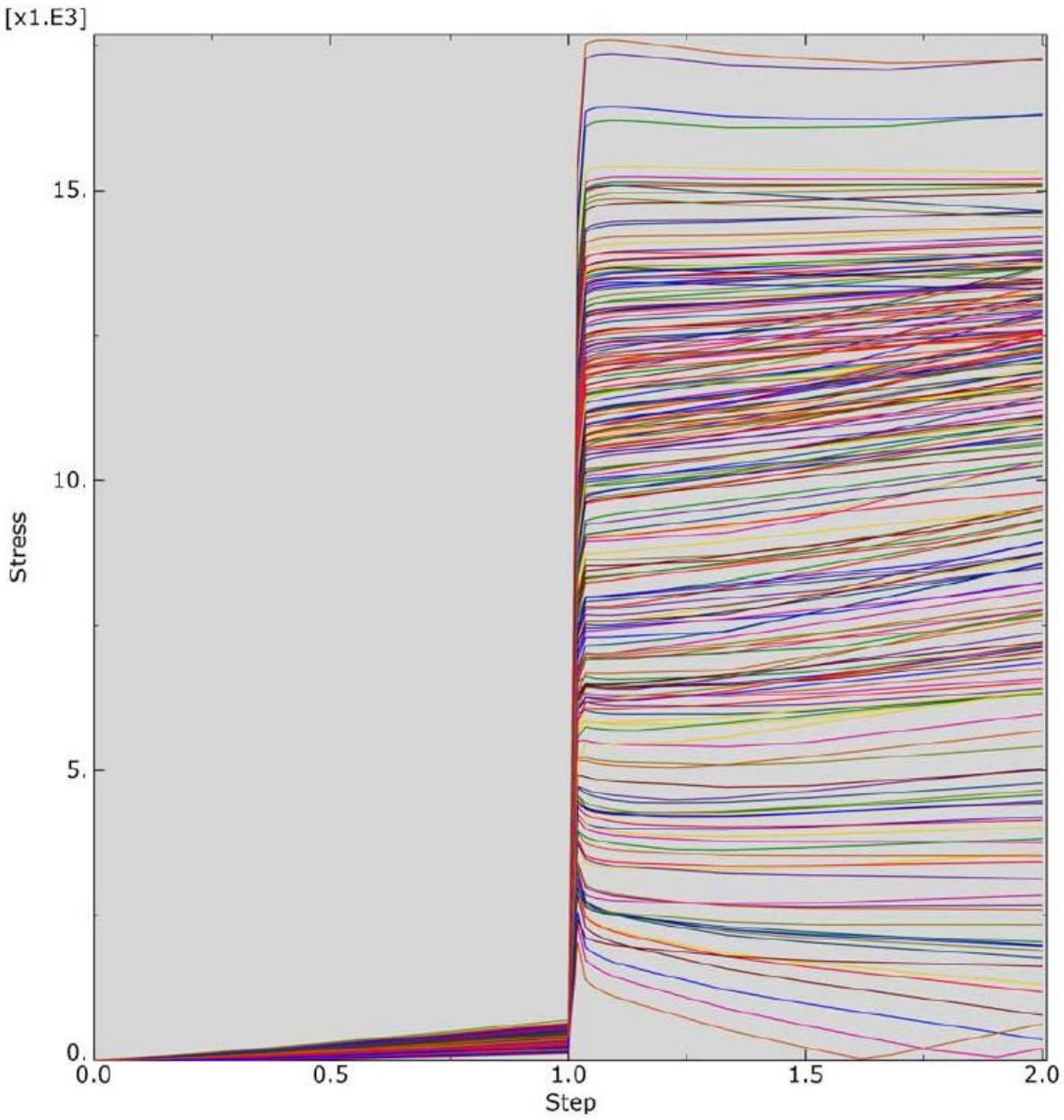

Figure 6.37. Story - von Mises Distribution for 30 Degree Skew

6.3 Shelby County 118 FE Model

A third FE model was created to resemble the construction of a bridge located in Shelby County, Iowa. The 400-foot long and 44-foot wide bridge will be located on US 59 over the West Nishnabotna River. Research activities for this bridge are limited to FE analysis with no field monitoring anticipated. The Shelby bridge is of interest because of its extremely high skew angle of 55°. The south abutment will be semi-integral, exceeding the current Iowa DOT skew limit of 45°. Bridge construction utilizes a self-expanding sealant system in the joint between the south approach abutment and the approach slab. Effects of the high skew at the joint location are unknown; therefore, a tied joint was not included in the design. The modeling techniques used for the previous two bridges allow for investigation of the performance of a theoretical tied approach connection.

Identical model element types, materials, contact properties, and similar boundary conditions to the Jasper and Story models. The Iowa DOT BR-205 Standard Road Plan approach connection in combination with the tie bar size and quantity taken from the J44 bridge plan standards were used to represent the tied approach connection. Twenty-two #8 stainless steel bars were spaced evenly across the joint and oriented vertically. Loading consists of a 100-degree temperature change per Iowa DOT LRFD BDM and the corresponding bridge abutment movement determined by the bridge length and girder material. The 12” thick approach slab is 44’ wide and 15’ long at the short side due to skew. Assembly of the model parts is done in the same manner as the previous FE models. A typical sleeper slab and 2’ thick soil layer are both 1’ wider that the approach slab to allow for sliding. Model geometry and boundary conditions can be seen in Figure 6.38.

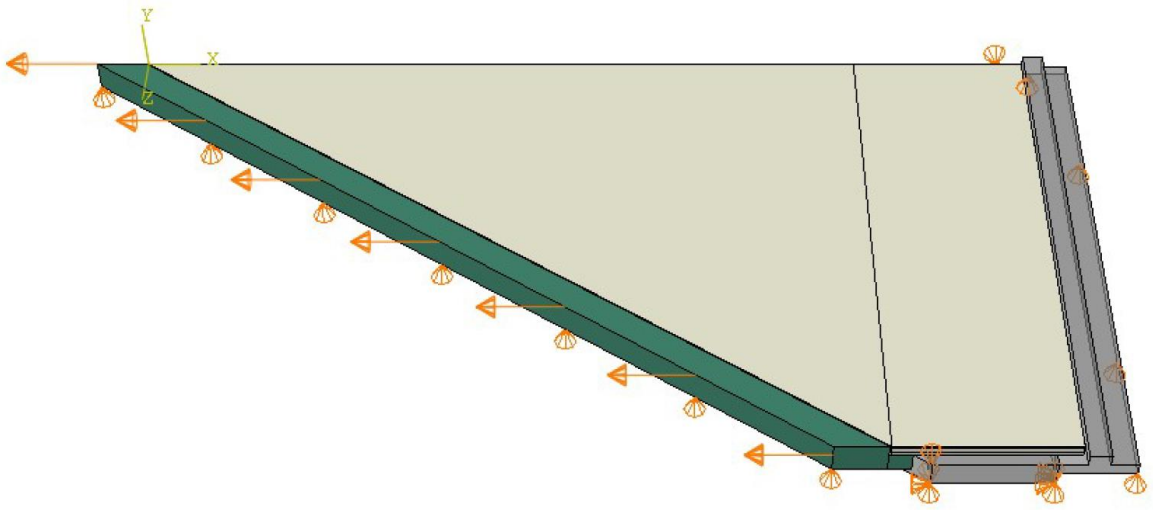

Figure 6.38. Shelby - Model Geometry and Boundary Conditions

6.3.1 Shelby County 118 FE Results

The objective of the Shelby FE analysis is to further examine the effect of skew on the tied approach connection. Previously a parametric study was completed using the Story bridge as a base model and analyzing skews of 0°, 15°, and 30°. Forces and stresses in the tie bars are in general distributed evenly across the tied joint for a rectangular slab with no skew. As the skew increases, the force distribution shifts and a gradient forms across the joint. The Shelby FE analysis examines the same concept for an extreme case of skew of 55°. The load-displacement curve for bridge contraction seen in Figure 6.39 shows a total force required to pull the slab of 240 kips. The maximum shear force seen in any single one of the twenty-two tie bars is 16.8 kips and the minimum is 4.1 kips. As expected, the maximum shear force occurs in the end bar at the acute bridge corner. The maximum principal concrete stress in the surface of the approach slab is shown in the contour plot in Figure 6.40. Contours follows the trends seen in the Story parametric study on skew angle. The maximum value occurs

along the side of the slab on the longer side corresponding to the acute slab corner. The stress of 235 psi does not exceed the rupture modulus of 480 psi per AASHTO.

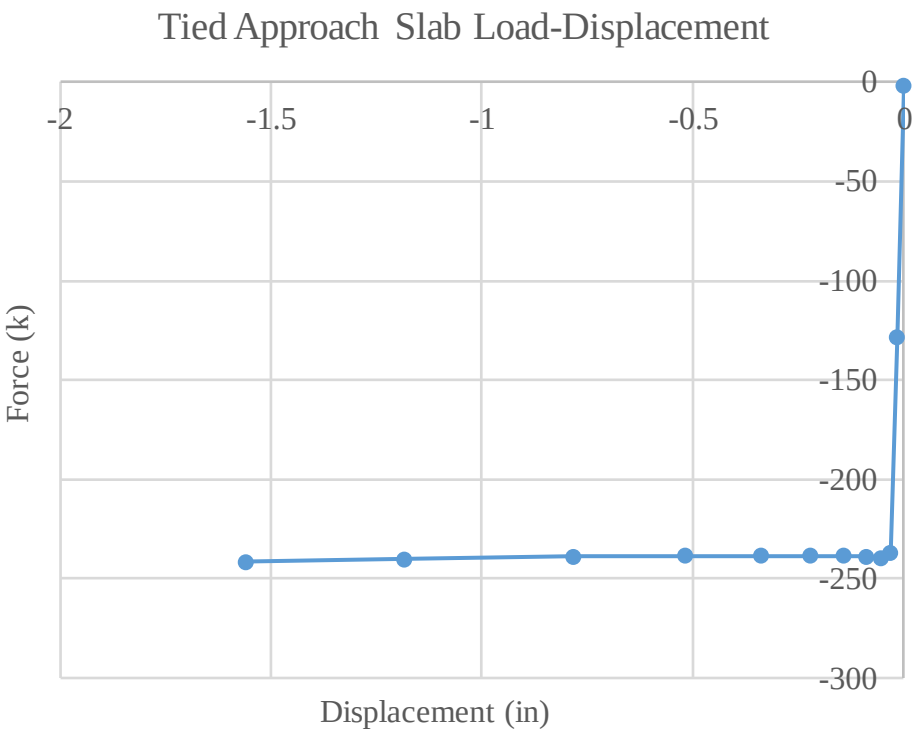

Figure 6.39. Shelby - Load Displacement Plot

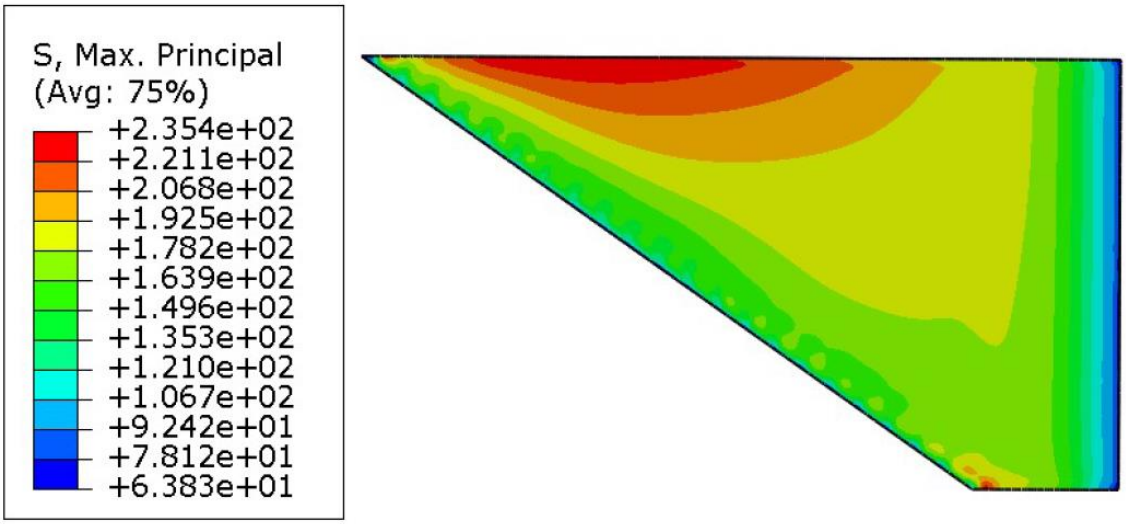

Figure 6.40. Shelby - Maximum Principal Stress

Trends in the force required to pull the slab generally occur in the von Mises stress seen by the tie bars. In the case of vertical bars, the shear force in the longitudinal direction account for the majority of the total stress. The von Mises stress distribution for all twenty-two bars seen in Figure 6.41 shows the stress after the application of gravity (Step 1) to the model to be under 5 ksi for every bar. Some axial force remains in the bars during bridge contractions as the maximum axial force in any single bar reached 8.7 kips. Transverse shear in the direction perpendicular to the bridge centerline shows opposite signs for bars at either end of the joint since the slab contracts and attempts to pull bars towards the middle. Von Mises stress in the bars ranges from 27.8 ksi to 1 ksi illustrating a significant difference between the magnitudes in bars across the joint. Although magnitudes are not directly comparable due to differences in slab size and the number of tie bars used, the distribution plots for the Story 30° skew model and the Shelby 55° skew model both show bar stresses distributed throughout the range between maximum and minimum stresses.

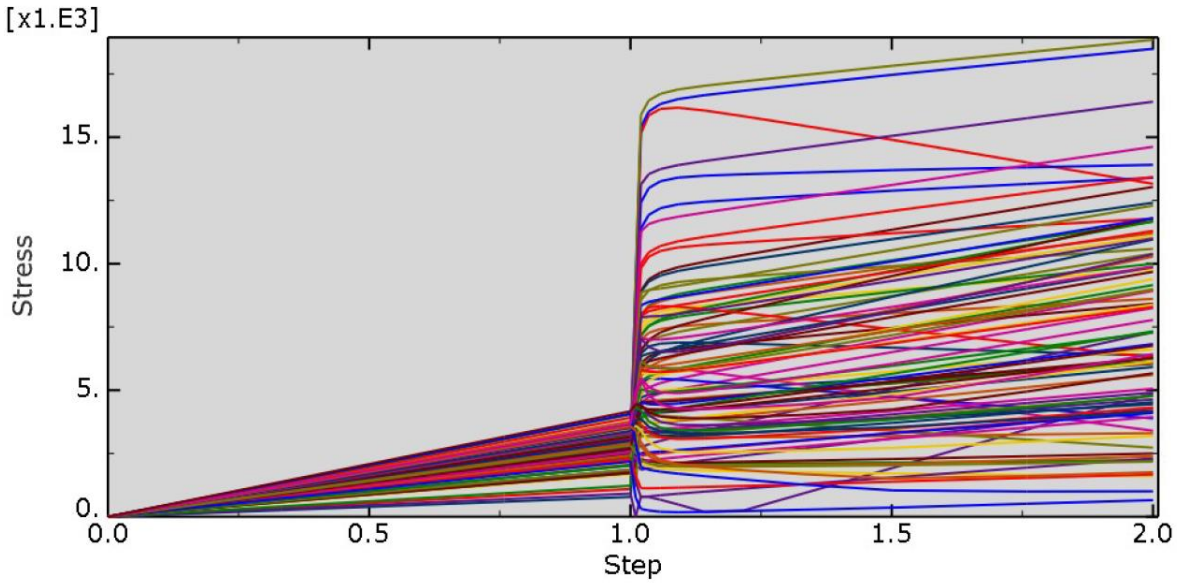

Figure 6.41. Shelby - von Mises Stress Distribution

CHAPTER 7. SUMMARIES, CONCLUSIONS AND RECOMMENDATIONS

The objectives outlined in Chapter 1 provided a path to make important conclusions based on the completed work. The summaries, conclusions, and recommendations made are separated by the research task for which they were completed.

7.1 Literature Review

Much of the literature provided approach slab and abutment details studied by other investigators with the goal of providing state DOTs and other transportation agencies with invaluable information on the performance of said details. The main conclusions drawn from the comprehensive review of literature performed in this thesis are summarized below.

Many states are currently attempting to find ways to achieve the benefits of integral and semi-integral abutments while avoiding the issues associated with pushing the limits of length and skew. One such example is the so-called “Virginia” abutment used by Virginia DOT which employs an integral backwall separated from another backwall by a large void. A joint is placed at the end of the bridge; however, the design prevents any water from reaching the bearings. The separation of the first backwall from the soil backfill eliminates most of the issues associated with integral abutments, especially for high skew or extreme length. The large void between the double backwalls allows easy drainage and maintenance since it is large enough and open on the sides of the bridge to allow for clearing of debris. The concept of the Virginia abutment would improve performance over a bridge with conventional bearings, but it would not be necessary for situations where other abutment types would be acceptable that have less complexity in constructability.

The deck-over-backwall concept is another abutment and approach slab detail that aims to realize the benefits of integral construction including the elimination of a traditional

joint at the deck end, while also trying to eliminate the expansion of the bridge into the backfill. Research conducted by Michigan DOT provides an example of a deck-over-backwall construction which uses a layer of expanded polystyrene between the backwall top surface and approach slab. The Butler County 118 demonstration bridge incorporates the deck-over-backwall concept at the East abutment and will be constructed in the near future.

Virginia DOT uses an abutment type hierarchy for new bridge designs. Based on length and skew limitations, the process prioritizes integral abutments, semi-integral abutments, deck-over-backwall, and finally the "Virginia" abutment. Iowa DOT provides a set of limitations on the use of integral abutments, but development of a similar hierarchy after finalizing investigation of new abutment details would prove beneficial to ensure the most effective type is chosen.

Corbels used to support the approach slab should be avoided if possible. The use of a corbel increases the difficulty of attaining proper compaction of backfill next to the abutment, a key contributor to minimizing approach slab settlement. Iowa DOT J-series bridge standards are an example of a paving notch as a part of the abutment. However, Story County 118 and Iowa DOT standard H-series include the use of a corbel. Corbels may not be eliminated as easily for semi-integral abutment conversions in which the existing abutment footing width is predetermined.

Inclined tie bars are recommended for use with semi-integral abutments to allow approach slab rotation at the tied joint. Backfill settlement under the approach slab inevitably leads to a rotation at the end of the slab, which is best accommodated by the inclined bars that do not transfer moment.

Concrete buttresses with rub plates are in use in Virginia with research leading to possible adoption by Michigan DOT. Buttresses and other bridge end guidance methods restrict thermal expansion to the longitudinal axis. Skewed bridges experience lateral earth pressure forces that cause a rotation of the entire bridge superstructure after repeated thermal loading cycles. Transverse displacement complicates tied approach slab behavior and other detailing aspects that may be best controlled by restricting expansion to the longitudinal axis.

Standard Road Plan BR-205 includes the use of a sleeper slab to support one end of the approach slab. A perforated subdrain is used under the EF joint in one direction from the sleeper slab and behind the abutment in the other direction from the sleeper slab. A joint exists between the approach slab and sleeper slab for which there is no subdrain. The formed curb at the side of the approach slab and sleeper slab is not continuous over the joint. An example from the literature shows drain collector pipes placed at the base of the sleeper slab (Abu-Hejleh et al. 2008). The lack of subdrain present at the sleeper slab for a tied approach slab conflicts with the design intent of having the entire bridge expansion accommodated at that location. The large movements expected at this location increases the possibility of surface water infiltration over time.

Approach slabs are designed to span the distance between abutment and sleeper slab should a loss of support from backfill occur. Sleeper slabs are placed on the same backfill material, so it follows that they may be susceptible to similar issues with settlement. It was shown that a thicker approach slab (e.g., 16”) and sleeper slab supported by soil reinforced with two geogrid layers improved the road profile (Chen and Abu-Farsakh 2016). It was shown that settlement of sleeper slabs was not a critical parameter for the bridges inspected

as part of this project; however, improvement of sleeper slab soil support may be an option should the issue arise.

Abutment backfill details for the bridges included for field monitoring use a geotextile layer placed behind the abutment before filling with porous backfill. The geotextile is described as “permeable” per Iowa DOT IM 4196.01, which would allow for a hydraulic short circuit should drainage become blocked. Water would make its way underneath the abutment possibly reaching foundation piles. A geomembrane was used in a similar manner to prevent such a hydraulic short circuit (Miller et al. 2013); however, the design choice of a geotextile may have been made in anticipation of blocked drainage to prevent accumulation of water behind the abutment. The choice of material should be evaluated with regards to the design intent.

7.2 Inspections

Four different bridge designs that used tied approach slabs, including six different structures, were inspected for condition as it relates to service life. The ¼” preformed tied approach joints used at every location measured between 3/8” and 1 5/8”. The joints are opening over time and not performing as intended. Decreased joint widths at the opposite ends of the approach slabs highlights that approach slabs are shifting away from the tied connection. Multiple bridges using the Iowa DOT BR-205 Standard Road Plan have been let within the past two years. The road plan includes the use of a tied approach with vertical paving notch dowel. Future inspections should be completed to determine the effectiveness of the tied approach joints. Ideally, inspections would take place at least one year after initial construction to allow the bridges to experience one full seasonal temperature cycle.

Condition and performance of the joint between wingwalls and the approach slab curb appeared unsatisfactory on multiple occasions. Noted problems include a 6” deep void

at the intersection of the approach to deck joint and wingwall, separation of the approach slab and wingwall and opening of the joint, concrete cracking at the beginning of the approach slab curb, and frequent poor drainage resulting in buildup of debris at the beginning of the curb. The poor performance of the joint between wingwall and approach slab together with recommendations made based on a review of literature indicate that barrier rails should be placed on top of the approach slab when approach slabs are tied to abutments. Strip seals are recommended for new construction integral and semi-integral abutments (Reza 2013). An example of the curb "kick-up" detail was provided, and a similar detail would be required to accommodate the continuous curb on the sleeper slab.

Abutment drainage was largely free of debris and able to drain water from behind the abutments should it infiltrate deck joints. A single bridge, 310 Jasper Southbound, had drain exits for which the openings were reasonably close to the abutment and blocked by soil.

7.3 Instrumentation

Field monitoring was completed for two different bridges in Iowa. The first is Jasper County 118, a 184.5' bridge with 45° skew. The Jasper semi-integral abutment conversion was designed with the intent that the West abutment was fixed, and the East abutment was moveable. Bridge displacement data taken from displacement transducers show movement of similar magnitudes for both abutments. Displacement transducers installed perpendicular to the bridge centerline measured displacements equal to 81% and 120% of longitudinal displacements for the 45° skew semi-integral abutment bridge.

Earth pressure sensors installed on the Jasper semi-integral abutment backwall just under the approach slab provided the range of pressures experienced over a four-month period from September to December. The maximum pressure at one of the three functioning sensors reached the calculated passive pressure value. A full yearly temperature cycle would

prove invaluable for monitoring earth pressures during a warming period of bridge expansion.

The second bridge included for monitoring was Story County 118, a 375' integral abutment bridge with 15° skew. Superstructure expansion of the Story bridge was captured using crackmeters installed at tied approach joints and approach slab to sleeper slab joints at both ends of the bridge. Displacement transducers require a fixed reference point which would have been difficult given the fact that the Story bridge was new construction and embankment settlement can alter displacement readings. By assuming sleeper slabs are fixed in place, all expansion of sleeper slabs and the superstructure was accounted for.

Crackmeters mounted on the story bridge barrier rails measured the tied approach slab joint without placing sensors on the road surface. While the initial data shows joints experiencing a cyclic opening and closing due to bridge expansion, the behavior is not simply a linear response. It is postulated that additional trends and opening of the joint may be revealed through long-term monitoring.

Strain gauges mounted on the tie bars between the approach slabs and abutments are not functioning as intended. Only one of the six gauges mounted on a tie bar appeared to capture the behavior of the bar instead of slab thermal expansion and contraction. It is recommended that the type of strain gauge used on tie bars for the other two bridges planned for field monitoring by Iowa DOT should be changed and allow for attachment directly to the bar itself. For example, a Geokon model 4150 may be more appropriate than the 4200. The gauges are also recommended to be attached closer to the joint itself, something that can be accomplished by using a small gauge.

7.4 Finite Element Analysis

Finite element models of both the Jasper and Story bridge ends were developed to study the effect of bridge thermal movement and the response of approach slabs. Various parameters such as approach slab friction, soil stiffness, tie bar style, and bridge skew were systematically investigated through FE simulations.

Load-displacement curves produced for the Jasper bridge approach slab with a tied connection show a lateral force in the tied joint of a similar magnitude to the longitudinal force. The force develops very quickly with only a fraction of the maximum displacement required to realize the movement of the slab in both directions. Tied joint design should account for large lateral forces. As mentioned previously, limiting bridge expansion in the transverse direction using buttresses could eliminate transverse displacement of the slab.

Comparisons of the Story bridge model with field monitoring data shows a similar magnitude of strain induced in the tie bars; however, tied approach joint expansion was slightly underestimated. The model shows a deformation in the tie bars before strain reaches a plateau and the entire approach slab begins sliding. In contrast, a continuous opening of the joint was observed for the joint behavior from the instrumentation data.

Varying coefficients of friction between the concrete approach slab and soil only served to increase the total force required to pull the slab. Stresses in the tie bars also increased proportionally while the force distribution across the bars remain relatively unchanged. The uncertainties involved in the approach slab friction was shown to have minimal effect on how forces are carried by the bars.

While soil stiffness did not affect the concrete or tie bars stresses during bridge contraction, It was unveiled that a stiffer soil can considerably increase concrete and tie bar stresses (i.e., maximum values) at the full range of thermal expansion.

Inclined tie bars experienced lower stresses during bridge contraction while pulling the approach slab. Concrete stresses showed no clear trends with regards to bar orientation.

Skew drastically changes stress distribution in tie bars across the tied approach joint. Force is shifted towards the acute approach slab corner/obtuse bridge corner. Stresses were simultaneously lowered in obtuse slab corner resulting in a greater range of stresses for increased skew angles. It was shown that equal force in each bar should not be assumed for skewed bridges. These results were consistent with the case of extreme skew for which the Shelby bridge model exhibited similar variance in stress in tie bars across the width of the tied approach joint during bridge contraction.

7.5 Future Research

The instrumentation placed on the Jasper and Story bridges was intended for long-term monitoring of up to two years. While invaluable information has been extracted and documented in this thesis, the relatively short periods of data available do not necessarily allow for capturing all the behavior that contributes to decreased bridge service life. An extended monitoring program can better capture the long-term effect of thermal behavior only occurring in cycles on a yearly scale. The extended program would see maximum and minimum extreme cases of temperature and bridge expansion where stresses in different structural elements could reach peak values.

The finite element modeling techniques developed for the Jasper and Story bridge models have shown the ability to provide further insight into how various factors influence the distribution of stresses in tie bars and concrete approach slabs alike. It would prove beneficial to carry this process forward and examine tie bar design in the tied approaches of Iowa DOT J40-series standards. The standards distribute tie bars evenly across the approach

slab to abutment joint regardless of skew ranging from 0° to 30° for abutments with steel piling.

As mentioned previously, the Iowa DOT-sponsored project includes monitoring of two additional bridges. Monitoring of these two bridges can provide supplementary information helpful for both evaluation of length limitations for semi-integral abutment bridges, and performance of details aimed at improving bridge drainage. One bridge is over the current Iowa DOT length limit for semi-integral abutments, so special attention will be paid to any negative effects caused by the large thermal movements. The final bridge includes experimental details for abutments, approach slabs, and bridge ends in general for evaluation in real conditions. Concrete barriers will be placed on approach slabs as recommended by this literature review, and a deck-over-backwall detail will be constructed as a possible alternative to semi-integral abutment when a tied approach slab is desired, but conditions do not allow.

Field monitoring presents many limitations and difficulties involved with placement of sensors and factors that cannot be accounted for in finite element modeling. Construction methods and errors are unpredictable and can influence the behavior of the structure. A laboratory setting allows for control of almost all elements of the construction. An experimental test of tie bar forces would prove beneficial. Approach slab friction reduction methods could be tested along with different bridge skews to check force distribution across the joint. It is believed that a combination of large-scale structural testing and FE simulations can be used to further the extent of knowledge of tied approach joint behavior. The joint is a key factor in increasing bridge end service life through managing drainage over the abutment and approach slab.

REFERENCES

Abu-Hejleh, N., Hanneman, D., Wang, T., & Ksouri, I. (2008). Evaluation and Recommendations for Flowfill and Mechanically Stabilized Earth Bridge Approaches. *Transportation Research Record: Journal of the Transportation Research Board, 2045*, 51–61.

Aktan, H., & Attanayake, U. (2011). *High Skew Link Slab Bridge System with Deck Sliding over Backwall or Backwall Sliding over Abutments Part II*. Research Report No. RC-1563. Michigan Department of Transportation Construction and Technology Division.

Aktan, H., & Attanayake, U. (2011). *High Skew Link Slab Bridge System with Deck Sliding over Backwall or Backwall Sliding over Abutments Part I*. Research Report No. RC-1563. Michigan Department of Transportation Construction and Technology Division.

Aktan, H., & Attanayake, U. (2011). *High Skew Link Slab Bridge System with Deck Sliding over Backwall or Backwall Sliding over Abutments Appendices*. Research Report No. RC-1563. Michigan Department of Transportation Construction and Technology Division.

Aktan, H., Attanayake, U., & Ulku, E. (2008). *Combining Link Slab, Deck Sliding over Backwall, and Revising Bearings*. Research Report No. RC-1514. Michigan Department of Transportation Construction and Technology Division.

Arenas, A., Filz, G., & Cousins, T. (2013). *Thermal Response of Integral Abutment Bridges with Mechanically Stabilized Earth Walls*. Research Report VCTIR 13-R7. Virginia Department of Transportation.

Arsoy, S., Duncan, J. M., & Barker, R. M. (2004). Behavior of a Semi-integral Bridge Abutment under Static and Temperature-Induced Cyclic Loading. *Journal of Bridge Engineering*, *9*(2), 193–199.

Bakeer, R., Mattei, N., Almalik, B., Carr, S., & Homes, D. (2005). *Evaluation of DOTD Semi-Integral Bridge and Abutment System*. Research Report No. FHWA/LA.05/397. Louisiana Transportation Research Center.

Biana, I. (2010). A semi-integral composite bridge of high skew. *Journal of Bridge Engineering*, *163*, 115–124.

Bonczar, C., Brena, S., Civjan, S., DeJong, J., Crellin, B., & Crovo, D. (2005). Field Data and FEM Modeling of the Orange-Wendell Bridge, 163–173. Integral Abutment and Jointless Bridges (IAJB 2005), March 16-18, 2005, Baltimore, Maryland.

Bonczar, C., Brena, S., Civjan, S., DeJong, J., & Crovo, D. (2005). Integral Abutment Pile Behavior and Design - Field Data and FEM Studies, 174–184. Integral Abutment and Jointless Bridges (IAJB 2005), March 16-18, 2005, Baltimore, Maryland.

Briaud, J., James, R., & Hoffman, S. (1997). *Settlement of Bridge Approaches (The Bump at the End of the Bridge)*. Synthesis Report 234, National Cooperative Highway Research Program, Washington, DC.

Chen, Q., & Abu-Farsakh, M. (2016). Mitigating the bridge end bump problem: A case study of a new approach slab system with geosynthetic reinforced soil foundation. *Geotextiles and Geomembranes*, *44*(1), 39–50.

Dicleli, & Albhaisi, S. (2003). Maximum length of integral bridges supported on steel H-piles. *Engineering Structures*, *25*, 1491–1504.

Dunker, K., & Abu-Hawash, A. (2005). Expanding the Use of Integral Abutments in Iowa. Proceedings of the 2005 Mid-Continent Transportation Research Symposium, August 18-19, 2005, Ames, Iowa.

Dupont, B., & Allen, D. (2002). *Movements and Settlements of Highway Bridge Approaches*. Research Report No. KTC-02-18/SPR-220-00-1F. Kentucky Transportation Cabinet.

Greimann, L., Phares, B., Faris, A., & Bigelow, J. (2008). *Instrumentation and Monitoring of Integral Bridge Abutment-to-Approach Slab Connection*. Research Report No. IHRB Project TR-530 & TR-539/CTRE Project 05-197 & 05-219. Iowa Department of Transportation.

Hassiotis, S., Khodair, Y., Roman, E., & Dehne, Y. (2006). *Evaluation of Integral Abutments*. *FHWA-NJ-2005-025*. New Jersey Department of Transportation.

Hoppe, E. J., & Eichenthal, S. L. (2012). *Thermal Response of a Highly Skewed Integral Bridge Standard Title Page -Report on Federally Funded Project*. Research Report No. FHWA/VCTIR 12-R10. Virginia Department of Transportation.

Hoppe, E., Weakley, K., & Thompson, P. (2016). Jointless Bridge Design at the Virginia Department of Transportation. *Transportation Research Procedia*, (*2016) 14*, 3943–3952.

Horvath, J. S. (2005). Integral-Abutment Bridges: Geotechnical Problems and Solutions Using Geosynthetics and Ground Improvement. *2005 FHWA Conference: Integral Abutment and Jointless Bridges*, (March), 281–291.

Idaho DOT. (2008). *Article 11.6.1.3 Design Guidelines for Integral Abutments*. Idaho DOT Bridge Design LRFD Manual.

Kaniraj, S. (1988). *Design Aids in Soil Mechanics and Foundation Engineering* (10th ed.). Tata McGraw-Hill Publishing Company Limited.

Kim, W., & Laman, J. A. (2011). Seven-Year Field Monitoring of Four Integral Abutment Bridges. *Journal of Performance of Constructed Facilities*, *26*(1), 54–64.

Kong, B., Cai, C. S., & Kong, X. (2015). Field monitoring study of an integral abutment bridge supported by prestressed precast concrete piles on soft soils. *Engineering Structures*, *104*, 18–31.

Kong, B., Cai, C. S., & Zhang, Y. (2016). Parametric study of an integral abutment bridge supported by prestressed precast concrete piles. *Engineering Structures*, *120*, 37–48.

LaFave, J. M., Fahnestock, L. A., Wright, B. A., Riddle, J. K., Jarrett, M. W., Svatora, J. S., … Brambila, G. (2016). *Numerical Simulations of Steel Integral Abutment Bridges under Thermal Loading*. Research Report No. FHWA-ICT-16-014. Illinois Department of Transportation (SPR) Bureau of Material and Physical Research.

LaFave, J. M., Riddle, J. K., Fahnestock, L. A., Brambila, G., Jarrett, M. W., Svatora, J. S., … Huayu, A. (2017). *Integral Abutment Bridges under Thermal Loading: Field Monitoring and Analysis*. Research Report No. FHWA-ICT-17-017. Illinois Department of Transportation (SPR) Bureau of Material and Physical Research.

Lenke, L. R. (2006). *Settlement Issues – Bridge Approach Slabs (Final Report Phase I)*. Research Report No. Report NM04MNT-02. New Mexico Department of Transportation.

Luna, R., Robison, J., & Wilding, A. (2004). *Evaluation of Bridge Approach Slabs, Performance and Design*. Research Report No. RDT 04-010. Missouri Department of Transportation.

Martin, R. D., & Kang, T. H.-K. (2013). Structural Design and Construction Issues of Approach Slabs. *Practice Periodical on Structural Design and Construction*, *18*(1), 12–20.

Maruri, R. F., & Petro, S. (2005). Integral Abutments and Jointless Bridges (IAJB) 2004 Survey Summary. Integral Abutment and Jointless Bridges (IAJB 2005), March 16-18, 2005, Baltimore, Maryland.

Mekkawy, M. M., White, D. J., Suleiman, M. T., & Sritharan, S. (2005). Simple Design Alternatives to Improve Drainage and Reduce Erosion at Bridge Abutments. Proceedings of the 2005 Mid-Continent Transportation Research Symposium, August 18-19, 2005, Ames, Iowa.

Miller, G. A., Hatami, K., Cerato, A. B., & Osborne, C. (2013). *Applied Approach Slab Settlement Research, Design/Construction*. Research Report No. FHWA-OK-13-09. Oklahoma Department of Transportation Planning and Research Division.

Mistry, V. C. (2005). *Integral Abutment and Jointless Bridges*. Integral Abutment and Jointless Bridges (IAJB 2005), March 16-18, 2005, Baltimore, Maryland.

Muttoni, A., Dumont, A., Burdet, O., Savvilotidou, M., Einpaul, J., & Nguyen, M. L. (2013). *Experimental verification of integral bridge abutments*. Rapport OFROU. Switzerland. 86 p.

Nadermann, A., Greimann, L., & Phares, B. (2010). *Instrumentation and Monitoring of Precast Bridge Approach Tied to an Integral Abutment Bridge in Bremer County*. Research Report No. InTrans Project 08-335. Iowa Department of Transportation Office of Bridge and Structures.

Nassif, H. H., Abu-Amra, T., Suksawang, N., Khodair, Y., & Shah, N. (2009). Field investigation and performance of bridge approach slabs. *Structure and Infrastructure Engineering*, *5*(2), 105–121.

Oliva, M. G., & Rajek, G. (2011). *Toward Improving the Performance of Highway Bridge Approach Slabs*. Research Report No. CFIRE 03-10. Research and Innovative Technology Administration United States Department of Transportation.

Olson, S. M., Holloway, K. P., Buenker, J. M., Long, J. H., & Lafave, J. M. (2013). *Thermal Behavior of IDOT Integral Abutment Bridges and Proposed Design Modifications*. Research Report No. FHWA-ICT-12-022. Illinois Department of Transportation Bureau of Materials and Physical Research.

Olson, S. M., Long, J. H., Hansen, J. R., Renekis, D., & Lafave, J. M. (2009). *Modification of IDOT Integral Abutment Design Limitations and Details*. Research Report No. FHWA-ICT-09-054. Illinois Department of Transportation Bureau of Materials and Physical Research.

Phares, B. M., White, D., Bigelow, J., Berns, M., & Zhang, J. (2011). *Identification and Evaluation of Pavement-Bridge Interface Ride Quality Improvement and Corrective Strategies*. Research Report No. FHWA/OH-2011/1. Ohio Department of Transportation.

Phares, B., & Dahlberg, J. (2015). *Performance and Design of Bridge Approach Panels in Wisconsin*. Research Report No. 0092-14-04. Wisconsin Department of Transportation Research & Library Unit.

Potyondy, J. (1961). Skin Friction between Various Soils and Construction Materials. *Geotechnique*, *11*(4), 339–353.

Puppala, A., Saride, S., Archeewa, E., Hoyos, L., & Nazarian, S. (2009). *Recommendations for Design, Construction, and Maintenance of Bridge Approach Slabs: Synthesis Report*. Research Report No. FHWA/TX-09/0-6022-1. Texas Department of Transportation Research and Technology Implementation Office.

Reza, F. (2013). *Synthesis of Bridge Approach Panels Best Practices*. Research Report No. MN/RC 2013-09. Minnesota Department of Transportation Research Services.

Robison, J. L., & Luna, R. (2004). Deformation Analysis of Modeling of Missouri Bridge Approach Embankments. *GeoTrans*, 2020–2027.

Seo, J., Ha, H., & Briaud, J.-L. (2002). *Investigation of Settlement at Bridge Approach Slab Expansion Joint: Numerical Simulations and Model Tests*. Research Report No. FHWA/TX-03/0-4147-2. Texas Department of Transportation Research and Technology Implementation Office.

Thiagarajan, G., Ajgaonkar, S., Eilers, M., & Halmen, C. (2013). Cost-Efficient and Innovative Design for Bridge Approach Slab. *Transportation Research Record: Journal of the Transportation Research Board*, *2313*, 100–105.

Varmazyar, M., Wozniak, R., & Walsh, R. (2017). *Utilizing Compressible Inclusions and Cement Stabilised Sand for Integral Bridges*. 10th Austroads Bridge Conference (2017) 10.

Weakley, K. (2005). VDOT Integral Bridge Design Guidelines. Integral Abutment and Jointless Bridges (IAJB 2005), March 16-18, 2005, Baltimore, Maryland. (pp. 61–70).

White, D. J., Mekkawy, M. M., Sritharan, S., & Suleiman, M. T. (2007). "Underlying" Causes for Settlement of Bridge Approach Pavement Systems. *Journal of Performance of Constructed Facilities*, *21*(4), 273–282.

White, H. (2007). *Integral Abutment Bridges: Comparison of Current Practice Between European Countries and the United States of America*. Research Report FHWA/NY/SR-07/152. New York State Department of Transportation.

Yasrobi, S. Y., Ng, K. W., Edgar, T. V., & Menghini, M. (2016). Investigation of approach slab settlement for highway infrastructure. *Transportation Geotechnics*, *6*, 1–15.

APPENDIX A. BRIDGE SERVICE LIFE SURVEY

Iowa State University - Abutment and Approach Slab Service Life Survey

Start of Block: Introduction

Q1.1 Please enter your contact information.

- First Name: _____
- Last Name: _____
- Title (e.g. Bridge Design Engineer): _____
- Organization (e.g. Iowa DOT): _____
- Email Address: _____
- Phone Number: _____

End of Block: Introduction

Start of Block: Abutments and Skew

Q2.1 What is the maximum degree of skew that you are comfortable with tying approach slabs to moveable abutments (e.g. integral, semi-integral, continuous deck)?

- My state does not tie approach slabs to moveable abutments.
- Enter maximum skew (degrees): _____
- Approach slabs can be tied no matter the skew.

Q2.2 Does your state account for transverse displacement (perpendicular to direction of travel) of skewed bridges at the tied approach slab connection? If so, how?

- ○ **N/A**, my state does not use tied approach slabs.
- ○ **No**, my state does not account for transverse displacement at the tied approach slab connection.
- ○ **Yes**. Please elaborate: _____

Q2.3 Does your state attempt to restrict transverse movement of the bridge end, especially for high skew bridges? Check all that apply.

- ☐ **No**, my state does not attempt to restrict transverse movement.
- ☐ **Yes**, with longitudinally guided bearings
- ☐ **Yes**, with buttresses and rub plates
- ☐ **Yes**, with shear keys in abutments
- ☐ **Other**. Please specify: _____

Q2.4 Are there any special accommodations made or unique details used for cases of high skew?

- ○ No.
- ○ Yes. Please elaborate: _____

Q2.5 The research team appreciates receiving any supporting documents regarding unique details for extreme skew. If possible, please upload files or share any links to design

documents or details. **Upload a file**:

Share a link:

_____

_____

_____

_____

_____

End of Block: Abutments and Skew

Start of Block: Sleeper Slabs/Grade Beams

Q3.1 Are there sleeper slabs or grade beams used in conjunction with approach slabs?

- **No**.
- **Yes, sleeper slabs** are used with approach slabs.
- **Yes, grade beams** are used with approach slabs
- **Yes**, **sleeper slabs and grade beams** are used with approach slabs.

Q3.2 Are there any methods used to reduce/eliminate settlement of the sleeper slab/grade

beam? Check all that apply.

- ☐ No attempts are made to reduce settlement other than use of compacted fill.
- ☐ Piles
- ☐ Geogrid
- ☐ Mechanically Stabilized Earth (MSE)
- ☐ Other. Please specify: _____

Q3.3 What kind of expansion joint/device is utilized between the approach slab and sleeper slab? Check all that apply.

- ☐ Strip Seal
- ☐ Finger Joint
- ☐ Joint Filler
- ☐ Other. Please specify: _____

Q3.4 What expansion devices does your state prefer in the case of large expected joint

movements? Check all that apply.

- ☐ Strip Seal
- ☐ Finger Joint
- ☐ Joint Filler
- ☐ Other. Please specify: _____

End of Block: Sleeper Slabs/Grade Beams

Start of Block: Erosion/Drainage

Q4.1 Is the concrete barrier rail typically placed on top of the approach slab (if present)? Does it continue the full length?

- ○ **No**, the barrier is not placed on the approach slab.
- ○ **Yes**, the barrier continues on the approach slab a **portion of its length**.
- ○ **Yes**, the barrier runs the **full** length on top of the approach slab.

Q4.2 What drainage maintenance is done at the bridge ends (bridge end includes the approach slab, abutment, embankment)?

_____

_____

_____

_____

_____

Q4.3 What challenges (if any) have accompanied bridge end drainage maintenance?

_____

_____

_____

_____

_____

Q4.4 Are there any specific drainage details that have performed extremely well?

- ○ No.
- ○ Yes. Please elaborate: _____

Q4.5 If possible, please upload files or share links for any drainage details that perform extremely well. **Upload a file:**

Share a link:

_____

_____

_____

_____

_____

End of Block: Erosion/Drainage

APPENDIX B. BRIDGE INSPECTION APPROACH SLAB SECTION PLANS

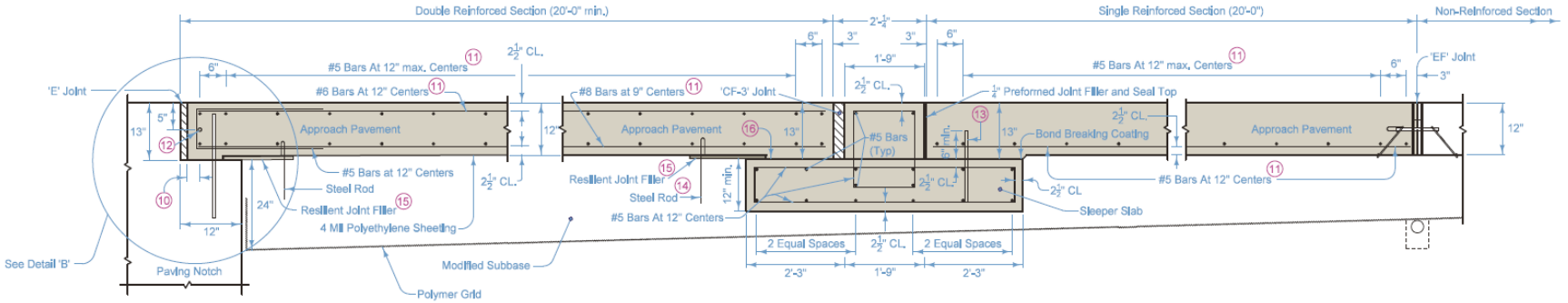

Figure B.1. 1215 Polk Approach Slab Section (Iowa DOT)

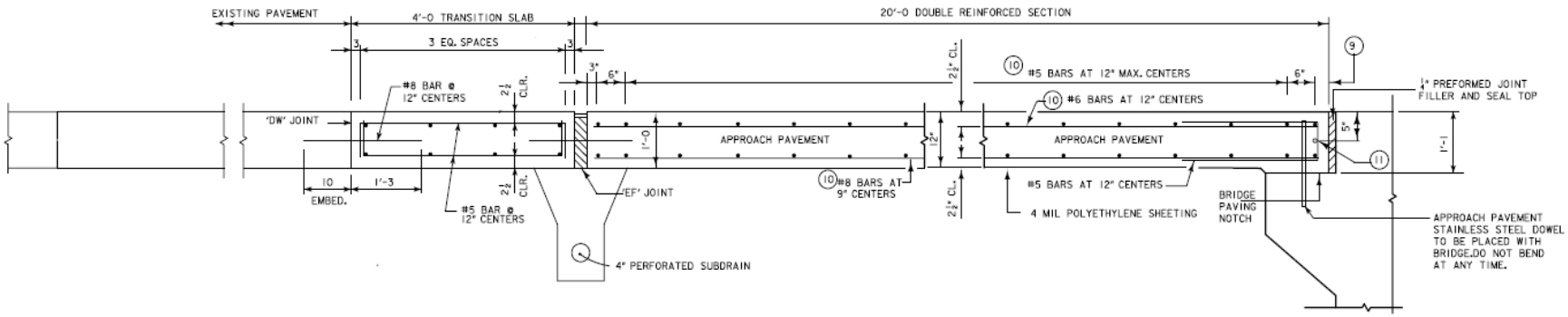

Figure B.2. 310 Jasper Approach Slab Section (Iowa DOT)

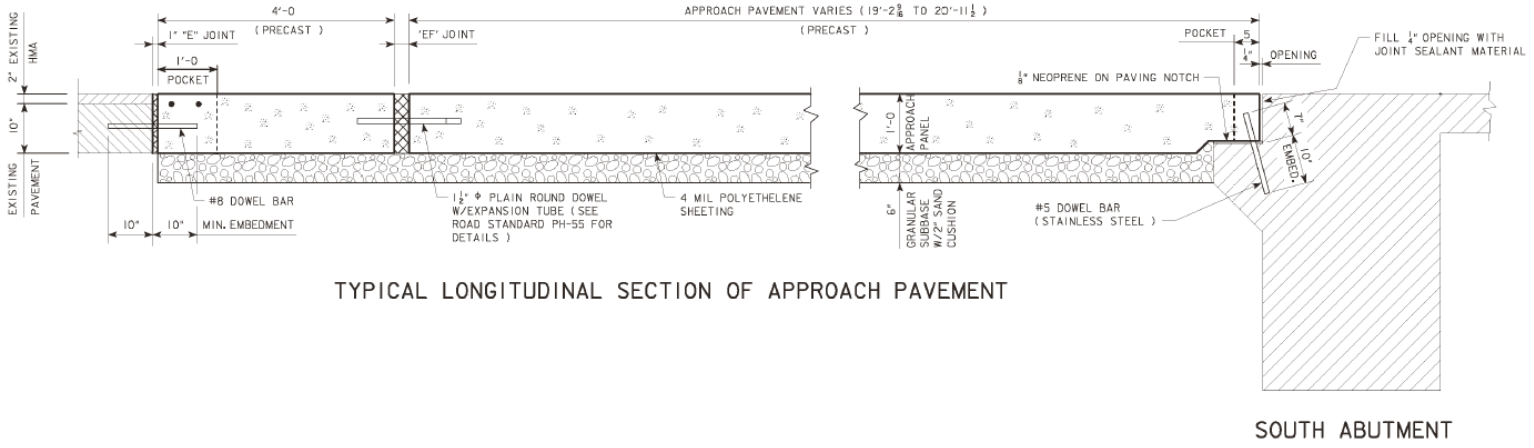

Figure B.3. 208 Bremer Approach Slab Section (Iowa DOT)

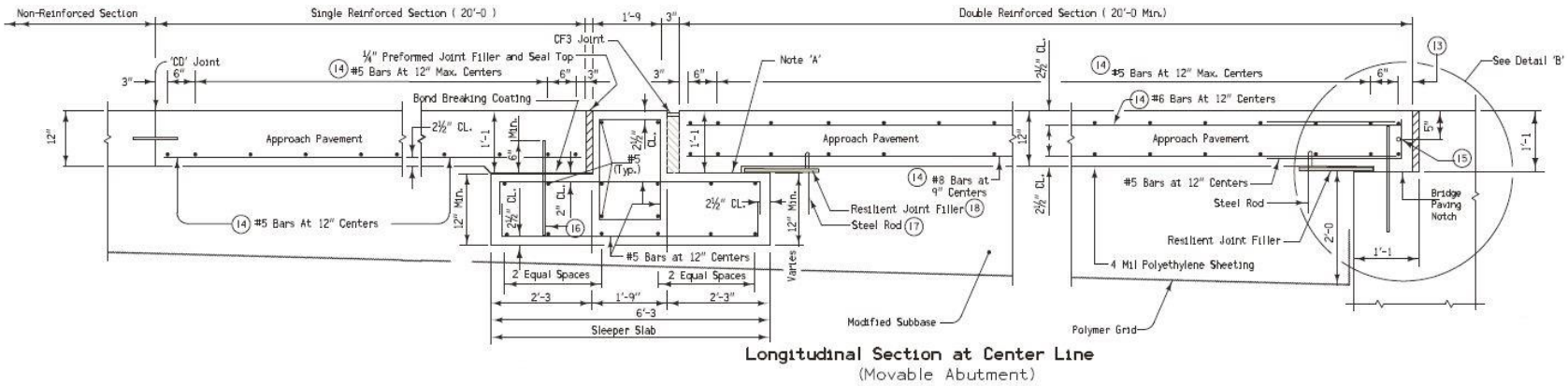

Figure B.4. 108 Blackhawk Approach Slab Section (Iowa DOT)

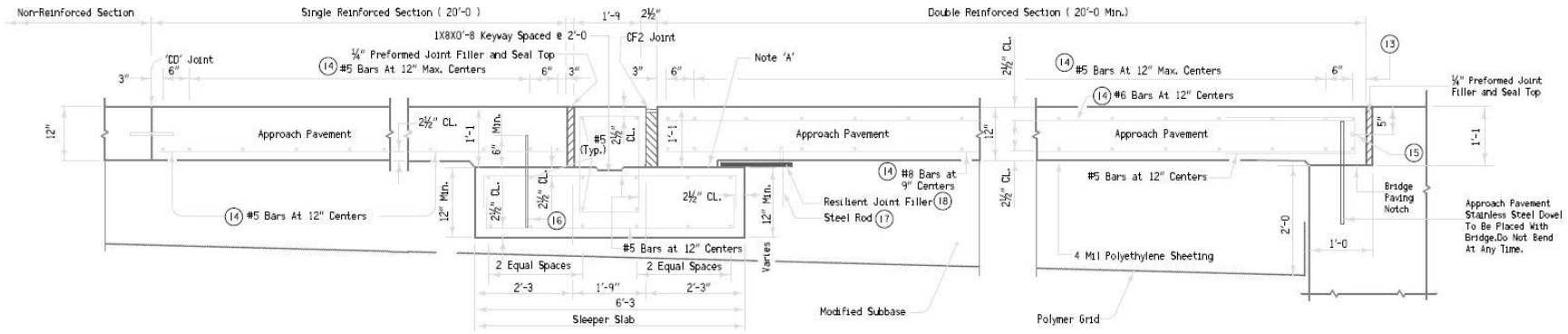

Figure B.5. 213 Cass Approach Slab Section (Iowa DOT)

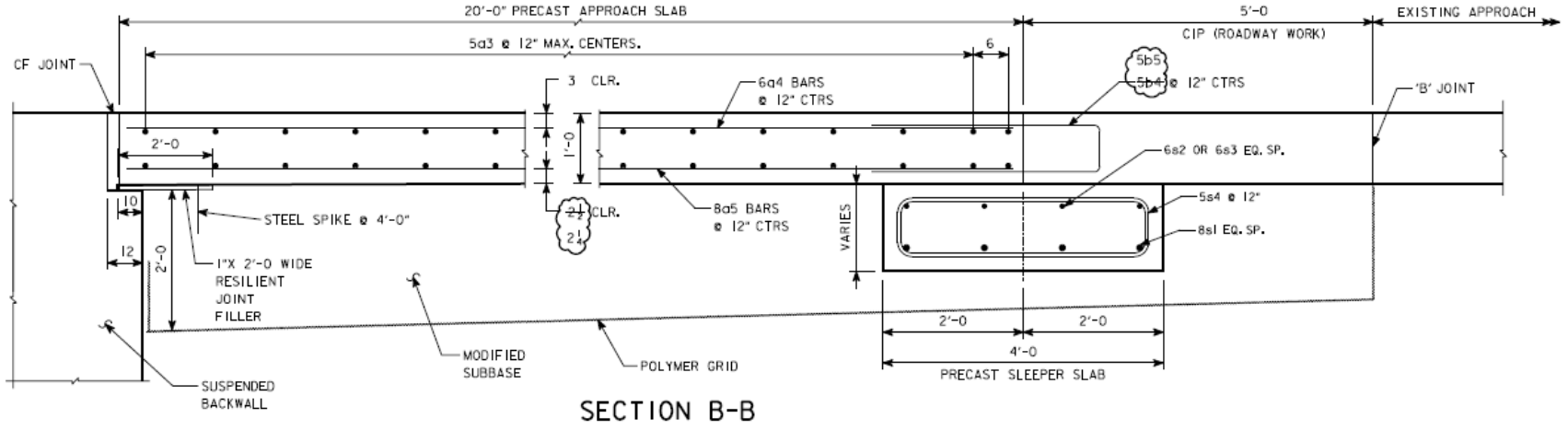

Figure B.6. 111 Pottawattamie Approach Slab Section (Iowa DOT)